

University of Denver

Digital Commons @ DU

Electronic Theses and Dissertations

Graduate Studies

1-1-2011

Trends in Heavy-Duty Diesel Emissions and Analyses of Colorado's Light-Duty Vehicle Inspection and Maintenance Program

Brent G. Schuchmann
University of Denver

Follow this and additional works at: <https://digitalcommons.du.edu/etd>



Part of the [Environmental Chemistry Commons](#)

Recommended Citation

Schuchmann, Brent G., "Trends in Heavy-Duty Diesel Emissions and Analyses of Colorado's Light-Duty Vehicle Inspection and Maintenance Program" (2011). *Electronic Theses and Dissertations*. 585.
<https://digitalcommons.du.edu/etd/585>

This Dissertation is brought to you for free and open access by the Graduate Studies at Digital Commons @ DU. It has been accepted for inclusion in Electronic Theses and Dissertations by an authorized administrator of Digital Commons @ DU. For more information, please contact jennifer.cox@du.edu, dig-commons@du.edu.

Trends in Heavy-Duty Diesel Vehicle Emissions and Analyses of Colorado's Light-Duty
Vehicle Inspection and Maintenance Program

A Dissertation

Presented to

The Faculty of Natural Sciences and Mathematics

University of Denver

In Partial Fulfillment

of the Requirements for the Degree

Doctor of Philosophy

by

Brent G. Schuchmann

November 2011

Advisor: Donald H. Stedman

©Copyright by Brent G. Schuchmann 2011

All Rights Reserved

Author: Brent G. Schuchmann
Title: Trends in Heavy-Duty Diesel Vehicle Emissions and Analyses of Colorado's
Light-Duty Vehicle Inspection and Maintenance Program
Advisor: Donald H. Stedman
Degree Date: November 2011

Abstract

Emission trends are reported and discussed resulting from the multi-year study of Heavy-Duty Diesel Vehicles (HDDV) at the Port of Los Angeles and at a weigh station in Peralta also in the L.A. basin. Remote sensing data were also collected from the Port of Houston and compared to the data from California. As part of San Pedro Bay Ports Clean Air Action Plan (CAAP) to fast track the turnover rate of cleaner trucks, many truck operators have been subject to modifying their trucks, or have purchased new trucks, with more advanced control technologies to reduce exhaust particulate matter (PM) and oxides of nitrogen (NO_x). These advanced control technologies have been proven to effectively reduce these emissions but have some unwanted effects such as increasing the NO_2/NO ratio in diesel exhaust which has the potential to increase ground level ozone. Ammonia (NH_3) was found to be an unexpected product from one of the new control technologies as almost all the NO_x is reduced to NH_3 . In addition to the HDDV comparison, two years worth of emissions records from Colorado's light-duty fleet Inspection Maintenance (I/M) program were matched and compared with the on-road measurements. This analysis shows that switching to an On-Board Diagnostics only program would cost 5-8 times as much as the currently used dynamometer tests and achieve only a fraction of emissions benefit from the current I/M program.

Acknowledgements

I would like to thank the University of Denver, Environmental Systems Products Holdings Inc., California Air Resources Board, Eastern Research Group, National Renewable Energy Laboratory, and South Coast Air Quality Management District for the opportunity and funding for the research presented within this document. Also, I wish to thank Dr. Gary Bishop and Dr. Donald Stedman for the guidance and direction they have provided. Their knowledge, understanding and willingness to accept my wishes to research remote sensing have been extremely exemplary. Finally I wish to graciously thank my parents Steve and Chris, my brother David, and my girlfriend Heather without whose love and support I would not have arrived at this juncture in my life nor my education.

Table of Contents

1.	Introduction.....	1
	Engine Operations and Emission Controls	1
	Instrumentation	7
	Remote Sensing Detector (RSD)	7
	Electrical Tailpipe Particle Sensor (ETaPS)	13
	RSD Calculations.....	14
	Assumptions.....	14
	RSD Theory	18
	Absorption Spectroscopy	18
2.	Heavy-Duty Diesel Vehicles.....	21
	Smoke Correlation of ETaPS/Dynamometer/RSD from HDDVs.....	21
	Introduction.....	21
	ETaPS Results.....	28
	Heavy Duty Diesel Vehicle Emissions in the Los Angeles Basin.....	36
	Setup	36
	California HDDV Results	42
	Methane Combustion	85
	Discussion	87
	HDDV Exhaust On-Road Sampling Prototype.....	91

3.	Light-Duty Gasoline Vehicles	111
	Comparison of Colorado’s Inspection Maintenance Program with OBD and RSD	111
	Cost Analysis of Colorado’s Inspection Maintenance Program with OBDII and RSD.....	131
	References.....	135
	Appendix A.....	139
	Appendix B	140
	Appendix C	141

List of Figures

Figure 1 Typical setup for the FEAT instrument.....	9
Figure 2 Schematic diagram of IR/UV detectors in the FEAT RSD.....	10
Figure 3 Averaged readings for each truck over each cycle driven. Errors bars are the standard deviations for each averaged data point. *No DPF **DPF bypassed ***DPF equipped.....	30
Figure 4 Averaged readings for each truck separated by cycle. The Urban Driving Dynamometer Schedule (UDDS) simulates city driving. The Cruise test simulates highway driving. The Acceleration (Acc) simulates intermediate emissions between the UDDS and Cruise tests. There are no error bars for the Acc cycle because only one run was performed for each truck.	30
Figure 5 Side view photograph of the ETaPS mounted onto the support rod which can be fastened to elevated exhaust pipes. The support rod has two right angle thumb screw clamps which would lock onto the two U-clamps that are placed around the exhaust pipe.	32
Figure 6 Side-view of the ETaPS in the 90 degree orientation.....	33
Figure 7 Close up photograph of the angle adjustment slide which allows the ETaPS to change its orientation 0-90 degrees to the horizontal.	34
Figure 8 Top-down photograph of the ETaPS body mount to the exhaust pipe apparatus.	35
Figure 9 A satellite photograph of the Peralta weigh station located on the eastbound Riverside Freeway (State Route 91). The scales are located on the inside lane next to the building in the top center and the outside lane is for unloaded trucks. The measurement location is circled at the upper right with approximate locations of the scaffolding, support vehicle and camera. This photograph was taken from Google maps.	38
Figure 10 Photograph at the Peralta Weigh Station of the setup used to detect exhaust emissions from heavy-duty diesel trucks.....	39
Figure 11 A satellite photograph of the Port of Los Angeles Water Street exit. The measurement location is circled in the lower left with approximate locations of the scaffolding, support vehicle and camera. This photograph was taken from Google maps.	40
Figure 12 Photograph at the Port of Los Angeles of the setup used to detect exhaust emissions from heavy-duty diesel trucks.....	41

Figure 13 Year over year NO _x and %IR opacity for both locations. Numbers above each bar are average fleet model year. The NO _x bar is separated into NO and NO ₂ but error bars are standard error of the mean calculated from the total NO _x which has been converted into NO ₂ units.....	48
Figure 14 Fleet fractions versus chassis model year for the Peralta Weigh Station and the Port of Los Angeles in 2010.	51
Figure 15 Fleet fractions versus chassis model year for the Peralta Weigh Station and the Port of Los Angeles in 2008.	51
Figure 16 Fleet fractions for the Peralta Weigh Station and the Port of Los Angeles for 2008 and 2010 plotted against binned gNO _x /kg.	52
Figure 17 Mean NO _x emissions for 2008-2010 measurement years at Peralta Weigh Station. The 1995 and newer fleet shows a general trend of decreasing mean NO _x as a function of chassis model year. Error bars are calculated from the standard error of the daily means.	55
Figure 18 Mean NO _x emissions for 2008-2010 measurement years at the Port of Los Angeles. Each year, newer than about 1995, shows a general trend of decreasing NO _x as a function of chassis model year. Error bars are calculated from the standard error of the daily means.	56
Figure 19 Cumulative NO _x fraction emissions plotted versus fraction of the truck fleet for the 2010 Peralta Weigh Station and the Port of Los Angeles.....	57
Figure 20 Ratio of NO ₂ /NO _x vs. chassis model year for HDDV's at each site in 2010. New technologies implemented to meet new EPA standards yield higher proportions of NO ₂ in MY 2008-2011 trucks. Uncertainties are standard errors of the mean. ...	58
Figure 21 Data sets from combined average smoke measurements of Peralta and the Port of Los Angeles in 2010 as a function of model year for the two remote sensing systems. The FEAT reports %IR opacity from the infrared and the ESP system reports smoke (g/kg) in the infrared and the ultraviolet. Model years dating before 1989 are removed because of low sample sizes and high uncertainty.....	61
Figure 22 Average %IR opacity plotted for different model year ranges corresponding to targeted PM reductions. Sample sizes are shown at the bottom of each bar and the average %IR opacity values are shown at the top of each bar. For comparison the 2008 measurement year has been age adjusted to the 2010 measurement so any differences in average opacity are not due to fleet age. Error bars are calculated as the standard error of the mean.	61
Figure 23 NO _x emissions as g/kg are plotted for each location of measurement in 2009. The fleet ages for Peralta and the Port of LA have been age adjusted according to the fleet age distribution at Houston in 2009. Uncertainty bars were calculated as	

standard error of the daily means for the Port of Houston and was then applied to Peralta and the Port of LA as a percentage of their age adjusted average.	66
Figure 24 Mean NO ₂ emissions versus model year for measurements collected in 2009 at the Port of LA, Peralta, and the Port of Houston. Error bars are calculated from the standard error of the daily means.....	67
Figure 25 Mean NO ₂ /NO _x ratios versus model year for measurements collected in 2009 at the Port of LA, Peralta and the Port of Houston. Error bars are calculated from the standard error of the daily means.....	68
Figure 26 Mean NO emissions versus model year for measurements collected in 2009 at the Port of LA, Peralta, and the Port of Houston. Error bars are calculated from the standard error of the daily means.....	69
Figure 27 Mean NO ₂ emissions binned by VSP for trucks measured at the weigh station at Peralta in 2008-2010.	70
Figure 28 Mean %IR Opacities versus model year for measurements collected in 2009 at the Port of LA, Peralta, and the Port of Houston. Uncertainty bars were removed for Houston MY 2009 and Peralta MY 1991 because they had smaller N values (< 2) and the large uncertainties distracted any observations from the whole figure.	71
Figure 29 Matched emission data sets combining Peralta and the Port of Los Angeles for the FEAT and ESP 4600 plotting the cumulative total emission for the infrared and ultraviolet smoke measurements. The fact that 10% of the fleet accounts for approximately 40% of the smoke emissions indicates that the distributions are only slightly skewed.....	74
Figure 30 Bar chart of truck emissions at the Port of Los Angeles separated by type of fuel burned for measurement years 2009 and 2010. Error bars are standard errors of the mean.	76
Figure 31 Individual SO ₂ emission readings by model year. The SO ₂ outliers present in the 2008 data are absent in this year's study.....	78
Figure 32 Individual SO ₂ emission readings observed in 2008 by model year. A vehicle that uses 15ppm ultra low sulfur fuel would average 0.03gSO ₂ /kg. The presence of apparent outliers in this graph indicates that some trucks were using illegal fuel with higher levels of sulfur. The larger triangles represent repeat measurement of the same truck.	78
Figure 33 A total of 1289 time aligned emission measurements for each pollutant collected at the Peralta weigh station by the two remote sensing systems in 2010. A least squares best fit line is plotted for each ratio and the equation for that line is included.....	82

Figure 34 A total of 1182 time aligned emission measurements for each pollutant collected at the LA Port by the two remote sensing systems in 2010. A least squares best fit line is plotted for each ratio and the equation for that line is included.	83
Figure 35 Cartoon drawing of a drive-through tent shed for a theoretical on-road HDDV IM program.	95
Figure 36 FEAT 5001 with attached air duct pointed at the fan blowing air out of the sampling pipe.	96
Figure 37 Point of CO ₂ injection into air inlet of FEAT 5001FEAT.	96
Figure 38 Point of where the 3'' sample pipe merges with the 4' pipe. A t-connector was used in place of an elbow adapter because the original design had two 25' pipes meeting at the center.	97
Figure 39 25' sample pipe with holes drilled about every foot. Two air sampling holes are pointed out by the arrows.	97
Figure 40 Point of CO ₂ injection at the far end of the sample pipe.	98
Figure 41 The results of the CO ₂ injection test. CO ₂ was injected five times and each time the FEAT registered two absorption peaks. The time difference between the maximum absorptions for each puff averaged about 40 points. Since data were collected as 10 Hz averaged samples this converts to 4 seconds.	99
Figure 42 Photograph of the DMM computer and the two Horiba Analyzers.	101
Figure 43 Photograph of the five foot sampling tube with half inch holes drilled one foot apart.	102
Figure 44 Photograph of the four inch diameter pipe perpendicular to the sampling tube. It is roughly five feet in length and is connected to the sampling tube with a right angle union.	103
Figure 45 Photograph of the four inch diameter pipe connected to the inline Fantech FG 4XL fan which draws air from the sampling tube and blows it in an aluminum air duct. Also shown is the air pump (blue) which supplies the two Horiba analyzers with the correct flow rates of sample exhaust.	104
Figure 46 Photograph of the Dekati Mass Monitor (DMM) along with the vacuum pump underneath it.	105
Figure 47 (Top) Four measured one liter injections into the tent sampling pipe from both calibration cylinders. The first two peaks shown are from the FEAT cylinder and the last two peaks are from the ESP cylinder. The cylinder concentrations are 6% CO, 6% CO ₂ , 0.6% HC, and 0.3% NO for the FEAT cylinder; and 3% CO, 12% CO ₂ , 0.15% HC, and 0.15% NO for the ESP cylinder. There is about a 10:1	

measured dilution. (Bottom) Signal traces for CO ₂ and soot for half a liter of synthesized particles diluted with half a liter of calibration gas. There is a two second lag in response time between the IM Analyzers and the DMM.	108
Figure 48 IM240 g/mi plotted against RSD ppm hydrocarbons for passenger vehicles of model year 1998. This was taken from Klausmeier <i>et al.</i> 2009 report to the state auditor.	114
Figure 49 This is also from Klausmeier <i>et al</i> which plots average IM240 g/mi against RSD ppm hydrocarbons by model year for the year 2008. As expected, there is a very good correlation between IM240 to RSD by model year.	120
Figure 50 IM240 g/mi plotted against RSD ppm for HC. Data were taken from Colorado's 2008 IM240 and RSD databases. Average emissions are plotted for model years 1983-2008. The correlation has an R-square of 0.988.	120
Figure 51 This is an attempt to recreate Figure 48 using more recent IM240 and RSD data for all model years. Please note the x-axis has been truncated to 4000ppm down from 35,000ppm so the origin can be clearly viewed. There are only a few points, less than 0.5%, of the measurements located outside the x-axis scale.	121
Figure 52 Hydrocarbon variability for vehicles remotely measured at least 50 times in 2009. Black bars represent the range of hydrocarbon emissions for an individual vehicle. The line represents each vehicle's average hydrocarbon emission.	124
Figure 53 Hydrocarbon variability of the dirtiest 1% of vehicles measured at least 50 times in 2009. This figure also shows that the top 1% of the dirtiest cars average 190ppm-1200ppm HC contain vehicles that consistently emit high HC and vehicles that have a large range of HC emissions.	125
Figure 54 Shows the average HC for the 28 vehicles from a criterion to select all vehicles being measured at least once of more than 5000ppm HC was applied to the vehicles in Figure 52. The dashed line shows the average for the 28 vehicles. Each x-axis point represents one vehicle and the triangles represent the vehicles that meet both criteria from Figure 54 and Figure 55.	127
Figure 55 Shows the average HC for the 26 vehicles from a criterion to select all vehicles being measured at least twice of more than 2000ppm HC was applied to the vehicles in Figure 52. The dashed line shows the average for the 26 vehicles. Each x-axis point represents one vehicle and the triangles represent the vehicles that meet both criteria from Figure 54 and Figure 55.	128
Figure 56 The dashed line shows the average for 9 vehicles. The triangles represent the vehicles that meet both criteria from Figure 54 and Figure 55.	129

List of Tables

Table 1 Breakdown of the number and type of tests performed on each truck on the chassis dynamometer.	26
Table 2 Table of all tested trucks at the West Virginia chassis dynamometer testing facility for the ETaPS project. The weather conditions on the testing days for the Thomas Bus interfered with the RSD measurements.	27
Table 3 Distribution of Identifiable Peralta License Plates separated by state in 2010. Matched plates are defined as the readable plates from the FEAT database that had a record in the state’s current registration database.....	43
Table 4 Distribution of Identifiable Port of Los Angeles License Plates separated by state in 2010. Matched plates are defined as the readable plates from the FEAT database that had a record in the state’s current registration database.	44
Table 5 Peralta Weigh Station and Port of Los Angeles FEAT Data Summary	47
Table 6 Measured exhaust species from the Port of Houston, Peralta and the Port of LA in 2009. The fleet ages for Peralta and the Port of LA have been adjusted to the fleet age distribution at Houston and are denoted by (AA). Values shown are in g/kg with uncertainty numbers calculated for the Port of Houston from the daily means. The percentage of uncertainty for the Port of Houston was applied to each of the California sites.	66
Table 7 Results of using the FEAT remote sensor to compare calibration cylinders.....	84
Table 8 Actual cylinder concentrations (left two columns). Calculated emission ratios to CO ₂ (middle two columns). Average measured ratios of two injections from each cylinder (right two columns). *Average measured HC are in ppm Carbon and are expected to be about three times the calculated HC as the HC used for calibration was propane therefore the calculated ratios for HC are multiplied by three. Measured uncertainties are calculated from a separate experiment of repeatability of the measurements using the ESP cylinder. Uncertainties are the square root of the sum of the squares for the cylinder certification and the standard error of the mean for each pollutant.	110
Table 9 Values shown are from vehicles identified using a remote sensing HC cut point of 300ppm. IM240 results were used to confirm the remote sensing results by looking at the vehicles that passed the overall emission test and the vehicles that failed the emission test. This 300 ppm cut point could be used to send home 91% of the fleet but at a loss of 12% of the IM240 failing emissions.....	122
Table 10 Values shown are from vehicles identified using a remote sensing HC cut point of 20ppm. IM240 results were used to confirm the remote sensing results by looking at the vehicles that passed the overall emission test and the vehicles that	

failed the emission test. This 20 ppm cut point could be used to send home 49% of the fleet but at a loss of 4.7% of the IM240 failing emissions..... 122

1. Introduction

Engine Operations and Emission Controls

Motor vehicle emissions have been well documented over the last 30 years (1-28). As on-road distributions of vehicles, fuels, and driving behavior have changed, so have the methods and strategies used to monitor the emissions. The remote sensing detector (RSD) was originally designed to measure low-level vehicular exhaust associated with light-duty cars where the exhaust pipe is only about a foot above the ground. The RSD design uses the body of the vehicle to block and unblock the optical beam which then triggers the instrument to record the emissions. This is very efficient when the exhaust pipe is at the rear of the vehicle, as in light duty cars. However, in the case of Heavy-Duty Diesel Vehicles (HDDVs) exhaust pipes are not only elevated above the truck cab and container, but are also directly behind the cab and not at the rear of the vehicle. RSD with special adaptation to HDDV was first used to measure HDDVs by the University of Denver in 1997 in Anaheim, California at the Peralta weigh station off of state highway 91 (29). The adaptations designed for the 1997 study were used in this work.

It is important to discuss the different fuel ignition processes, as they will directly influence the composition in the engine-out exhaust. Heywood (30) presents a very detailed discussion of internal combustion engine processes. Spark ignition, which is predominantly used for gasoline light-duty vehicles, is accompanied by an injection of a

pre-mixed volume of fuel and air into the combustion cylinder where it is compressed and then is ignited by a high voltage spark. Gasoline is mainly composed of shorter carbon chains than other hydrocarbon fuel, around 5-12 carbon atoms per molecule, and is generally a mix of alkanes, cycloalkanes, aromatics and alkenes. The composition of gasoline renders it more vulnerable to knocking if certain constraints are not in place for proper combustion. Knocking is a combustion phenomenon where the fuel-air mixture will combust spontaneously as a result of adiabatic compression and prior to the spark. Knocking is very sensitive to chemical make-up of the fuel and its corresponding response to the high temperatures and high pressures found in the engine cylinder. One way to reduce these high temperature and pressures is to reduce the compression ratio of the cylinder. The compression ratio is the ratio of the volume of the total cylinder to the volume of the cylinder when the piston is at Top Dead Center (TDC). Spark ignition engines will therefore have a lower compression ratio, in order to lower the temperature of air that is compressed. Compression ratios for spark ignition engines are commonly around 10. The pre-mixed fuel that is injected into the cylinder is well controlled and maintained at the stoichiometric ratio for combustion using the free oxygen in air as the oxidant. For gasoline, a typical mass-based value for the stoichiometric air/fuel ratio is about 14.6.

Compression ignition is used for diesel fuel. Unlike spark ignition, compression ignition initiates combustion by only providing fuel when combustion should be initiated and using high temperature and pressure from previously compressing a

stoichiometrically excess amount of air into the cylinder. Relative to gasoline, diesel fuel has longer carbon chains which can get as high as 28-30 carbon atoms per molecule. In a compression ignition engine the diesel fuel is directly injected as a spray into the combustion cylinder, usually just before the piston reaches TDC. This process does not achieve a uniform air/fuel distribution since the reactants are not pre-mixed like spark ignition. Since there is no spark to initiate combustion, compression ignition relies solely on the injection timing and high temperature (~800 K) and pressure (~4 MPa) and takes advantage of larger compression ratios to reach these conditions. Typical compression ratios for compression ignition engines can achieve values in the low twenties.

An important pollutant formed during combustion for both spark and compression ignition is NO_x . For vehicular pollutants, NO_x is defined as the sum of NO and NO_2 present and the NO is commonly converted into the same units of NO_2 using molecular weight as an adjustment factor. For both spark and compression ignition systems NO is the main component of total NO_x emissions. Nitric oxide formation in engine cylinders is very complicated and dependent on temperature, fuel mixing and air/fuel ratio. All of these dependencies can vary between spark and compression ignition and different concentrations of NO and NO_x are produced. High temperatures and pressures are produced ahead of the flame front from the initial combustion inside the cylinder and these increase the reaction rates for the NO production pathways (31). Compression ignition will generate more NO, relative to spark ignition, under normal operating conditions and the NO_2/NO ratio can achieve values up to 30% for lighter loads(32,33).

Diesel combustion is always lean and often high temperature; therefore HDDVs have been the dominant source of on-road NO_x emissions. Recently some alternative fuels, such as natural gas, have been used for newer trucks; many remain operated at very lean air to fuel ratios (A/F). Carbon monoxide (CO) and hydrocarbon (HC) emissions from HDDVs are almost always low for the same reasons they have higher NO_x . Newer emission controls for HDDVs are expected to be responsible for large reductions of NO_x and particulate matter (PM). PM reduction from newer vehicles can arise from both fleet age turnover and the use of diesel particle filters (DPF) on newer trucks.

Diesel trucks have various ways of controlling exhaust pollutants of which NO and PM are the major pollutants of concern as the lean burning conditions of diesel engines produce little CO and HC. NO catalysis is difficult with oxidation catalysts in diesel vehicles because conversion efficiency of NO to N_2 is dependent on the presence of reducing species, mainly CO and HC, which are not in high enough concentrations under diesel combustion. Diesel PM, which is predominately soot, can be trapped with downstream diesel particulate filters (DPF), which then need to be cleaned. Diesel particles usually ignite around 500-600 Celsius which is above normal exhaust temperatures. DPFs are therefore usually accompanied with oxidation catalysts to convert NO to NO_2 and then use the NO_2 to oxidize the accumulated particles on the filter because this can occur at lower temperatures. Other methods of oxidizing diesel particles, such as fuel injection at the front of the filter, attempt to increase the exhaust

temperature to achieve the ignition. Lower temperatures of oxidation reduce damage to the catalyst and will increase the lifetime and are therefore more preferred.

An incentive program offered under the San Pedro Bay Ports Clean Air Action Plan (CAAP) consists of up to 50% in monetary support for truck operators wishing to switch to alternatively fueled trucks (34). Two methods of burning liquefied natural gas (LNG) have recently been demonstrated for drayage trucks operating at the Port of Los Angeles. One method uses a dual-fuel mixture of LNG and a small amount of diesel. The fuel is ignited under compression, like a diesel engine, but the natural gas does not ignite efficiently like pure diesel. In this dual fuel, the small amount of diesel is injected under the compression stroke and the pre-mixed natural gas is ignited from the generated flame from the diesel. This lean burn LNG process produces similar exhaust pollutants relative to normal diesel exhaust (35). The second method uses a pre-mixture of vaporized LNG and air which is spark-ignited like a normal gasoline engine. The stoichiometric condition of this spark-ignited fuel uses a three-way catalyst to oxidize the CO and HC to CO₂ as well as to reduce NO_x to N₂ (36).

Only recently have some HDDVs been equipped with three-way catalysts (TWC) to comply with NO_x and PM emission standards. There is a potential disadvantage for trucks attempting to spark-ignite alternative fuels with TWC. The LNG supplies excess hydrogen across the catalyst and NO_x is further reduced to ammonia. This ammonia byproduct is not new as light-duty gasoline fleets produce the same phenomenon where the excess hydrogen is produced not by the fuel but by the water-gas shift reaction where

carbon monoxide and gaseous water under the right thermodynamic conditions make carbon dioxide and hydrogen. Bishop, *et al.* (26) found that the average California on-road light duty fleet emits 0.49 grams of ammonia per kilogram of fuel, and for the newest model years (MY) up to 60% of the fixed nitrogen species in the exhaust are emitted as ammonia, which is not currently a regulated pollutant.

A non-intrusive method for predicting future emissions of light-duty vehicles was implemented for vehicular model year 1996 and newer which monitors oxygen concentrations and other emission control conditions throughout the vehicle from the engine to the tailpipe. This monitoring system is controlled by an onboard diagnostics computer (OBD) and is currently in its second phase of operation commonly referred to as OBDII. This system is known to drivers by the “check engine” light. Studies of the functionality and accuracy of OBD in an Inspection Maintenance (I/M) program have been evaluated over the years (37-39). A recent study by the EPA on high-mileage vehicles evaluates the cost-effectiveness of the OBD system in an I/M program using the IM240 dynamometer test(40). The IM240 test collects the tailpipe emissions of a vehicle that is driven on a dynamometer for 240 seconds. A total of 153 vehicles were selected for this study that had been driven 100,000 miles or more. The ultimate goal of this study was to procure 300 vehicles and their published conclusions reflect results from the halfway point of the study. Repairs were performed on vehicles that exclusively had their malfunction illumination light (MIL) on; vehicles that failed the IM240 test but whose MIL was not illuminated; and vehicles that failed their Federal Test Procedure

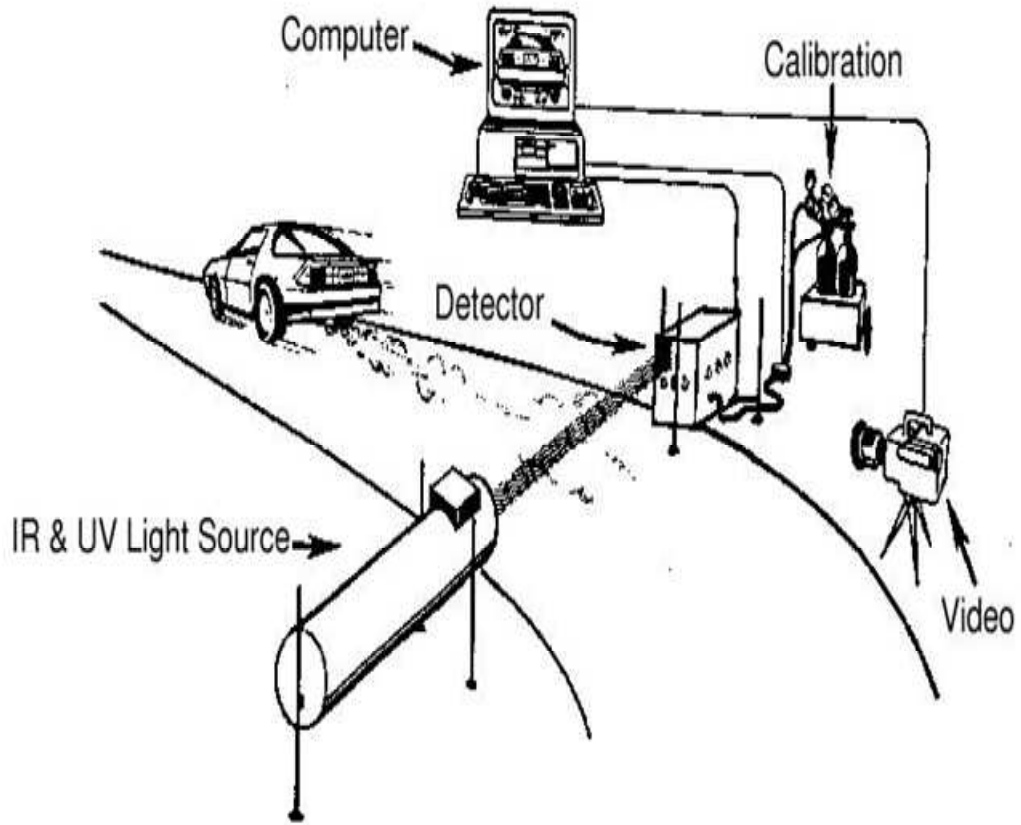
(FTP) with emissions that exceeded the full-useful-life standards by greater than 50%. Of the 153, 54 were chosen for repairs based on illuminated MILs (46) or failed IM240 cycles (8). It was concluded that air quality benefits from an OBD test are greater than those identified by an IM240 cycle. Quantitatively, the IM240 cycles captured 75-88% of the identified emissions by OBD. However, the emissions benefits of the OBD program were the result of repairing 30% of the sampled fleet (46 vehicles) and the emissions benefits of the IM240 program were the result of repairing only 5% of the sampled fleet (8 vehicles). The cost of repairs per vehicle for the OBD program averaged \$453 while the cost of repairs for the IM240 program were 30% less at \$316. The overall cost of the OBD program to repair identified broken cars was a little over 8 times the overall cost of the IM240 program.

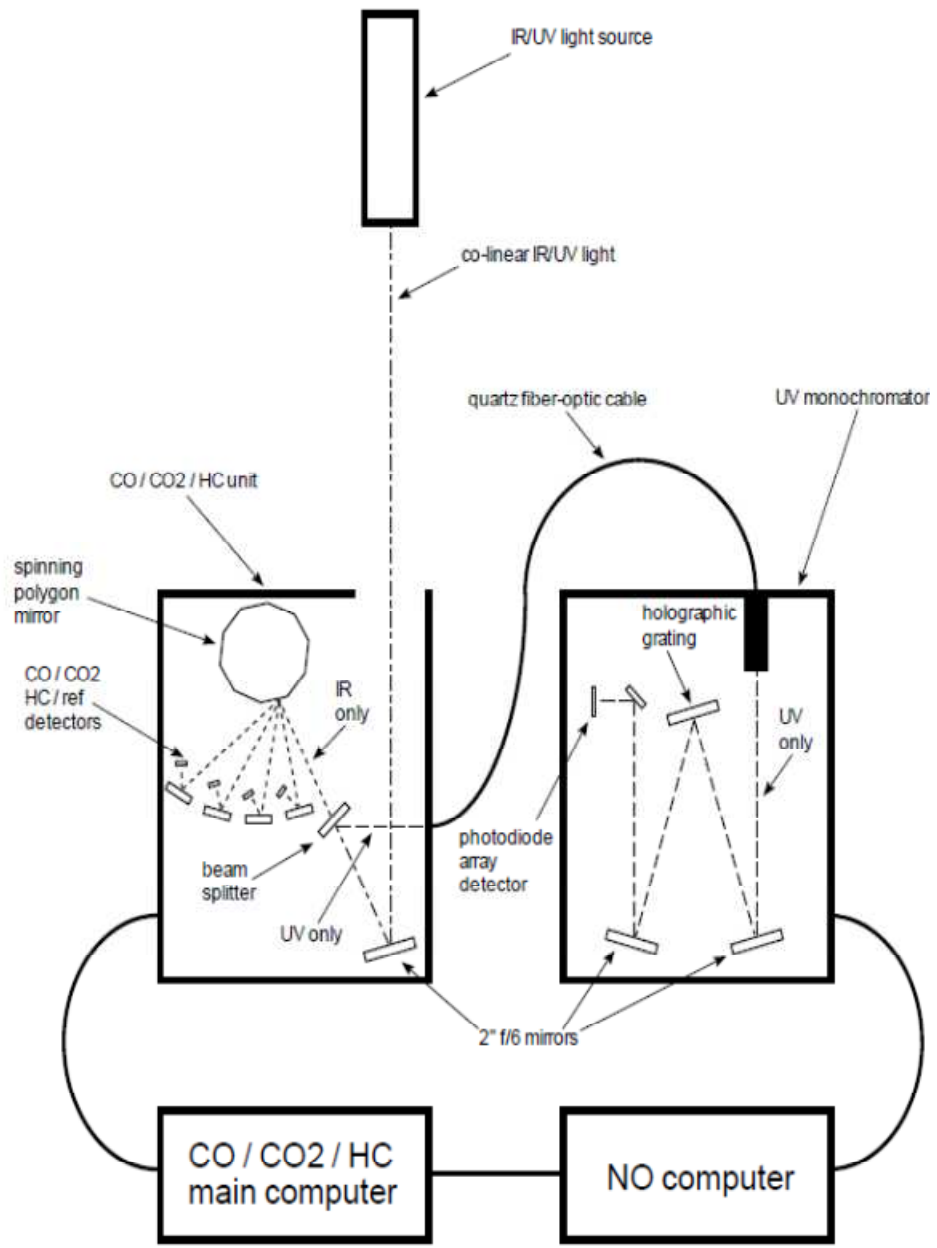
Instrumentation

Remote Sensing Detector (RSD)

There were two RSDs used in these experiments. The first is the University of Denver's Fuel Efficiency Automobile Test (FEAT) 3000 series. The second is the commercially available Environmental Systems Products (ESP) RSD 4600 series. Both instruments use non-dispersive infrared (IR) spectroscopy to measure carbon monoxide (CO), hydrocarbons as propane (HC), carbon dioxide (CO₂) and smoke opacity (measured as absorbance at the reference wavelength). They also both use dispersive

ultraviolet (UV) spectroscopy to measure nitric oxide (NO). In addition to these measured species, the FEAT has the capability to measure ammonia (NH₃), sulfur dioxide (SO₂), and nitrogen dioxide (NO₂) by dispersive UV spectroscopy. The ESP instrument also measures smoke opacity in the UV at 230 nm, in addition to its smoke opacity measurement in the IR whereas the FEAT instrument only measures smoke opacity in the IR. In both instruments, collinear beams of IR and UV light are directed across the road and eventually reach a detector. The FEAT light source and the detector are placed on opposite sides of the road in different boxes. The on-road setup for the FEAT instrument is shown in Figure 1. The ESP instrument houses the light source and detector in the same unit and reflects the collinear beams off a retroreflective mirror. A dichroic mirror reflects the UV light into the spectrometer through a fiber optic cable. The IR light passes through the dichroic mirror and onto a spinning polygon mirror. The spinning mirror reflects the IR light onto the four appropriate detectors, which are mounted with interference filters corresponding to the desired wavelength. This process enables all detectors to receive all of the signal part of the time rather than use beam splitters that reduces signal intensity. This process is shown in Figure 2.





RSD triggering and data collection for ground level exhaust

Both the FEAT and ESP instruments start their triggering process in the same fashion when measuring light-duty fleets. The ESP 4600 additionally waits for a large enough absorption of CO₂ to signal the start of the exhaust plume. As shown in Figure 1, the RSD instrument is placed on the road and the optical beam is situated roughly around the average height of ground level exhaust pipes. Absorbance is continually measured. As a vehicle passes through the RSD and blocks the optical beam the instrument records the absorbencies of each channel for 200 ms before the vehicle and then checks for the lowest reference voltage which is the zero offset. Once the optical beam is unblocked at the rear of the vehicle, the computer records data for 0.5 seconds and subtracts out the zero offset for all points. The computer interrogates the data for each channel, in the 0.7 seconds devoted to each vehicle, looking for the highest CO₂ voltage or the least polluted 10 ms data average. This is the Clean Air Reference (CAR). The 0.5 seconds of data are ratioed to the reference channel and then against CAR to correct for fluctuations in the optical beam. After data corrections, the data sets for each exhaust species are converted to pollutant path integrated concentrations and then ratioed against the CO₂ data set. These ratios are then used to calculate grams of pollutant per kilogram of fuel. Results can also be reported as expected exhaust concentrations using the combustion equation and correcting for excess oxygen and water vapor.

RSD triggering and data collection for high level exhaust

Data collection for exhaust plumes that do not originate near the ground (i.e. Heavy Duty Diesel Vehicles) can be difficult as exhaust pipes can vary anywhere between 9-13 feet above the road surface and 8-15 feet from the front of the tractor cab. Also, exhaust systems for these vehicles are not located at the rear but instead are located most likely on the passenger side of the tractor cabs. The tractors are usually hauling trailers with containers so an RSD programmed to wait for an unblocked optical beam will not work because the exhaust plume would have disappeared by the time the container exited the optical beam. In order to successfully measure on-road emissions of Heavy Duty Diesel Vehicles (HDDVs) two major things need to be considered, these are as follows; 1) a structurally sound scaffolding unit must be tightly fastened to the ground with guy wires to prevent misalignment of the optical beam, and 2) the trigger must be accurate to tell when the exhaust pipe is about to pass directly under the optical beam so the computer can begin data collection.

For the FEAT instrument, data collection begins as the front of the tractor cab passes a Banner infrared trigger placed down road from the optical beam. This distance will vary based on the speed of traffic. For speeds averaging five miles per hour this distance is about six feet. For speeds averaging fifteen miles per hour this distance is about twelve feet. Once the FEAT is triggered, data are collected for one second and not

the traditional 0.5 seconds. This change helps overcome the variability of both the speed and placement of the exhaust pipe on the tractor cab. The correction process and signal ratios are maintained for HDDVs data collection.

For the ESP instrument, data collection begins after a two step process. The first step involves the use of a laser trigger which is blocked by the front of the tractor cab and placed at a distance down road of the optical beam with the same conditions as the FEAT Banner trigger. After the ESP instrument receives a trigger block the computer will wait for a CO₂ absorbance above a certain threshold which is supposed to indicate the presence of an exhaust plume. Since the ESP instrument attempts to identify the front of the exhaust plume it still uses the 0.5 second data collection software.

Electrical Tailpipe Particle Sensor (ETaPS)

The data that were collected in West Virginia for the ICAT smoke correlation study utilized RSD, a gravimetric filter associated with chassis dynamometer Constant Volume Samplers (CVS), and the Electrical Tailpipe Particle Sensor (ETaPS). The theory, operation, and equations associated with the ETaPS are described elsewhere(41,42). Briefly, the ETaPS is an electrical charger creating an effective corona which is placed directly in hot, raw exhaust. There is a feedback loop monitoring the power required to maintain the corona as particles travel through the electrical field. The signal can be related to the active surface area of particles. Assuming a certain particle diameter, size distribution and flow rate one can obtain particle mass and concentration.

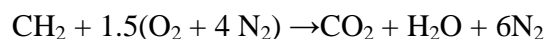
More effectively, when correlated to a dynamometer, the ETaPS will report in units of Volt*sec/milligram. Typical values are 0.5-1.0 Volt*sec/milligram depending on the driving cycle.

RSD Calculations

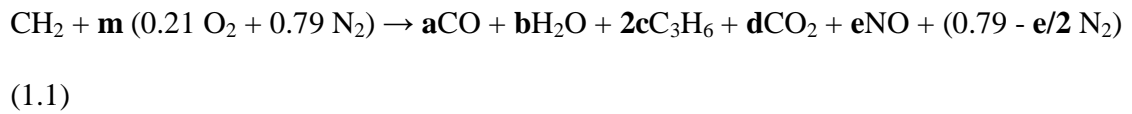
Assumptions

- Fuel is C:H ratio is 1:2 and is non-oxygenated (acceptable for gasoline and diesel)
- Exhaust is corrected for excess air not involved in combustion
- Fuel out tailpipe hydrocarbons have the same C:H ratio as fuel and is measured as propane using a certified calibration cylinder
- Equal amounts of seen and unseen hydrocarbons in the exhaust (43)

If a normal gasoline car with a proper air/fuel ratio completely converts fuel to carbon dioxide and water and we assume a simplified O₂:N₂ ratio the combustion equation becomes



However, using air as an oxidant in the combustion equation ultimately forms engine out nitric oxide (NO) under the high temperatures and pressures in the engine manifold. If a more accurate O₂:N₂ ratio is used and any unburned hydrocarbons in the exhaust are accounted for, the above equation becomes



The factor $2c$ comes from Singer *et al.* (43) findings that IR absorption at the wavelengths used for RSD detects only about half the carbon mass measured with a flame ionization detector. The hydrocarbon bandpass is centered at 2941 cm^{-1} with about a 140 cm^{-1} bandwidth to capture the absorption of C-H stretches from alkanes. Alkenes and aromatic C-H stretches are weak within this bandwidth or fall outside this range.

The three measured ratios of pollutants are then set against CO_2 .

$$Q = \frac{CO}{CO_2} = \frac{a}{d} \text{ or } a = dQ$$

$$Q' = \frac{HC}{CO_2} = \frac{c}{d} \text{ or } c = dQ'$$

$$Q'' = \frac{NO}{CO_2} = \frac{e}{d} \text{ or } e = dQ''$$

If equation 1.1 is balanced individually by carbon, hydrogen and oxygen then,

- Carbon balance: $a + 6c + d = 1$ (1.2)

- Hydrogen balance: $2b + 12c = 2$ (1.3)

- Oxygen balance: $a + b + 2d + e = 0.42m$ (1.4)

Substituting in the Q , Q' and Q'' ratios into equations 1.2-1.4, rearranging and simplifying

- Carbon balance: $dQ + 6dQ' + d = 1$ (1.5)

- Hydrogen balance: $b = 1 - 6dQ'$ (1.6)

- Oxygen balance: $dQ + b + 2d + dQ'' = 0.42m$ (1.7)

Substituting equation 1.6 into equation 1.7 yields

$$dQ + (1 - 6dQ') + 2d + dQ'' = 0.42m \quad (1.8)$$

Dividing by d from equation 1.8

$$Q + \left(\frac{1}{d}\right) - 6dQ' + 2 + Q'' = \frac{0.42m}{d} \quad (1.9)$$

Dividing equation 1.5 by d and rearranging yields

$$\frac{1}{d} = Q + 6Q' + 1 \quad (1.10)$$

Substituting equation 1.10 into equation 1.9 and dividing

$$Q + (Q + 6Q' + 1) - 6Q' + 2 + Q'' = \frac{0.42m}{d} \quad (1.11)$$

Simplifying equation 1.11

$$2Q + 3 + Q'' = \frac{0.42m}{d} \quad (1.12)$$

The mole fraction of CO₂ in the exhaust can be written

$$f_{CO_2} = \frac{d}{a+2c+d+e+0.79m-\frac{e}{2}} \quad (1.13)$$

Multiplying the numerator and the denominator both by (1/d) and substituting in the correct Q values

$$f_{CO_2} = \frac{1}{Q+2Q'+1+0.5Q''+\frac{0.79m}{d}} \quad (1.14)$$

Multiplying the numerator and denominator both by 0.42 and substituting equation 1.12 into the denominator yields

$$f_{CO_2} = \frac{0.42}{2.79+2Q+0.84Q'+Q''} \quad (1.15)$$

The mole fraction of CO₂ in the exhaust can now be calculated from the measured ratios of pollutants.

%CO₂ can be calculated by multiplying equation 1.15 by $\frac{100}{0.42}$

$$\%CO_2 = \frac{100}{6.64+4.76Q+2Q'+2.38Q''} \quad (1.16)$$

The other pollutants can also be calculated as percents by multiplying the appropriate Q value and the %CO₂. However it is a more likely practice to report RSD measurements in units of grams of pollutant per kilogram of fuel burned. To do this, the measured carbon species in the exhaust are used to back calculate the mass of fuel burned and the assumed fuel CH₂ has mass carbon fraction of 860 grams per kilogram of fuel.

For example, the calculation for gCO/kg of fuel is

$$gCO/kg \text{ of fuel} = \left(\frac{28gCO}{mole}\right) * \left(\frac{860gC}{kg}\right) * \left(\frac{mole}{12gC}\right) * \left(\frac{Q}{Q+6Q'+1}\right) \quad (1.17)$$

Reporting RSD measurements in this way is particularly useful because it makes no assumption about fuel density or fuel economy. Similarly, gHC/kg and gNO/kg are calculated using the appropriate Q values and molecular weights. There is a factor of 2 added to the numerator in the gHC/kg calculation to account for the hydrocarbons that are not seen by infrared absorption as previously stated.

$$gHC/kg \text{ of fuel} = 2 * \left(\frac{44gHC}{mole}\right) * \left(\frac{860gC}{kg}\right) * \left(\frac{mole}{12gC}\right) * \left(\frac{Q'}{Q+6Q'+1}\right) \quad (1.18)$$

$$gNO/kg \text{ of fuel} = \left(\frac{30gNO}{mole}\right) * \left(\frac{860gC}{kg}\right) * \left(\frac{mole}{12gC}\right) * \left(\frac{Q''}{Q+6Q'+1}\right) \quad (1.19)$$

If, for instance, natural gas is used instead of gasoline or diesel, then the formula for fuel becomes CH_4 . The appropriate scaling factors are used for detecting methane with IR absorption. Singer *et al.* (43) reports that NDIR will measure about half the carbon mass measured with a FID so a factor of two is used when calculating exhaust hydrocarbons as in equation 1.18. Singer *et al.* (43) goes on to report that NDIR is one third as sensitive measuring methane compared to propane when used in a remote sensor. This is, in large part, due to the interference filter at 2941cm^{-1} which does not capture the individual absorption lines of methane in that region of the electromagnetic field. Therefore, another factor of three is used in calculating exhaust hydrocarbons and the factor 2 in equation 1.18 becomes 6 and the denominator of the fourth term in equations 1.17-1.19 becomes $Q + 18Q' + 1$. The FEAT RSD still reports these hydrocarbons as propane units because propane is used as the calibration gas.

RSD Theory

Absorption Spectroscopy

The concentration of an unknown analyte can be determined using absorption spectroscopy. An analyte of any phase of matter can absorb electromagnetic radiation of specific frequencies that correspond to the analyte's excited states. These absorption spectra can be used as fingerprints to identify single compounds. In the case of vehicle

exhaust, it is possible to use narrowband interference filters, in the IR, as the compounds of interest absorb at different frequencies and there are hardly any other absorbing species that interfere at those frequencies.

Quantitatively, the resulting change in light intensity, I , can be ratioed to the incident light intensity, I_o , to determine % transmittance, %T, of the absorbing frequency.

$$\%T = \frac{I}{I_o} * 100 \quad (1.20)$$

The absorbance, A , of a sample is calculated from %T by

$$A = \log\left(\frac{I_o}{I}\right) = -\log(T) \quad (1.21)$$

Absorbance can be represented as a function of concentration, c , typically measured in parts per million (ppm) or molarity, the pathlength of the absorbing species, l , typically measure in cm, and the absorption coefficient, ϵ , which is an intrinsic measure of the species' cross-section to absorb a photon. The units of ϵ are such that allow A to be unitless. These factors are commonly shown in the Beer-Lambert Law or

$$A = cl\epsilon \quad (1.22)$$

For the purpose of remote sensing, which operates in an open pathlength mode, the pathlength of any given plume cannot be determined; therefore direct concentrations cannot be calculated. However, the combustion equation can be used to back calculate the grams of pollutant per kilograms of fuel burned by ratioing absorptions to all the measured carbon species in the exhaust as a measure of fuel as previously stated. This open pathlength is easily dealt with as the absorbed frequencies of light that reach the detector can be interrogated to measure the integrated plume from behind the vehicle or

the product of $c * l$ represented in units of ppm.cm. This integrated product is what is used to ratio against species representing fuel burned. This is a successful way to measure exhaust gases on-road because during the short residence time of the exhaust plume, behind a vehicle, the individual species present in the turbulent exhaust plume do not have sufficient time to separate during dilution.

2. Heavy-Duty Diesel Vehicles

Smoke Correlation of ETaPS/Dynamometer/RSD from HDDVs

Introduction

The University of Denver, in coordination with West Virginia University and the California Air Resources Board (CARB), conducted a six week study to correlate the smoke measurement capabilities between a RSD's on-road technique, a chassis dynamometer's gravimetric filter, and an Electric Tailpipe Particle Sensor's (ETaPS) electrical charging technique. Currently there is no Federal Test Procedure for HDDVs after the engine has been certified, and an inexpensive, less-time consuming test relative to a HDDV chassis dynamometer test would be very useful. The remote sensor used in this study, supplied by Environmental Systems Products (ESP), can measure % opacity in the UV and the IR in less than a second. The ETaPS has been shown to measure HDDV exhaust on-road under real driving conditions(41).

According to the original ETaPS ICAT project proposal, the goal statement was:

“Trucks with particle emissions which are significantly higher than they should be, need to be identified and repaired. If the outcome of the ICAT experiment is as positive as we hope, then we can imagine determination of “probable cause” using RSD, for instance as the vehicle accelerates from a stop at a weigh station. The trucks so identified could then be quickly instrumented and subjected to a road load ETAPS investigation, the outcome of which could be used to trigger enforcement action and calculate mass emission credits upon repair.”

The theory and model equations used for the ETaPS are found in the literature(41,42). Basically the ETaPS is a corona charger which is placed in raw exhaust, unlike dynamometer testing which dilutes incoming exhaust, and monitored with a feedback loop determining the power required to maintain the corona. The ETaPS literature indicates that the ETaPS voltage signal is linear to particle flux and particle surface area which, under certain assumptions about particle diameter and size distributions, one can relate the ETaPS signal to particle concentration. Since ETaPS is placed in raw exhaust, it has trouble seeing semi-volatiles that later condense on a much cooler gravimetric filter, thus some complications might arise from correlations studies of a hot ETaPS to cooler comparison devices.

Data were collected from eight unique HDDVs and two diesel transit buses. Five were pre-2007 MY with no diesel particle filter (DPF) and five were post-2007 MY equipped with functioning DPFs. The five post 2007 MY HDDVs were then re-tested after installing a bypass around the DPF to simulate a failed DPF. The bypass used a butterfly valve that was partially opened and tested prior to dynamometer runs as to not saturate the ETaPS voltage output. Each HDDV underwent testing of three different cycles on the chassis dynamometer; an Urban Dynamometer Driving Schedule (UDDS) transient to simulate urban driving, a Cruise cycle to simulate highway driving, and an Acceleration cycle to simulate intermediate emissions between the UDDS and Cruise cycles, which can be found in Pope's thesis(41). The complete list of number of runs for each test is shown in Table 1 and the complete list of the vehicles tested with average

readings is shown in Table 2. Exhaust %CO₂ measurements and Tapered Element Oscillating Microbalance (TEOM) measurements were also recorded. Each truck was also driven three or more times at three different speeds through the RSD for a total of 149 measurements. It was determined that the unshielded configuration of the mounted ETaPS on a HDDV was highly susceptible to power line interference and could not be used for the on-road portion of this study. This power line interference was examined back at the University of Denver and found that it could be avoided if the corona is placed inside a t-connector pipe that would shield it from any electric fields(41).

The United States Environmental Protection Agency (EPA) has recently mandated stricter emissions standards for on-road HDDVs(44). The standards are specifically for reduction of particulate matter (PM), non-methane hydrocarbons (NMHC), and oxides of nitrogen (NO_x). However, beginning in 2007 most diesel engine manufacturers opted to meet a Family Emission Limit (FEL) with EPA allowing engine families with FEL's exceeding the applicable standard to obtain emission credits through averaging, trading and/or banking. This will allow some diesel engine manufacturers to meet 2010+ standards with engines that do not meet a rigid NO_x limit of 0.2 g/bhp-hr subsequent to the 2010 model year.

In California the National EPA Highway Diesel Program is just a part of a number of new regulations that will be implemented over the next decade. The San Pedro Bay Ports Clean Air Action Plan (CAAP) enacted at the Ports of Long Beach and Los Angeles (34) banned all pre-1989 model year trucks starting in October 2008. For all of

the remaining trucks, it further requires them to meet National 2007 emission standards by 2012. This requirement applies to all trucks, including interstate trucks, which move containers into the South Coast Air Basin and beyond. The CAAP required by the end of 2009 that all pre-1994 engines be retired or replaced and all 1994 to 2003 engines must meet an 85% PM reduction and a 25% NO_x reduction (34). By the end of 2013, all drayage trucks, state-wide, must meet 2007 emission standards. This rule applies to all trucks with a gross vehicle weight rating of 33,000 pounds or more that move through port or intermodal rail yard properties for the purposes of loading, unloading or transporting cargo (45).

In addition, CARB's Statewide Truck and Bus Regulations will phase in most PM requirements for all trucks between 2012 and 2015 and will phase in NO_x emission standards between 2015 and 2023 (46). These regulations will dramatically alter the composition and emission standards of the current South Coast Air Basin's HDDV fleet. HDDVs are currently estimated to account for 40-60% of PM and NO_x emissions in the on-road mobile inventory (47,48).

Before advanced aftertreatment systems, control of NO_x and PM emissions were constrained relative to technologies that trade-off the control of these two pollutants. However, advanced control technologies deployed in the post-2007 timeframe for compliance with the U.S. EPA and CARB heavy-duty engine emission standards will not experience this trade-off. These advanced technologies will include a combination of diesel particle filter, selective catalytic reduction, and advanced exhaust gas recirculation

(EGR) control strategies. In addition, diesel fuel composition can play a role in emission reductions. The compositions are not studied in this research; however, by measuring sulfur dioxide (SO₂) emissions, we can infer the use of illegal high-sulfur fuels. Overall, understanding the expected impacts of future deployment of advanced emission control technologies will facilitate interpretation of data as it is generated throughout the course of this multi-year research project.

Truck	Bypassed?	Test			# Tests	# Runs
		UDDS	Cruise	Accel		
1995 Mack	N/A	3	3	1	3	7
1996 Peterbilt	N/A	3	3	1	3	7
1994 Freightliner	N/A	3	3	1	3	7
1999 Peterbilt	N/A	3	3	1	3	7
2005 Thomas Bus	N/A	3	3	0	2	6
2009 Thomas Bus A*	No	3	3	1	3	7
2008 Volvo A*	No	3	3	1	3	7
2008 Penske A*	No	3	3	1	3	7
2008 Volvo Day Cab A*	No	3	3	1	3	7
2007 Prostar A*	No	3	3	1	3	7
2009 Thomas Bus B*	Yes	3	3	1	3	7
2008 Volvo B*	Yes	3	3	1	3	7
2008 Penske B*	Yes	3	3	1	3	7
2008 Volvo Day Cab B*	Yes	3	3	1	3	7
2007 Prostar B*	Yes	3	3	1	3	7
* denotes DPF equipped					44	104

Truck	MY	DPF	PM	ES2	UV
Mack	1995	N/A	0.266	84.3	0.258
Peterbilt	1996	N/A	0.449	306	0.213
Freightliner	1994	N/A	0.297	243	0.559
Peterbilt	1999	N/A	0.469	295	0.145
Thomas Bus	2005	N/A	0.350	222	0.200
Thomas Bus A	2009	Non-Bypassed	0.006	1.01	N/A
Volvo A	2008	Non-Bypassed	0.008	1.37	0.018
Penske A	2008	Non-Bypassed	0.007	0.94	0.021
Volvo Day Cab A	2008	Non-Bypassed	0.007	0.80	0.017
Prostar A	2007	Non-Bypassed	0.012	0.85	-0.081
Thomas Bus B	2009	Bypassed	0.150	133	N/A
Volvo B	2008	Bypassed	1.106	92.6	0.037
Penske B	2008	Bypassed	0.070	118.	0.080
Volvo Day Cab B	2008	Bypassed	0.074	47.00	0.031
Prostar B	2007	Bypassed	0.168	105	0.132

PM- PM (g/mile)

ES2- ETaPS Signal (volt sec/mile)

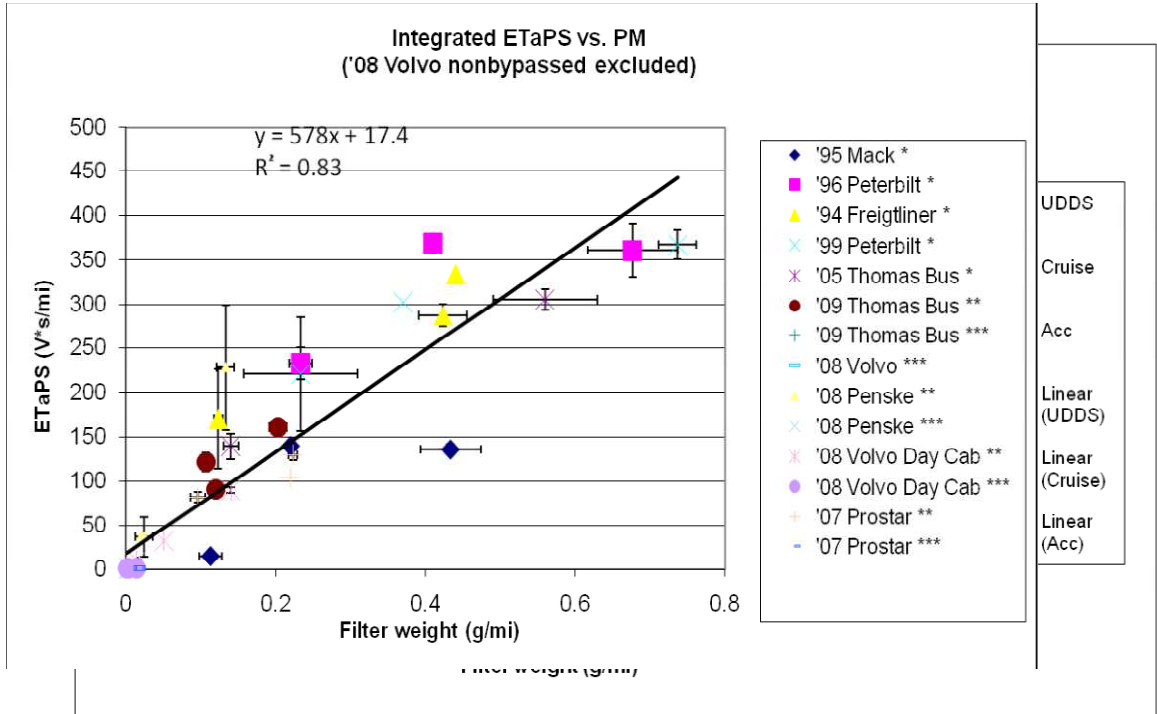
UV- UV smoke factor (Sec. 1)

ETaPS Results

The full, detailed results can be found in Pope's thesis (41). This section will outline the summarized results as well as a description of the mounting process of ETaPS on elevated exhaust pipes.

ETaPS shows correlations with r^2 between 0.83 and 0.98 against a gravimetric filter for each driving cycle be it UDDS, cruising or accelerating. Of the trucks tested, only one a 2008 Volvo did not express the same correlations as the rest of the tested fleet. Upon further examination, the ETaPS readings for the 2008 Volvo were much lower as a result of higher concentrations of hydrocarbon semi-volatiles that condense later on the cooler gravimetric filter. No further analysis was performed to determine why the 2008 Volvo was emitting higher hydrocarbon semi-volatiles. These hydrocarbon readings ranged anywhere from 4-20 times higher than the average of the rest of the tested fleet. As a result the 2008 Volvo was then removed from further analysis to determine the correlations for the rest of the fleet. Distance based ETaPS signal (Volt*sec/mile) correlates well with distance based gravimetric filter weight (g/mile) for all trucks and cycles with an r^2 of 0.83. Average readings were determined for each truck based on the cycle driven and are shown in Figure 3. Error bars represent the standard deviations of each averaged data point. Emissions are cycle dependent and as expected so are the correlations. Figure 4 shows the same data from Figure 3 separated by cycle. Even though the data have been divided into smaller groups the correlations are better for two

of the cycles (Cruise and Acc) and the same for the third (UDDS) compared to the overall correlation.



ETaPS did not correlate very well with remote sensing due to large electrical interference caused by overhead power lines above the RSD setup. As described below, the ETaPS was mounted on elevated exhaust in an open configuration. This configuration places the corona of the ETaPS just at the opening of the exhaust pipe. In a conventional ETaPS configuration the corona is inserted into a T-connector adapter which effectively shields the corona from any outside electrical interference.

The apparatus used to mount the ETaPS consists of a metal rod with Y-shaped metal holder where the ETaPS body sits. This Y-shaped piece can rotate 0-90 degrees against the vertical and is the main reason why this apparatus can accommodate any exhaust pipe. Elevated exhaust pipe openings can vary in dimension and angle therefore it is important for the ETaPS to be able to adjust to whatever exhaust pipe it encounters. The base of the ETaPS has slide adjusters screwed on both sides to support ETaPS weight and whatever configuration the ETaPS is in. U-bolts were fastened around the exhaust pipe and are attached to the metal rod with right angle clamps. The complete setup can take anywhere from 5-10 minutes depending if hand tools or power tools are used to secure the bolts. Figure 5- Figure 8 show the close up ETaPS apparatus before being mounted on an elevated exhaust pipe. Mounted ETaPS photos can be found in Pope's thesis(41).









Setup

At the Peralta Weigh Station, data measurements were made between the hours of 8:00 and 17:00 on the lane reentering Highway 91 eastbound (the Riverside Freeway, CA-91 E) after the trucks had been weighed. This weigh station is just west of the Weir Canyon Road exit (Exit 39). A satellite photo showing the weigh station grounds and the approximate location of the scaffolding, motor home and camera is shown in Figure 9. Figure 10 shows a close up picture of the measurement setup. The uphill grade at the measurement location averaged 1.8° . The hourly temperature and humidity data for the 2010 study collected at nearby Fullerton Municipal Airport are listed in Appendix A.

At the Port of Los Angeles, measurements were made between the hours of 8:00 and 17:00 just beyond the exit kiosk where truckers had checked out of the port. This location is just west of the intersection of West Water Street and South Fries Avenue. A satellite photo of the measurement location is shown in Figure 11 and a close up picture of the setup is shown in Figure 12. The grade at this measurement location is 0° .

The detectors were positioned on clamped wooden boards atop aluminum scaffolding at an elevation of 13'3", making the photon beams and detector at an elevation of 14'3" (see Figure 10 and Figure 12). The scaffolding was stabilized with three wires arranged in a Y shape. A second set of scaffolding was set up directly across the road on top of which the transfer mirror module (ESP) and IR/UV light source

(FEAT) were positioned. The light source for the RSD 4600 is housed with the detector in the instrument and is shone across the road and reflected back. Behind the detector scaffolding was the University of Denver's mobile lab housing the auxiliary instrumentation (computers, calibration gas cylinders and generator). Speed bar detectors were attached to each scaffolding unit which reported truck speed and acceleration. A video camera was placed down the road from the scaffolding, taking pictures of license plates when triggered.

At the Peralta weigh station, detection took place on the single lane at the end of the station where trucks were reentering the highway. Most trucks were traveling between 10 and 20 mph in an acceleration mode to regain speed for the upcoming highway merge.

The Port of Los Angeles testing site was located at an exit near the intersection of Fries Avenue and Water Street near Wilmington, CA. The exit has three lanes allowing trucks to leave (one reserved for bobtails), and the University of Denver's equipment was set up in Lane #1 about 30 feet down the road from a booth where trucks stopped to check out of the Port. At the Port location the trucks were accelerating from a dead stop generally not reaching speeds higher than 5 mph.









California HDDV Results

The five days of data collection using the University of Denver FEAT remote sensor at the Peralta weigh station in 2010 resulted in 2120 measurements that contain readable license plates. Plates were not read for the ESP equipment. While California plated trucks constituted the large majority of the trucks measured, there were 350 measurements from trucks registered outside of California. Table 3 details the registration, the total measurements and the number of unique trucks they represent. License plates were matched for California, Arizona, Washington, Texas, Oklahoma and Illinois trucks.

Data collected during the five days of measurements using the University of Denver FEAT remote sensor at the Port of LA site in 2010 resulted in 2109 license plates that were readable. The plates were not read for the ESP equipment at this site. There were only 146 out-of-state plated trucks measured at the Port. Table 4 details the registration, the total measurements and the number of unique trucks measured. License plates were matched for the California, Illinois, Texas and Arizona vehicles.

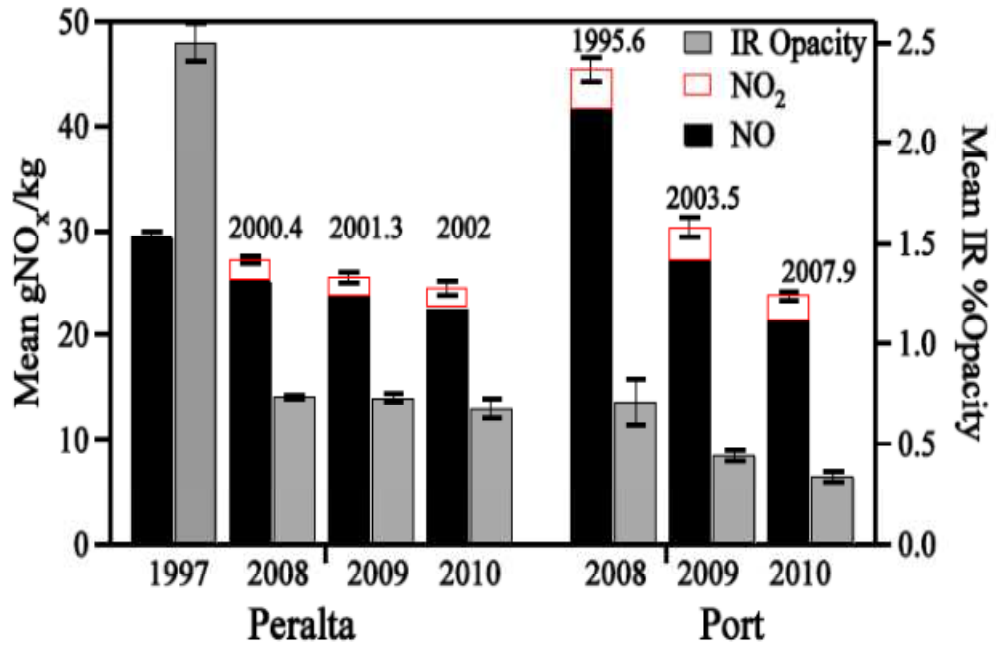
State / Country	Readable Plates	Unique Plates	Matched Unique Plates	Total Measurements
Alabama	3	3	0	0
Arizona	38	36	30	32
California	1770	1432	1420	1761
Colorado	1	1	0	0
Florida	4	4	0	0
Georgia	2	2	0	0
Iowa	5	5	0	0
Idaho	3	3	0	0
Illinois	45	41	41	45
Indiana	82	78	0	0
Kansas	2	2	0	0
Louisiana	1	1	0	0
Massachusetts	1	1	0	0
Michigan	2	2	0	0
Minnesota	6	6	0	0
Montana	3	2	0	0
North Carolina	11	11	0	0
North Dakota	2	2	0	0
Nebraska	4	4	0	0
New Jersey	5	5	0	0
New Mexico	2	2	0	0
Nevada	7	7	0	0
New York	1	1	0	0
Ohio	10	10	0	0
Oklahoma	21	17	16	20
Oregon	23	20	0	0
Pennsylvania	3	3	0	0
Tennessee	14	11	0	0
Texas	15	15	6	6
Utah	14	14	0	0
Washington	8	8	7	7
Wisconsin	4	4	0	0
Canada	8	8	0	0
Totals	2120	1761	1520	1871

State	Readable Plates	Unique Plates	Unique Matched Plates	Total Measurements
Arizona	29	17	7	8
California	1963	1103	1095	1956
Illinois	3	3	3	3
Indiana	54	40	0	0
New Jersey	1	1	0	0
Ohio	29	19	0	0
Oklahoma	7	2	1	2
Oregon	6	5	0	0
Texas	16	11	10	15
Utah	1	1	0	0
Totals	2109	1202	1116	1984

Table 5 provides a data summary of the previous and current measurements that have been collected at the two measurement sites. From 1997 to 2010 reductions in CO (34%) and HC (15%) and NO (23%) emissions have been observed at Peralta. License plates were not read and matched during the 1997 measurements, so we are unable to comment with any certainty on how fleet changes during the past twelve years may have contributed to these reductions. Figure 13 provides the year over year changes in NO_x and %IR opacity for both locations. The average fleet model year for each category is above each bar. The total NO_x bars are converted into NO₂ units and separated into NO and NO₂. The %IR opacity proportionality constant to mass based units is not well known but a 0.5% IR opacity corresponds to between 0.5 and 2 grams of soot/kg of fuel burned. Figure 13 shows how emissions have changed at the Port of Los Angeles over a two year interval. At Peralta, there has been a large reduction of PM since 1997 yet very little PM reduction over the last three years. Since license plates were not recorded in 1997 there are limited conclusions that can be deduced as why this large PM reduction is observed yet is not apparent for NO_x emissions. The little change in PM or NO_x emissions at the weigh station in Peralta can be attributed to the small change in average fleet age. Assuming that HDDVs behave similar to LDVs where average fleet age progresses one year newer for every measurement year, then the fleet of HDDVs measured in Peralta is actually getting older by 0.5 model year. Changes in emission reductions similar to those at the San Pedro Bay Ports are not observed further inland at the Peralta weigh station. This can be attributed to average fleet age and driving modes

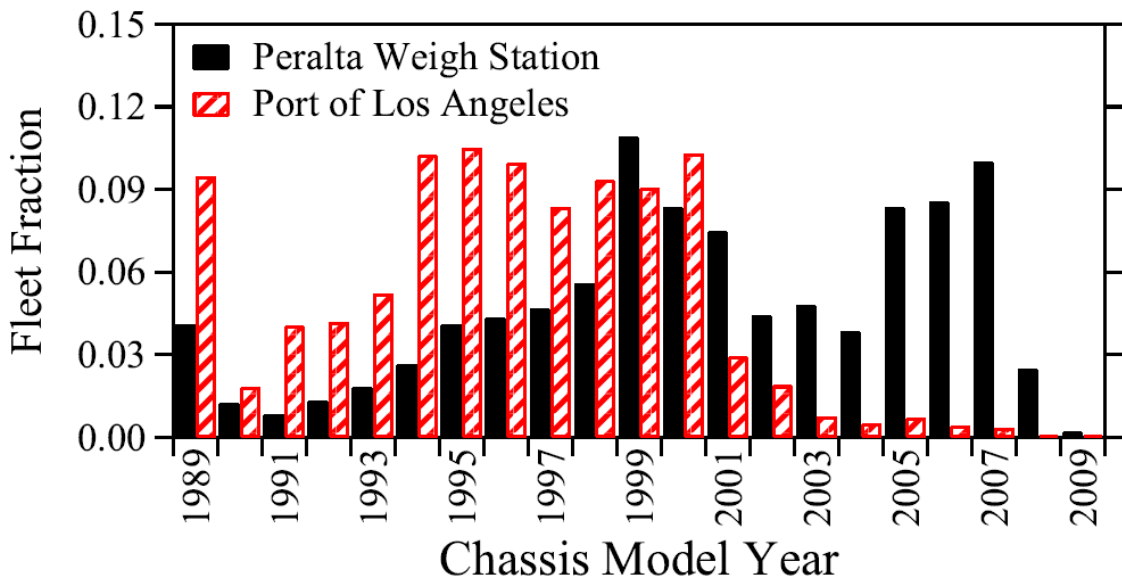
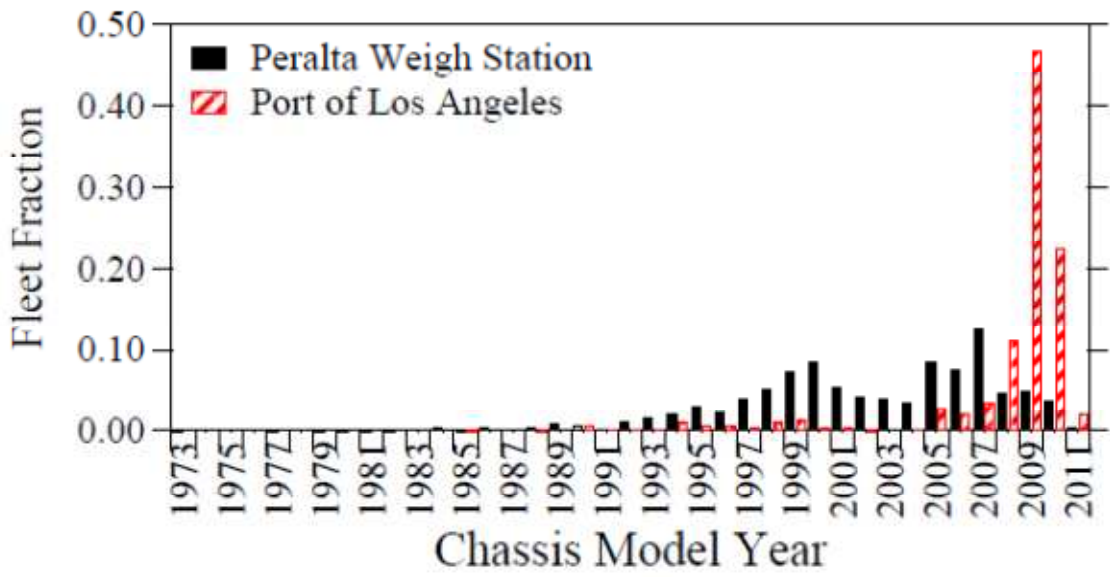
differences between the two sites. The lower speeds and higher loads, combined with possible colder starts from trucks leaving the port from multiple paper processing stations can lead to higher NO_x emissions because of the higher speeds of HDDVs leaving the Peralta weigh station. The NO₂ fraction of NO_x emissions at the port is increasing each year even though the total NO_x is decreasing. The large change in average model year in just a two year measurement interval is mainly responsible for the total NO_x reductions at the port. However, these newer trucks are intentionally making NO₂ to burn soot from their filters and as a result both locations have seen increased levels of NO₂ for newer model years. The higher speeds of trucks measured at Peralta results in lower NO_x emissions relative to the port, but Peralta has not yet had the same restrictions to force the fleet to turnover. It is unclear at this time whether or not the fleet emissions at Peralta will see similar reductions when new statewide regulations will force all on-road trucks to meet an 85% PM reduction and 25% NO_x reduction starting in January 2014 (34). If Peralta's fleet turnover behavior is similar to the port, then the average model year at Peralta should see a large change in 2014 and one would predict similar emissions reductions.

Location Study Year	Peralta 1997	Peralta 2008	Peralta 2009	Peralta 2010	Port of LA 2008	Port of LA 2009	Port of LA 2010
Mean CO/CO ₂ (g/kg of fuel)	0.008 (16.1)	0.005 (10.0)	0.005 (10.6)	0.005 (10.0)	0.006 (12.7)	0.004 (7.6)	0.005 (8.6)
Median gCO/kg	9.3	6.7	6.6	6.6	10.6	4.0	2.7
Mean HC/CO ₂ (g/kg of fuel)	0.0008 (5.0)	0.0004 (2.7)	0.0007 (4.8)	0.0007 (4.2)	0.0009 (5.3)	0.0009 (5.4)	0.0009 (5.2)
Median gHC/kg	3.7	2.1	2.9	2.9	4.2	3.3	2.5
Mean NO/CO ₂ (g/kg of fuel)	0.009 (19.2)	0.008 (16.4)	0.007 (15.4)	0.006 (14.7)	0.013 (27.1)	0.008 (17.7)	0.006 (13.6)
Median gNO/kg	18.0	15.2	14.3	13.5	24.8	14.9	12.4
Mean SO ₂ /CO ₂ (g/kg of fuel)	NA	0.00006 (0.26)	0.00004 (0.16)	-0.00004 (-0.22)	0.00004 (0.18)	-0.000004 (-0.016)	-0.00005 (-0.23)
Median gSO ₂ /kg	NA	0.22	0.11	-0.2	0.16	-0.003	-0.2
Mean NH ₃ /CO ₂ (g/kg of fuel)	NA	0.00003 (0.03)	0.00002 (0.003)	0.000007 (0.008)	0.00001 (0.02)	0.0002 (0.2)	0.0004 (0.4)
Median gNH ₃ /kg	NA	0.02	0.016	0.006	0.02	0.01	0.02
Mean NO ₂ /CO ₂ (g/kg of fuel)	NA	0.0006 (2.1)	0.0006 (1.9)	0.0005 (1.9)	0.001 (3.9)	0.001 (3.3)	0.0008 (2.5)
Median gNO ₂ /kg	NA	1.6	1.4	1.4	3.4	2.4	1.2
Mean gNO _x /kg	NA	27.3	25.4	24.5	45.4	30.4	23.3
Median gNO _x /kg	NA	25.2	23.6	22.3	41.7	26.1	21.9
Mean Model Year	NA	2000.4	2001.3	2002.0	1995.6	2003.5	2007.9
Mean Speed (mph)	NA	13.4	13.5	13.4	~<5	4.6	5.0
Mean Acceleration (mph/s)	NA	1.1	0.9	0.8	NA	0.5	0.5
Mean VSP(kw/tonne) Slope (degrees)	NA 1.8°	6.3 1.8°	5.8 1.8°	4.9 1.8°	NA 0°	1.0 0°	1.0 0°



Fleet composition and driving mode are again noticeably different between the two sites sampled in 2010. The Port of Los Angeles fleet is almost six years newer than the Peralta fleet and the measurements observe a high load, low speed acceleration as the trucks move away from the checkout gate. Figure 14 shows the fleet fractions (calculated by dividing the number of HDDV in each model year by the total number of HDDV vehicles in the database for that location) as a function of model year for Peralta and the Port in 2010. There has been a large and fast change in the average fleet age at the Port as part of the CAAP getting about 10.2 years newer over the two year interval 2008-2010. The average fleet age at Peralta has regressed getting about half a year older, not newer, over the same time period. The age distribution at Peralta shows that the fraction of model years 2008 and newer HDDV is very low compared to the Port. A higher purchase rate of 2007 HDDVs prior to the introduction of new technology engines combined with the national economic downturn in 2008 may have reduced the emissions reductions that otherwise might have occurred at the Peralta site. Figure 15 shows the fleet fractions for both sites in the 2008 measurement year. Note the difference in scale on the y-axis. In 2008, the fleet distribution is dominated by model years older than 2001. This distribution completely changes for the 2010 measurement year as the three newest model years make up over half of the fleet. Unlike the large fleet distributional changes at the port, the fleet distribution at Peralta the changes are slight. The bimodal distribution at Peralta is present in both measurement years with small increases in the newest model years.

The dramatic reductions in NO_x at the Port of Los Angeles can best be illustrated by comparing the emissions distributions from 2008 to 2010. Figure 16 shows fleet fraction versus binned gNO_x/kg. Each bin of gNO_x/kg reports the average of all NO_x emissions that are between that bin and the next highest bin. For example the 10 gNO_x/kg bin reports the average of all NO_x emissions that are at least 10 gNO_x/kg and less than 15 gNO_x/kg. The top plot shows the distributions for both locations in 2008 and the bottom plot shows the distributions for both locations in 2010. While there is some distributional change at Peralta with the lowest bin being more populated and depopulation of some higher bins over the two year interval, these are small when compared to the dramatic distributional shift observed at the port. While the influence of fleet age can contribute to the lower NO_x emissions observed at Peralta, the limiting factor is driving mode. The driving mode can be defined by many things which include; speed, acceleration, and load. Even when the fleet age at Peralta is normalized to the fleet age at the Port, the NO_x emissions at Peralta are still 27% lower in 2008. There were also 44 trucks that have been observed at both sites since 2008. These trucks account for 60 measurements at Peralta and 88 measurements at the port with a mean chassis model year of 2004.3. These trucks show 47% lower NO_x emissions at Peralta with the difference increasing with newer model year suggesting that driving mode is the main reason for the differences.



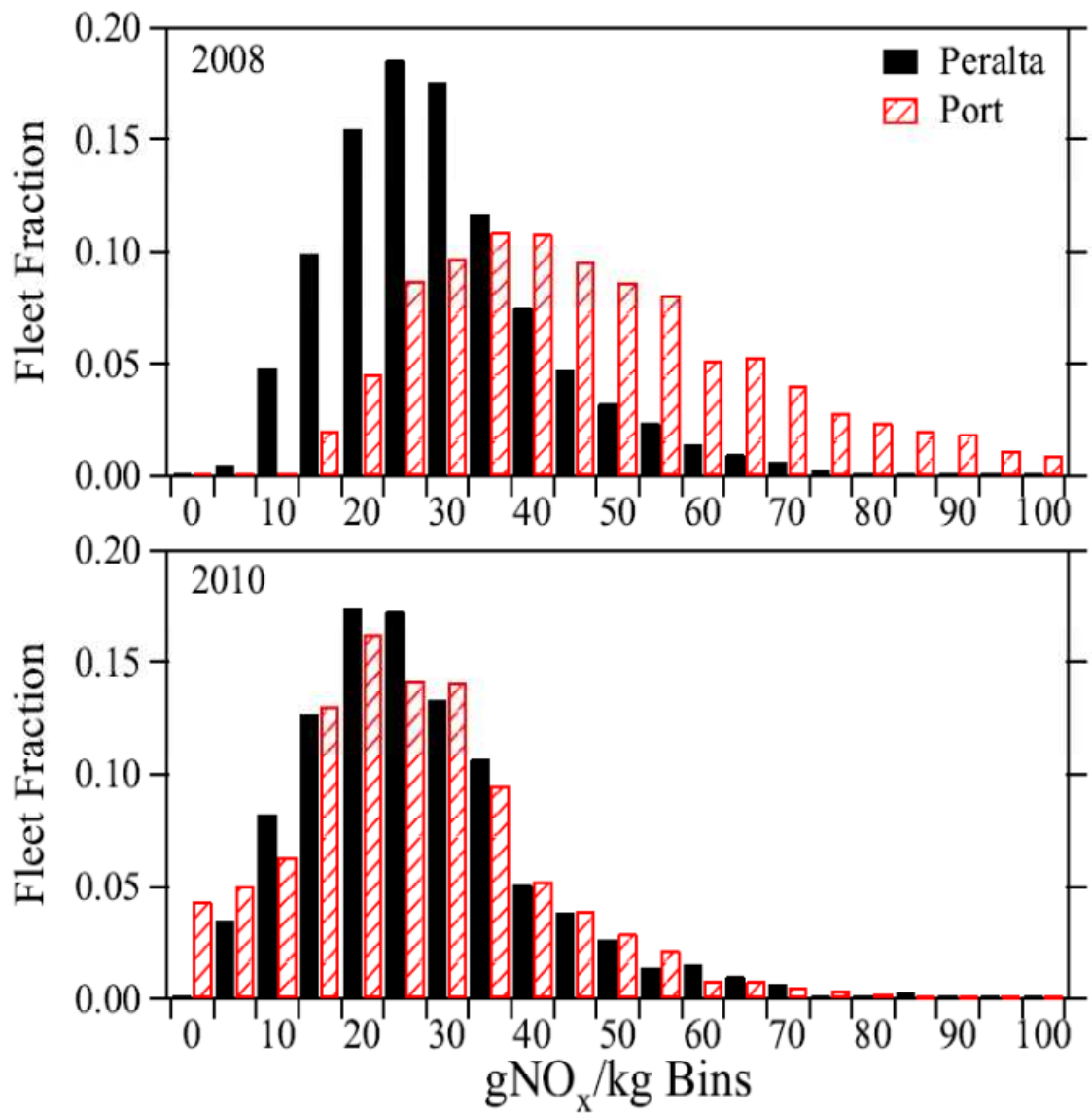
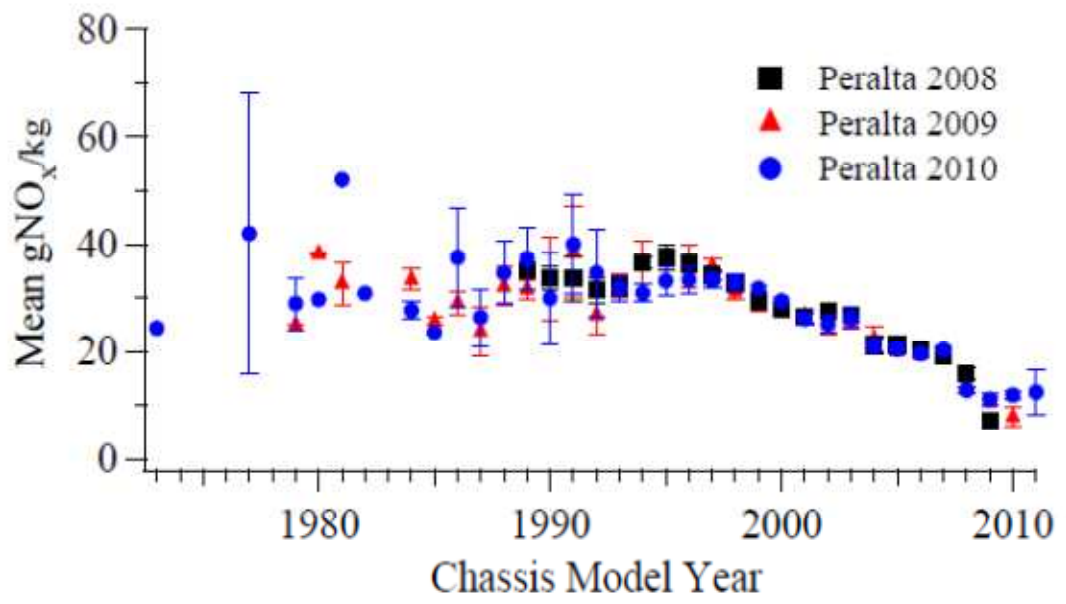


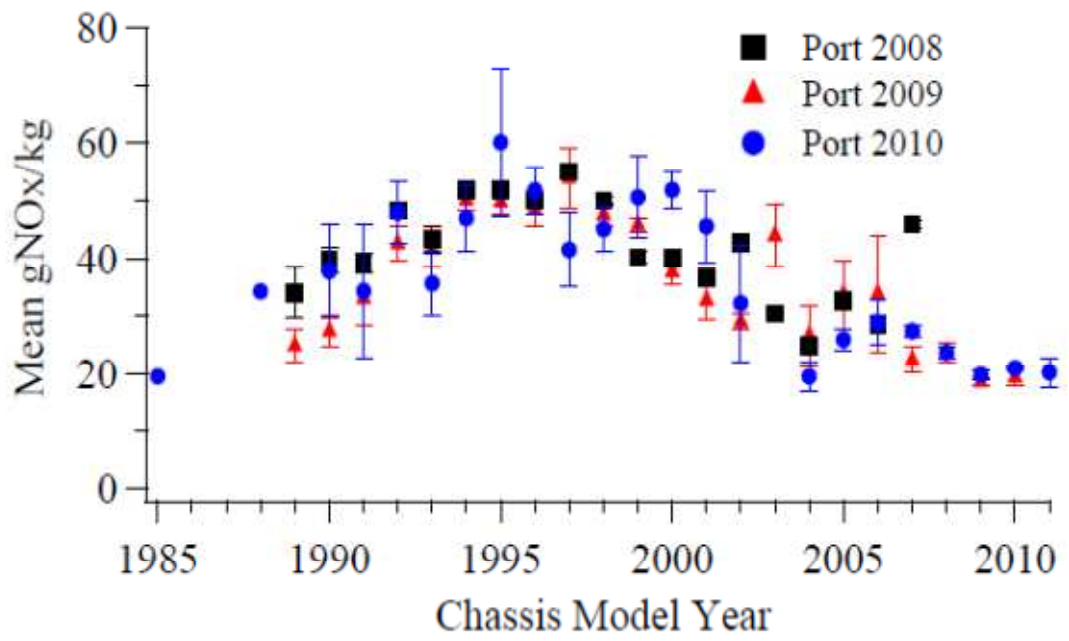
Figure 17 and Figure 18 plot mean NO_x emissions at both locations as a function of chassis model year for the measurement years 2008 through 2010. These are the only consecutive on-road HDDV measurements in the field taken from the same sites. Measurements at Peralta show good agreement for both years with decreasing mean NO_x emissions as a function of chassis model year. Measurements at the Port decrease as well but there are no comparative measurements for model years 2008-2010 taken in 2008. Figure 19 plots the cumulative fraction of NO_x emissions against the fraction of the fleet. In 2008 the distributions were nearly identical. For measurements made in 2009, there was a measurable separation of emission distributions with 10% of the Peralta fleet producing 20% of NO_x emissions and 10% of the Port fleet producing 24% of emissions. This difference was thought to be a result of the interjection of new trucks at the Port starting in 2009, but in 2010 the distributions are nearly identical which is similar to measurements in 2008. The NO_x emissions reductions in the new fleet are encouraging but the 2010 NO_x standard of 0.2 g/bhp-hr corresponds to about 1.3 g/kg well below the current observations.

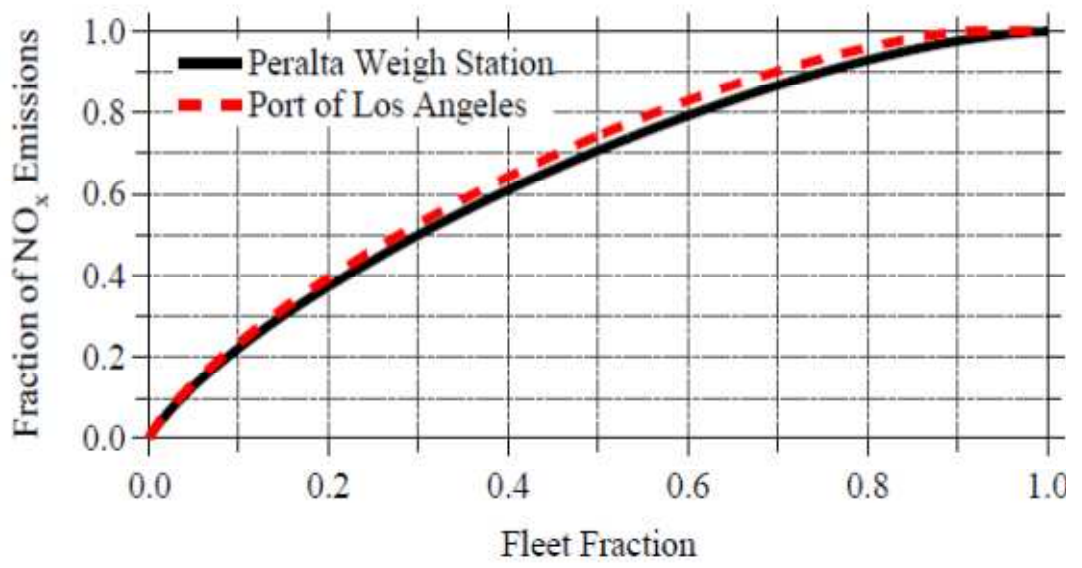
The National and California emission regulations that have targeted major reductions in PM emissions have been met with the introduction of diesel particle filters (DPF). Because these filters physically trap the particles, they require a mechanism to oxidize the trapped particles to keep the filter from plugging. One approach used to date has been to install an oxidation catalyst upstream of the filter and to use it to convert engine-out NO emissions to NO₂. NO₂ is then capable of oxidizing the trapped particles

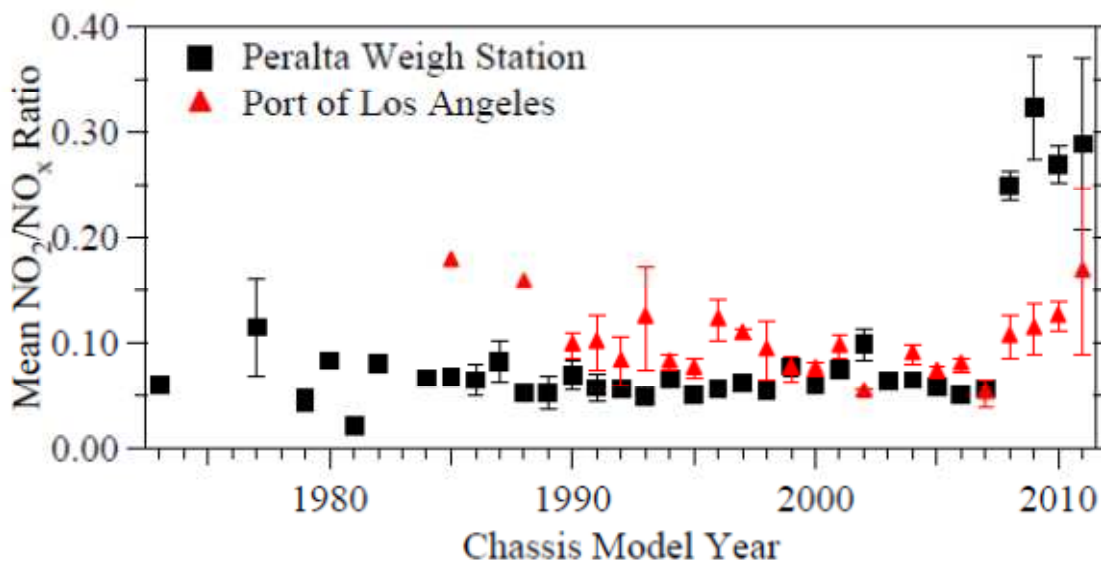
to regenerate the filter and is able to accomplish this at lower temperatures than is possible with other species. However, if the production of NO_2 is not controlled well it can lead to an increase in tailpipe emissions of NO_2 , and the unintended consequence of increased ozone in urban areas (49,50).

European experiences with increasing the prevalence of DPF's have shown a correlation with increases in urban NO_2 emissions(51). California has codified this concern by passing rules that limit any increases in NO_2 emissions from the uncontrolled engine baseline emissions for retrofit DPF devices(52). Nationally, new vehicle manufacturers are constrained with only a total NO_x standard that does not differentiate between NO and NO_2 emissions. Traditionally diesel exhaust NO_2 has comprised less than 10% of the tailpipe NO_x emissions; however this ratio has increased in the new trucks in some cases as high as 30%. Figure 20 presents on-road data for NO_2/NO_x ratio of HDDV emissions by model year. Nearly the entire fleet of the newest trucks (model year 2008-2011) have been fitted with one of these PM-reducing devices in accordance with the new EPA standards. The result is an observed increase in the NO_2/NO_x ratio in line with the expectation of increased emissions of NO_2 .



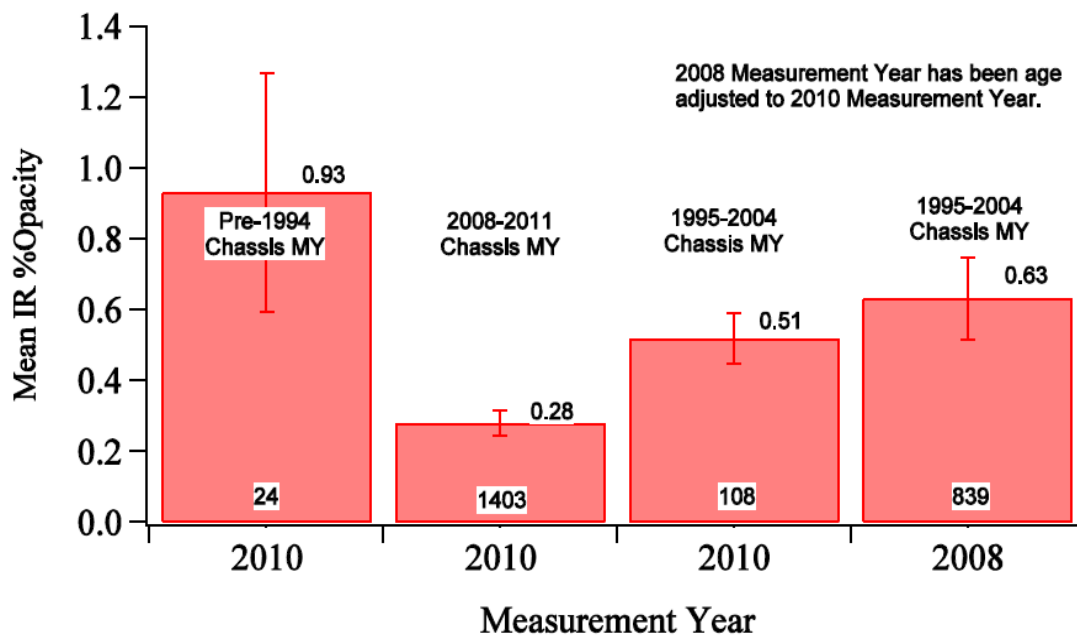
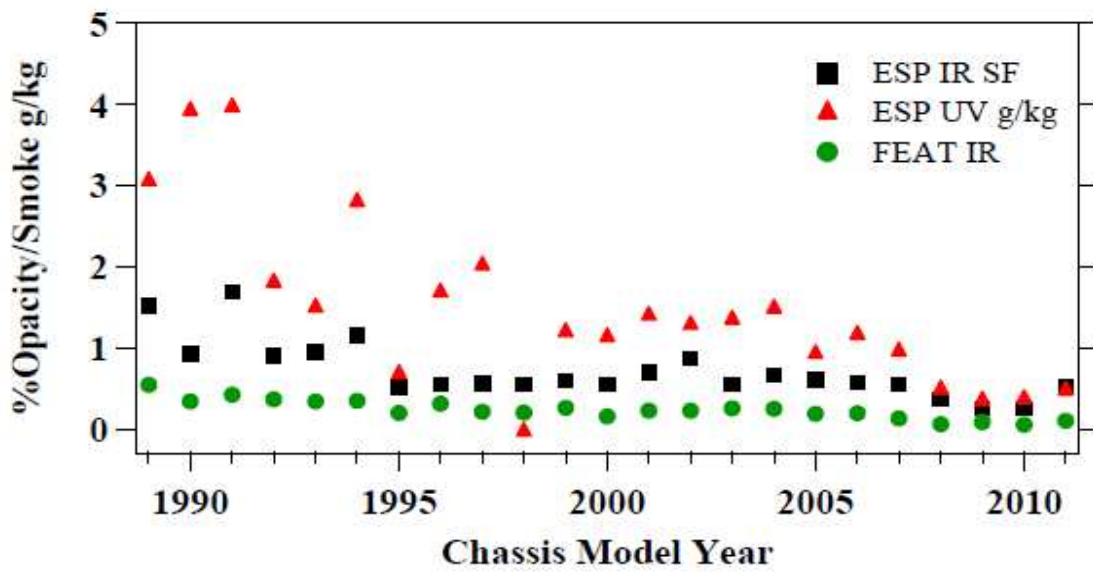






As the diesel particle filters are being phased into the fleet, we would expect to observe large reductions in PM emissions. Figure 21 shows the average PM emissions against chassis model year recorded by the two remote sensing systems for the combined datasets of both sites. Combining both sites PM emissions was decided after observing that the slope intercomparisons of the three measurement channels were identical for both sites. The FEAT system measures percent opacity in the infrared while the RSD 4600 reports a smoke factor value in both the infrared and the ultraviolet. A UV smoke factor of 0.1 is equivalent to 1 gram of soot per kilogram of fuel and the results presented here are in these units. As shown in Figure 21, decreased particle emissions are observed with both systems beginning with the 2008 model chassis. The PM standard of 0.01 g/bhp-hr translates to a cycle average of about 0.07 g/kg. The 2009 measurements showed that the newer model years were certainly approaching this value. The 2010 measurements continue to show low smoke values for the newer model years 2007-2011. An unintended result from the CAAP January 2010 deadline left truck operators with the choice of either retrofitting engine model year trucks 1994-2003 with DPFs to meet the 85% PM reduction or to purchase new trucks. One goal of the emissions analysis for the port was to see if these 1994-2003 engine model years show any reductions in %IR opacity as a measure of reduced PM. Figure 22 plots average %IR opacity for different chassis model year ranges in 2010 as well as a base comparator for chassis model years 1995-2004 measured in 2008. For the newest model years measured in 2010 the average %IR opacity is 0.28 with small uncertainty. This fleet of new trucks is statistically

distinguishable from the base case in 2008. This suggests that all 1995-2004 chassis model year trucks retrofitted in 2010 to meet an 85% PM reduction should also be distinguishable from the 2008 base case. This is not the case. The average %IR opacity for the 2010 retrofitted trucks is indistinguishable from the 2008 base case but is distinguishable from the newest model years measured in 2010. Upon further examination into why there is no observed %IR opacity difference, it was discovered that, of the truck operators that did not purchase new trucks, very few decided to retrofit their trucks. Instead, those trucks that did show up with chassis model year 1995-2004 were actually Class 7 trucks which were exempt from the new PM regulation. This effectively gives truck operators a free two year extension to meet the new regulations at the port until 2012 when all trucks must meet the 2007 EPA standard.



Another option for truck operators is to take their business elsewhere to other ports. In the summer of 2009, a two week study was conducted at the Port of Houston in Texas measuring trucks entering the port. This was the first such study at the Port of Houston. Three trucks that were registered in California in 2008 and measured at the Port of Los Angeles were observed operating at the Port of Houston in 2009. The two week Houston study resulted in 4,525 measurements with mean chassis model year 1998.8. The average speed and acceleration of trucks measured in Houston is similar to the average speed and acceleration of trucks measured in Peralta while the average vehicle specific power (VSP) is more in common with the Port of Los Angeles. VSP is a measure for the instantaneous power of an on-road vehicle. The proposed equation used is comprised of four terms calculating the work needed for a vehicle to climb the slope of the road, the work need to accelerate the vehicle, the estimated friction, and the aerodynamic resistance (53). VSP has the units kw/tonne and is calculated from the speed, acceleration, and road slope. Similar speed and acceleration suggest that the NO_x emissions should be similar between Houston and Peralta. Figure 23 compares the mean emissions of the fleets measured at the Peralta Weigh Station in 2009, the Port of Los Angeles in 2009 and the Port of Houston in 2009. The fleet ages for both California locations have been age adjusted to match the fleet age distribution at Houston and any difference in emissions observed can be attributed to driving mode. According to Figure 23, the mean emissions at the Port of Houston in 2009 are more similar to the mean emissions measured at Peralta in 2009. A closer examination reveals that both Peralta and

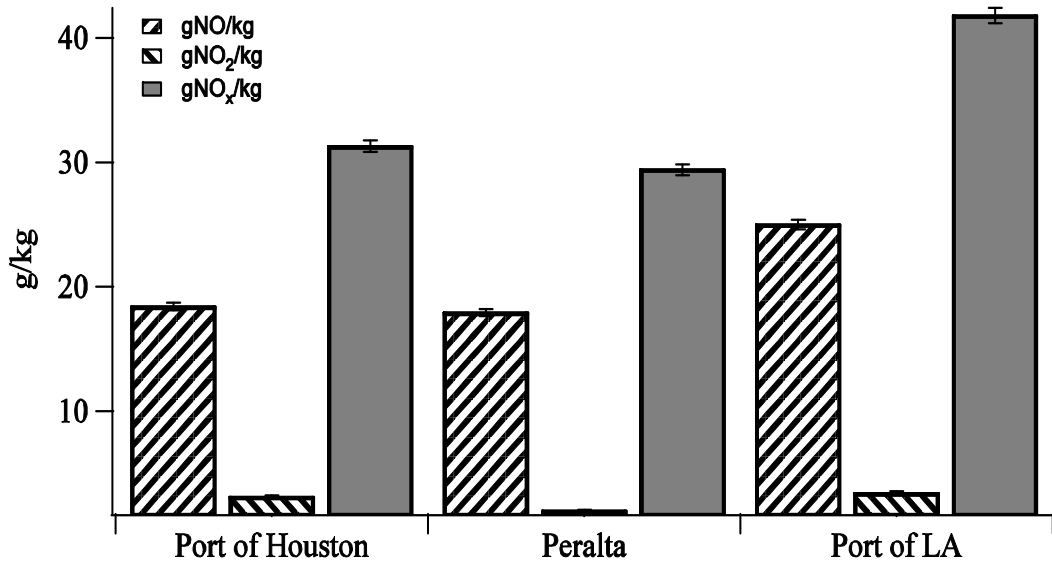
the Port of Houston have at least 25% lower NO_x emissions compared to the Port of LA site. Table 6 lists the measured exhaust species for the Port of Houston, Peralta, and the Port of LA in 2009. The uncertainties were calculated as standard error of the daily means for the Port of Houston measurements and the resulting percent error was then applied to the California means. Similar emissions between Houston and Peralta suggest that speed and acceleration are important contributors for total NO_x . However, NO_2 emissions at Houston are more similar to the Port of LA. Figure 24 shows gNO_2/kg emissions versus chassis model year for all three sites. It is important to distinguish the source of NO_2 emissions at Houston and the Port of LA. Starting at model year 1992, NO_2 emissions at Houston and at the Port of LA are significantly higher relative to Peralta. These mid-range model years, 1995-2003, contribute less than half of the NO_2 to the fleet average since these trucks only make up about 34% of the fleet at the Port of LA. The rest of the NO_2 at the Port of LA comes from newer trucks, 50% of the fleet were 2009 model year and newer and were equipped with a variety of control technologies. At Houston the largest contribution of NO_2 comes from these mid-range model years, 1995-2003, that make up 79% of the fleet. Figure 25 shows the NO_2/NO_x ratio for all three sites. There is a general trend starting with model year 1990, of increasing NO_2/NO_x ratio going from Peralta, to the Port of LA, and finally to Houston. For each site, there is at least a two-fold increase in this ratio for the newest model years. An unexpected result for these newest model years is that the ratios at Peralta are significantly larger than Houston and the Port of LA. For the newest model years at

Peralta, the apparent jump in NO_2/NO_x ratio is a result of much smaller NO emissions. Figure 26 shows NO emissions versus chassis model year for all three sites and what is most important is the larger reduction of NO for the newest model years at Peralta relative to Houston and the Port of LA. This NO reduction largely decreases the overall NO_x and effectively increases the NO_2/NO_x ratio.

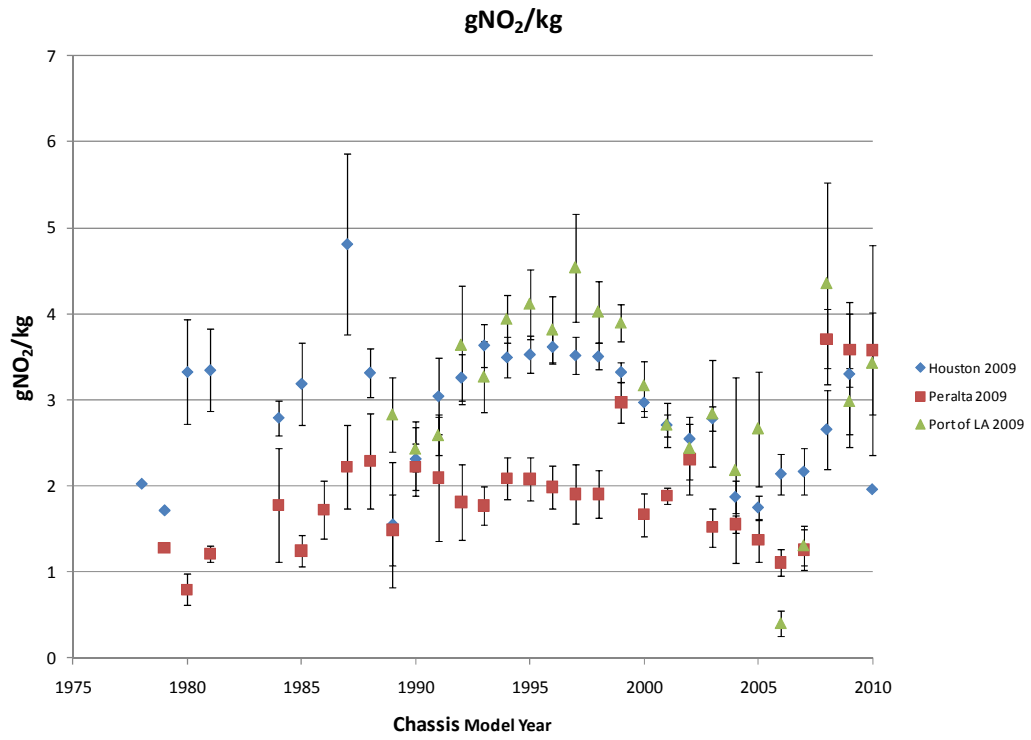
The data in Figure 27 show average NO_2 emissions from all three measurement years at Peralta binned by VSP. For all measurement years the two VSP bins 0 and 5, produce the highest average NO_2 . These bins contain VSPs from -5 to +5. Both the Port of LA and Houston have similar average VSP less than 2. Peralta, on the other hand, has an average VSP of almost 6. According to Figure 27, the larger average VSP of Peralta should produce less NO_2 than locations with lower VSP like Houston and the Port of LA. This result agrees with the literature that the fraction of NO_2 in diesel exhaust decreases with increasing load (54).

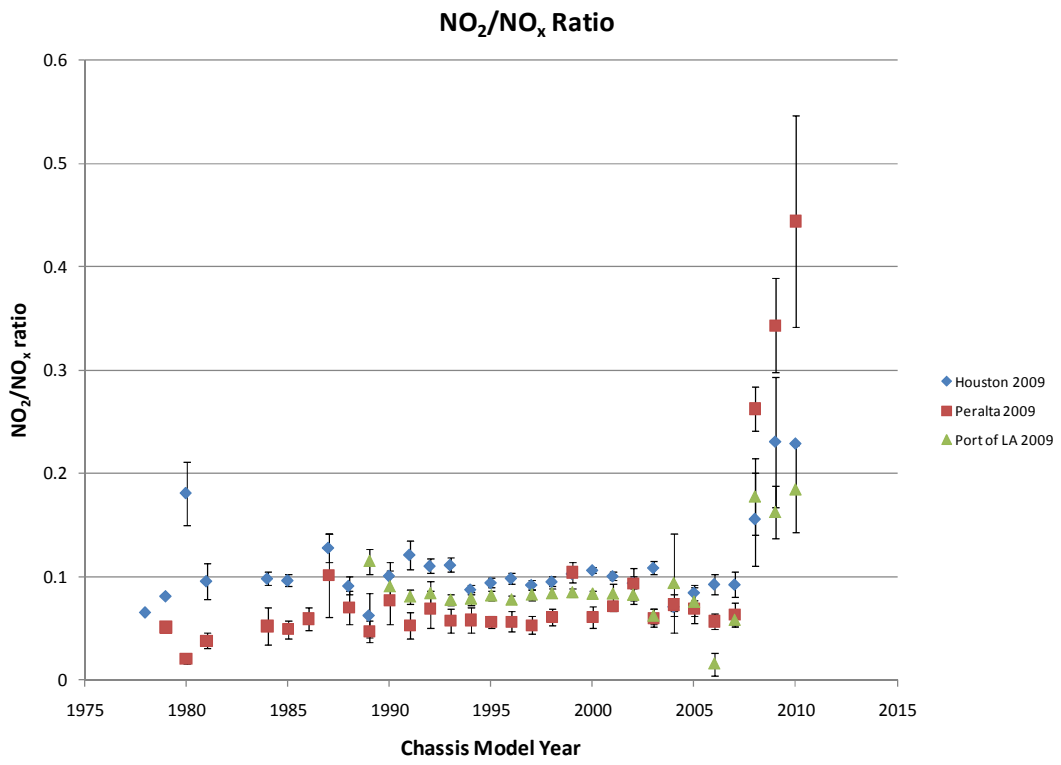
Smoke data measured as %IR opacity were also compared for the three different sites and are shown in Figure 28. Uncertainty bars were removed for Houston MY 2009 and Peralta MY 1991 because their N values (< 2) were small and the large uncertainties protruded so far into the negative portion of the y-axis that it distracted any observations for the whole figure. Starting with model year 1995, on average Houston trucks produce twice as much smoke than the Port of LA and Peralta. Each location does show a decreasing smoke trend for the newest four model years. However, the 2007 EPA PM

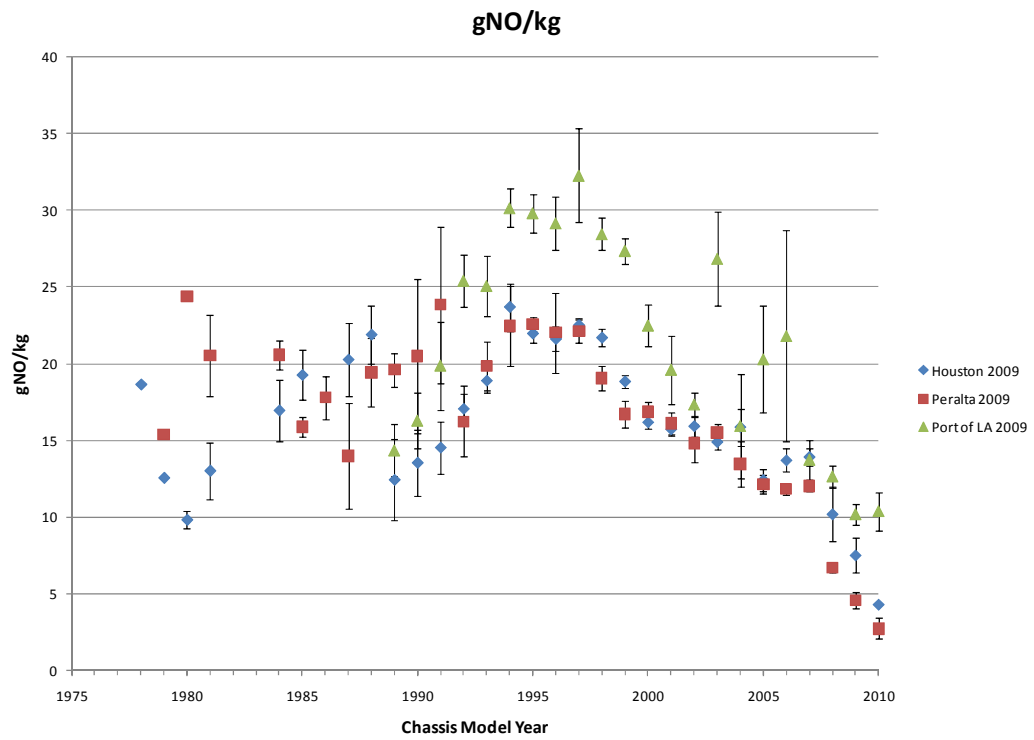
standard of 0.01 g/bhp-hr approximately translates to %IR opacity of 0.035. Even the newest MY trucks have room for improvement to meet the new PM standards.



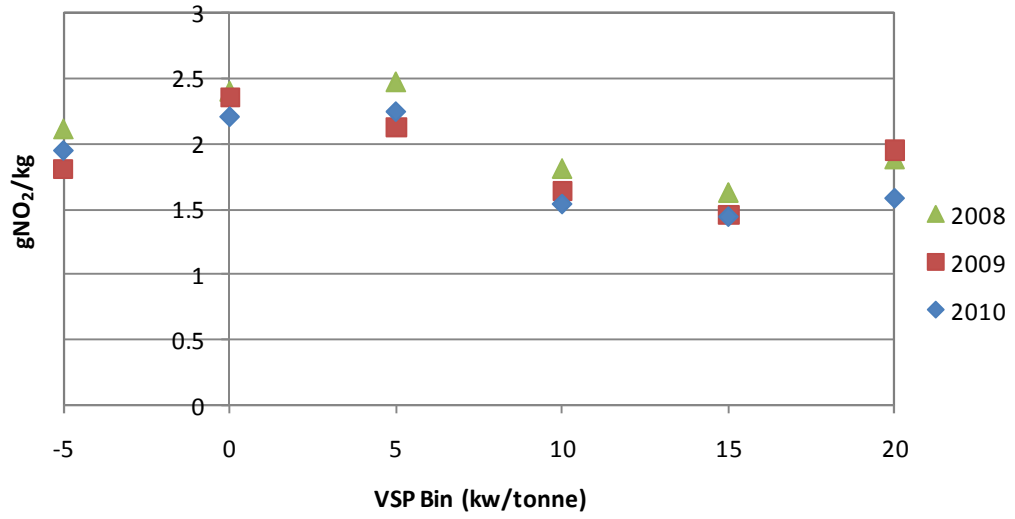
Location	CO_GKG	HC_GKG	NO_GKG	SO2_GKG	NH3_GKG	NO2_GKG	NOX_GKG
Houston 2009	14.0 ± 0.74	3.6 ± 0.36	18.4 ± 0.29	0.13 ± 0.073	0.04 ± 0.003	3.1 ± 0.12	31.3 ± 0.46
Peralta 2009(AA)	11.4 ± 0.6	4.9 ± 0.49	17.9 ± 0.27	0.19 ± 0.1	0.02 ± 0.002	2 ± 0.08	29.4 ± 0.43
Port 2009 (AA)	9.8 ± 0.52	5.9 ± 0.59	25 ± 0.4	0.014 ± 0.007	-0.001 ± 0.00008	3.4 ± 0.14	41.8 ± 0.61







Peralta



%IR opacity

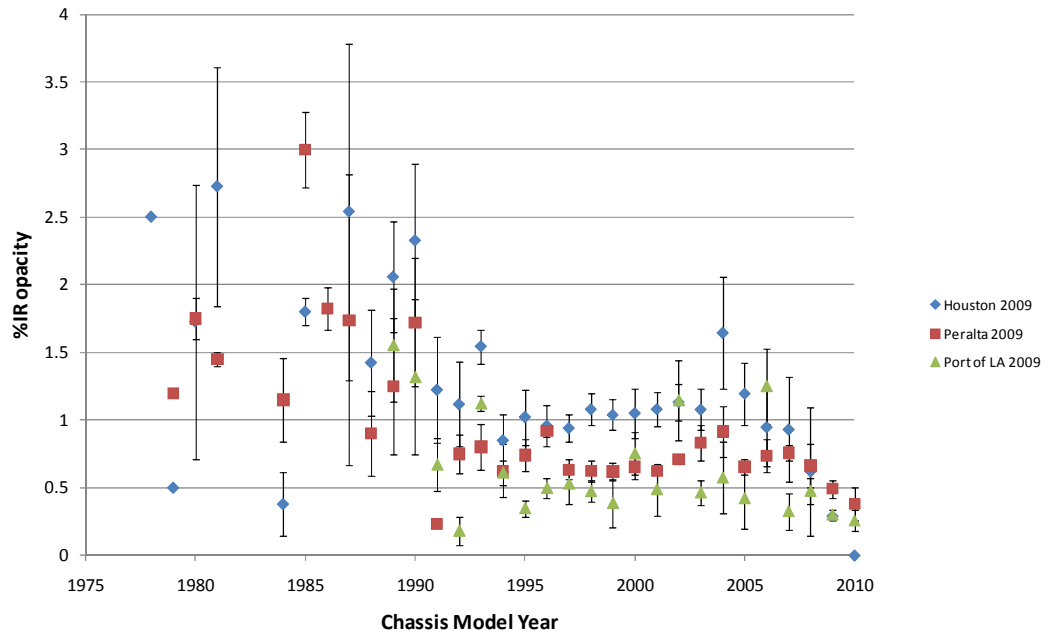


Figure 29 shows the cumulative smoke emission distributions from the 2010 California campaign for the three metrics and it indicates that the overall emissions distribution for smoke, at the combined Peralta and Port of LA sites, is not heavily skewed towards high emitters. The apparent emission fraction greater than 1.0 results from negative smoke readings that arise from measurement error and inherent emission variability.

Another goal of the research was to quantify ammonia emissions over the five-year period. Ammonia is a potential byproduct of methods to be implemented to reduce NO_x emissions in diesel trucks to meet the 2010 EPA standards. In a recent study on light-duty vehicles, Bishop *et al.* (26) found that the mean ammonia emitted by California cars to be 0.49 g/kg. These emissions come about as a by-product of NO reduction in the presence of hydrogen by three-way catalysts in the light-duty vehicles.

The 2010 measurements observed the same two types of vehicles, that were documented in 2009, at the Port which burn natural gas as their combustible fuel. The first was a group of Cummins ISL-G engines that have been installed in Sterling, Peterbilt and Freightliner trucks that are fueled with liquefied natural gas (LNG) and combust using spark ignition at nominal stoichiometry with a three-way catalyst. The second was a group of Kenworth vehicles with Cummins ISX engines fueled with LNG but operated under very lean air/fuel (A/F) ratio conditions similar to diesel engines with an oxidation catalyst. The Cummins ISL-G engine is a gasoline equivalent spark ignition engine combined with Exhaust Gas Recirculation (EGR). The EGR system takes a

measured amount of exhaust gas and passes it through a cooler to reduce temperature before mixing it with fuel and incoming air. This helps lower combustion temperature and is said to improve power density (55). These ISL-G engines have an average CO of about 48 g/kg, which is high compared to an average diesel HDDV CO reading of about 5 g/kg. These ISL-G engines are therefore operating rich of the stoichiometric air/fuel ratio. Under these circumstances, the methane does not completely burn and the catalyst can be overwhelmed by excess hydrogen. Ammonia is then an expected byproduct of the reducing conditions of the three-way catalyst where the excess hydrogen reduces NO to ammonia. Methane combustion is further discussed in the next section. The Cummins ISX engine is a dual fuel (diesel and LNG) compression ignition system that operates under very lean conditions. The oxidation catalyst serves to oxidize non-methane hydrocarbons, carbon monoxide and particles, but does not have the required reducing conditions to reduce NO to ammonia. By itself, methane combusts very poorly under compression ignition, and to ignite the premixed methane the Cummins ISX injects a small amount of diesel fuel to the cycle. This produces many tiny diesel droplets combusting in the cylinder and acting as flame ignition points for the lean methane air mixture. By comparison, the Cummins ISL-G has only one flame ignition point which is the spark plug.

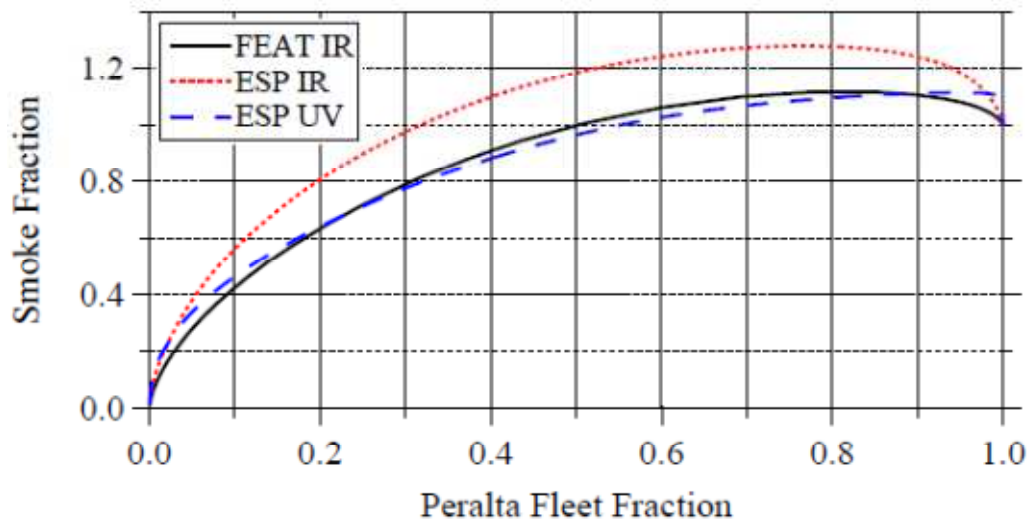
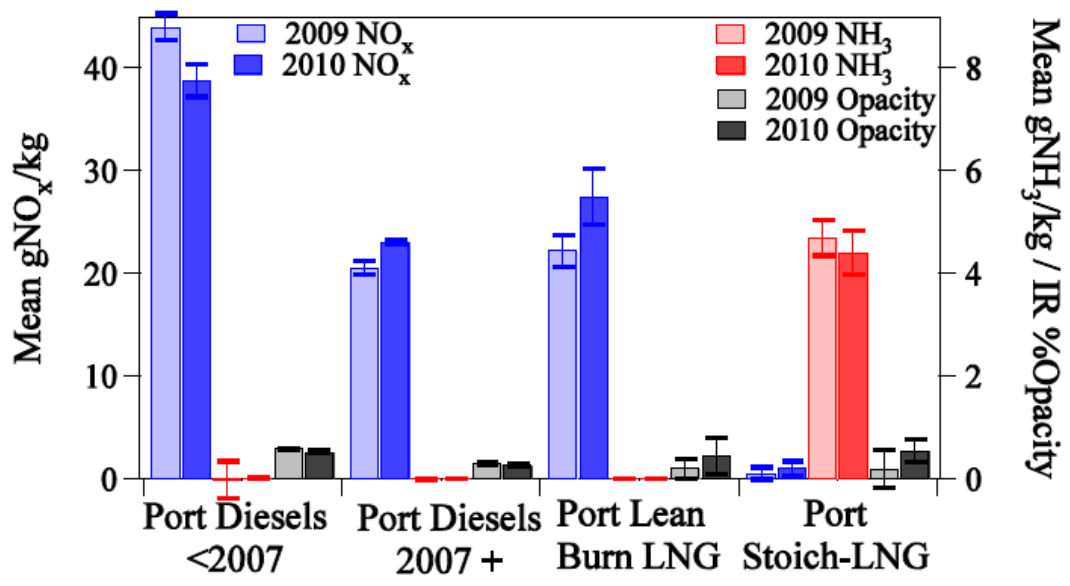


Figure 30 is a bar chart separating trucks at the Port into the types of fuel they burn and the corresponding mean emission for NO_x, ammonia and opacity. The lean burning natural gas NO_x and opacity emissions are similar to the similarly aged diesel emissions. The average opacity of the lean burn natural gas trucks is similar to the average opacity of diesel trucks of equivalent model year; however the average diesel opacity is distinguishable from zero while the lean burn natural gas trucks with much smaller N are indistinguishable from zero. On the other hand the stoichiometric burning natural gas emissions are very dissimilar than the other fuel types. They emit very little NO_x and PM but emit a very large amount of ammonia (~5g/kg). In 2010, the average PM for the stoichiometric natural gas engines is higher than the average for equivalent model years of diesel trucks. The 2007-2011 model years of diesel trucks are required to meet the PM standard of 0.01 g/bhp-hr and most trucks do so with a DPF. However, while diesel trucks use DPFs to reduce PM emissions natural gas engines do not utilize DPFs because they should have low PM emissions.



The use of 15 ppm ultra-low sulfur diesel fuel has been required by law in North America starting from September 2006 (56). An analysis of the 2010 SO₂ emissions from both locations, shows that the average for HDDVs in 2010 is -0.22 g/kg and that there are no high SO₂ emitters which were present in the Bishop *et al.* 2008 report (57). Figure 31 is a plot of all of the valid measurements from both locations in 2010. In this format it was easy to spot any outliers that may be using >15ppm or high-sulfur fuel. However, the 2010 measurements show no outliers compared to measurements taken in 2008. The SO₂ outliers that were present in 2008 are shown in Figure 32. The exhaust SO₂ of a truck using 15 ppm ultra-low sulfur fuel would be read as 0.03g/kg by a remote sensor.

Emission measurements were matched for trucks captured by both remote sensing devices with readable plates. Each day's database was compared, using the recorded photographs, to determine the time differences between the two data sets. After determining this difference it was possible to time align the two sets of measurements to within ± 1 second for the entire day's data. The readings were then manually matched with each other and any questionable matches were resolved using the video images.

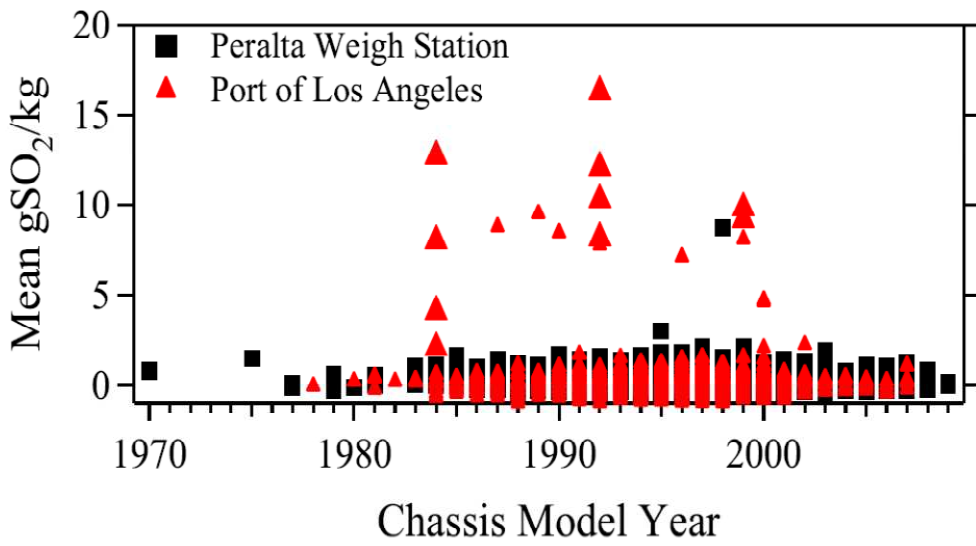
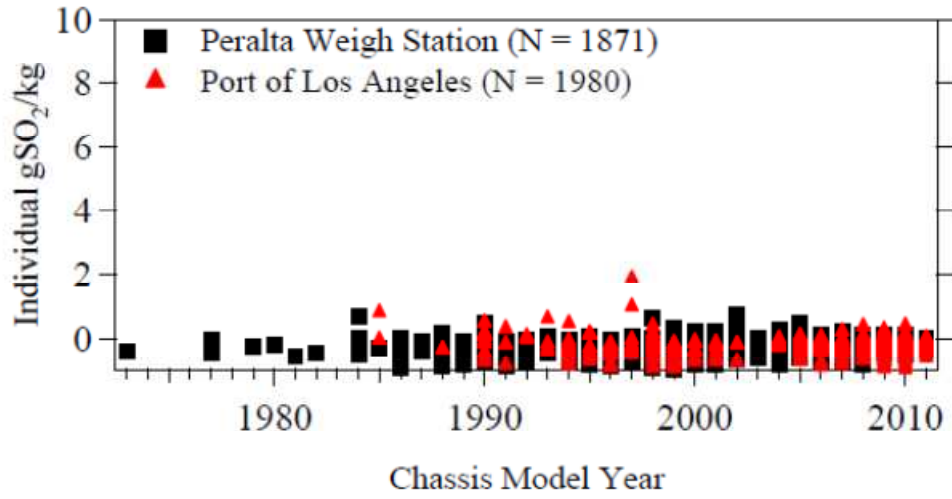


Figure 33 and Figure 34 compare the two time-aligned databases for CO, HC and NO with the line plotted being a least squares fit through the data points. The equation included provides the slope and intercept for the least squares line. At Peralta there are 1289 matched measurements and at the LA Port there are 1182 matched measurements. The data collected at the Port have noticeably more noise than the measurements collected at Peralta, and this is likely a consequence of the low-speed driving mode observed at the Port. In addition there are a number of negative readings reported by the FEAT while the ESP equipment has few if any negative readings. This is a result of the two different ways that the remote sensors calculate the emission ratios. The FEAT determines the emission ratios from a least squares line fit through the correlated emissions plume data. Fits close to zero will always have positive and negative results. The ESP equipment on the other hand uses an integral method where each species plume data are summed and then the ratios are calculated from these sums. This method produces fewer negative results.

Generally only the NO measurements have enough spread to lend themselves to being compared. While the noise is greater for the NO data collected at the Port both data sets have a similar slope with the ESP instrument consistently reporting lower NO emissions when compared with the FEAT measurements. Keep in mind that the two remote sensing beams were separated by about three feet and we did not try to collocate them and as such some disagreement, because of differences in driving mode, will be

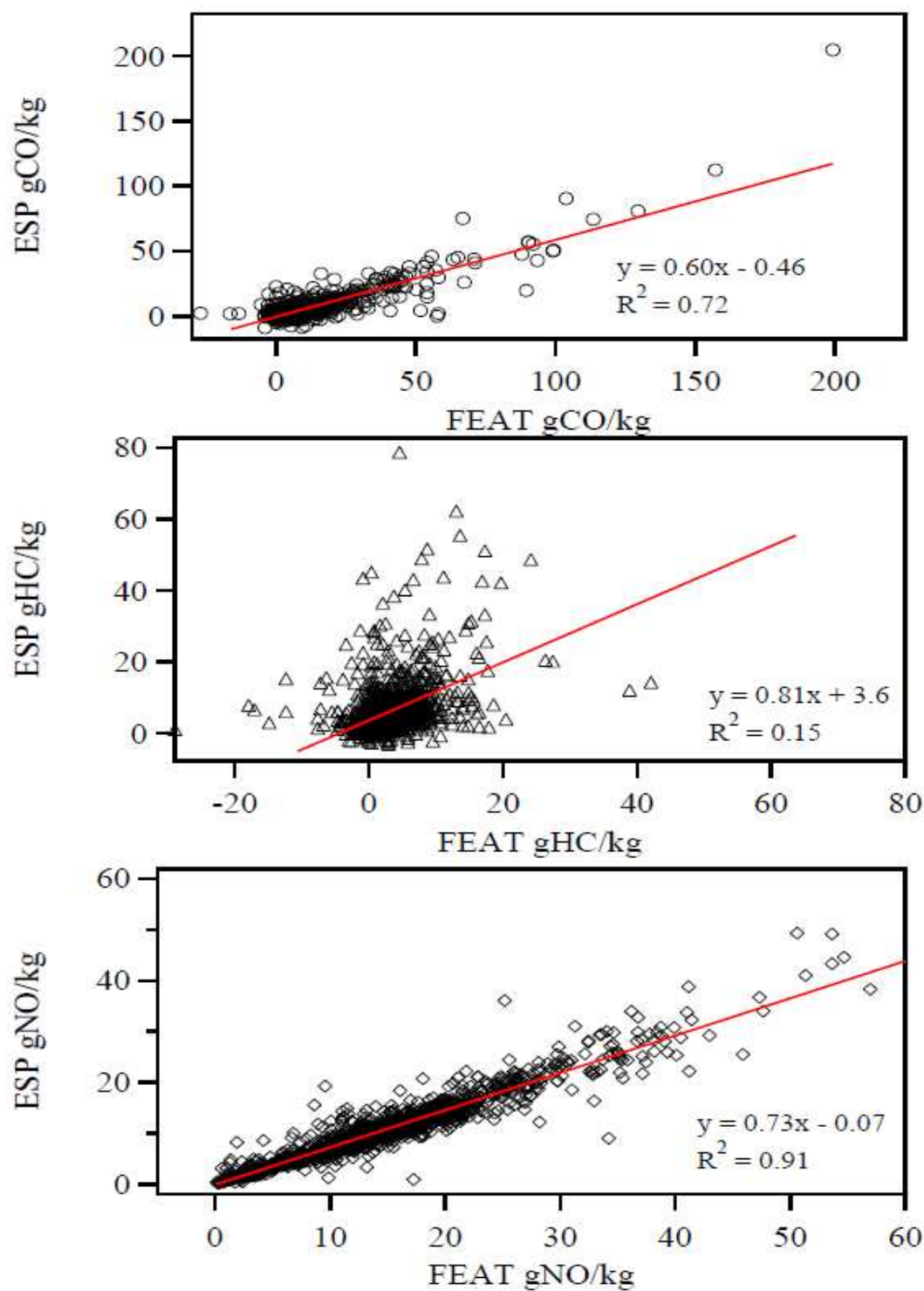
unavoidable. However, the systematic underreporting of NO by the ESP equipment appears to be much larger than one would expect a driving mode difference to produce.

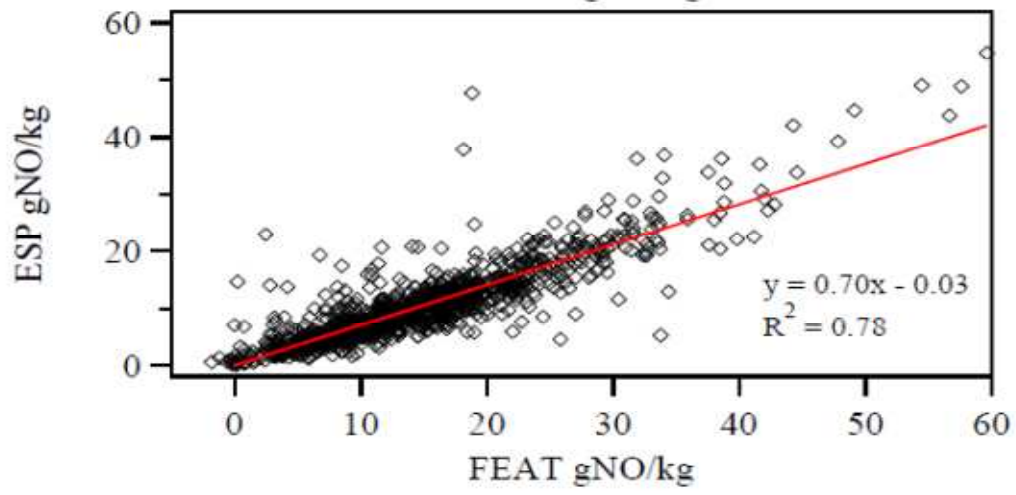
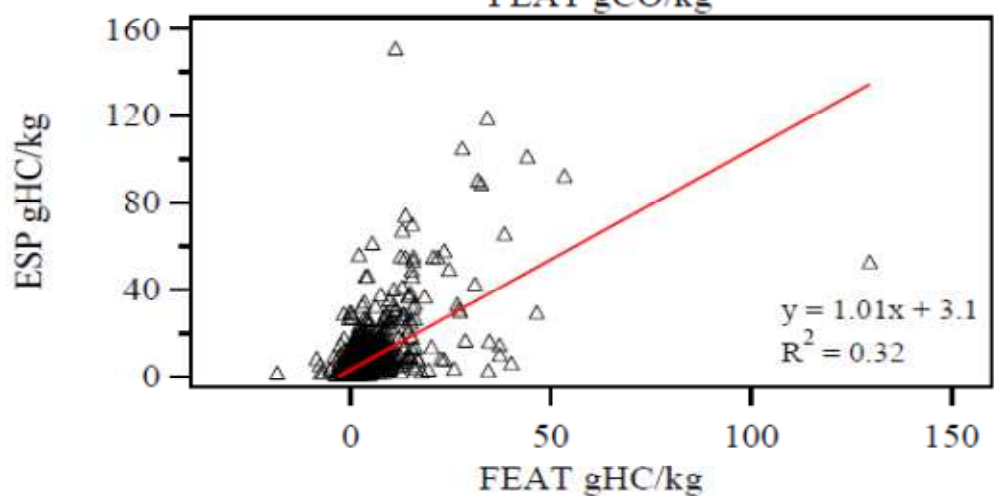
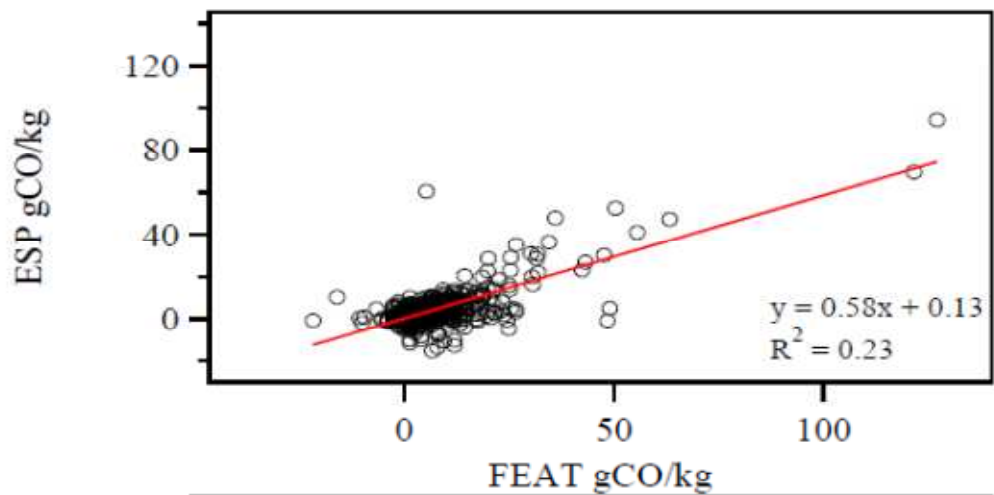
While there are major operational differences between FEAT and the RSD 4600 they both basically operate as comparators that compare the ratios of a standard gas cylinder with the ratios measured from the passing trucks. Since the systematic difference between the two instruments was observed in the field at Peralta it was decided to compare the two calibration cylinders at the LA Port. It was a simple matter to use ESP's cylinder on the FEAT instrument and using the Port setup we first used the FEAT to measure its calibration cylinder and then we repeated measurements on the ESP cylinder. Both cylinders were products of Scott Specialty Gases and Table 7 details those measurements performed from the 2010 campaign. The fact that the ESP cylinder calibrations are all larger relative the FEAT cylinder indicates that the two certified cylinders do not agree on their contents and that the FEAT would underreport each ratio if the ESP cylinder was used for calibration. From this comparison it is impossible to say which cylinder is correct but the disagreement between the two cylinders NO/CO₂ ratios possibly explains the observed differences in slopes between the comparisons of truck emissions with the two remote sensors. The lower slopes at Peralta were 60 and 73% for CO and NO respectively.

We chose not to consider HC emissions here because they are consistently low and the correlations are poor at both locations. If we simply add the percent discrepancy for the ESP cylinder versus the FEAT cylinder, we obtain the results 86% (CO) and

118% (NO) which implies that both instruments were actually measuring the same phenomenon within the constraints imposed by the calibration cylinder disagreement.

If we believe the FEAT cylinder is correct then all NO and NO_x results are as reported. If however we believe that ESP's cylinder is correct then our reported NO values should be decreased by about 30%, according to Figure 33 and Figure 34 which will then further decrease total NO_x.



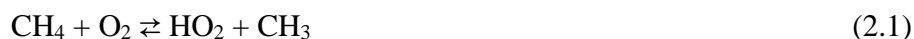


	FEAT Cylinder			ESP Cylinder		
	CO/CO ₂	HC/CO ₂	NO/CO ₂	CO/CO ₂	HC/CO ₂	NO/CO ₂
	0.985	0.1019	0.046	0.296	0.01176	0.01573
	0.978	0.1014	0.047	0.287	0.01203	0.01563
	1.017	0.1062	0.046	0.287	0.01195	0.01499
Mean	0.993	0.1032	0.046	0.290	0.01191	0.01545
Cylinder Ratio	1	0.0996	0.0499	0.2326	0.0116	0.0116
Cal Factor	0.99	1.04	0.92	1.25	1.03	1.33
Percent Difference				+26%	Negligible	+45%

Methane Combustion

Methane combustion at high-temperatures and rich fuel/air conditions is very complex. There are as many as 127 reactions in the detailed mechanism (58). To simplify the discussion, this mechanism can be reduced to 24 reactions. Ten of the more important reactions are discussed in this section.

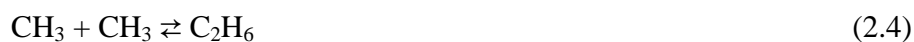
Methane combustion initiates from the reaction of methane and oxygen.



Methane can also react with HO_2 and OH radicals, which are created from other reactions as part of this process.



The methyl radicals from reactions 2.1-2.3 will react with each other, when there is insufficient oxygen, to produce ethane or will react with oxygen to produce formaldehyde and a hydroxyl radical.



Methyl radicals will also react with HO_2 to produce a methoxy radical and a hydroxyl radical. Methoxy radicals will produce formaldehyde and hydrogen which will eventually go on to make more hydroxyl radicals.



Additionally the hydrogen peroxide created in reaction 2.2 decomposes to form two hydroxyl radicals.



The hydroxyl radical plays an important role in methane combustion over H or O at both low and high temperatures. H and O should not be neglected at high temperatures as there are important reactions that shuffle hydrogen and oxygen; but the rich fuel/air conditions described for the Cummins ISL-G engines will not provide sufficient oxygen to this chain reaction, therefore the H and O can be considered negligible (58). The subsequent reactions, which are not included from the 24-step mechanism, will produce the normal combustion products of carbon dioxide, water, and carbon monoxide since there is a rich fuel/air ratio. The formation of hydrogen comes from reaction 2.8, and the water-gas shift reaction. The water-gas shift reaction turns carbon monoxide and water into carbon dioxide and hydrogen. This excess hydrogen will reduce nitric oxide over the catalyst to ammonia (59).



Discussion

Fifteen days of field work at each of two sites between 2008 and 2010 were conducted, resulting in 11,974 HDDV emission measurements. The sites chosen were Peralta Weigh Station on California State Route 91 (the Riverside Freeway) in Anaheim near the Weir Canyon Road exit and a truck exit on Water St. at the Port of Los Angeles in San Pedro. The Peralta Weigh station site was previously used in 1997 to collect measurements and adds a historical perspective to those measurements. Emissions analysis was performed on measurements that recorded a valid emission flag on the FEAT instrument for all gas species not including opacity. The heavy-duty fleet observed at Peralta in 2010 was about six years older than the vehicles in use at the Port location (2002 vs. 2007.9) and was measured at higher operating speeds than the vehicles in use at the Port location (~13 mph compared with ~5 mph). The fleet age at the Port has changed significantly between our sampling campaigns in 2009 and 2010, averaging about four years newer (2003.5 in 2009 vs. 2007.9 in 2010). Remote sensing measurements of HDDV exhaust at the Peralta site between 1997 and 2010 show large reductions in carbon monoxide (CO, 29%), hydrocarbons (HC, 16%), and nitric oxide (NO, 23%). A database for each site was compiled at Peralta and the Port, respectively, for which the states of Arizona, California, Illinois, Oklahoma, Texas and Washington provided make and model year information. This database, as well as any previous data our group has obtained for HDDV's can be found at www.feat.biochem.du.edu.

The introduction of lower EPA standards of 0.01 g/bhp-hr for PM and 0.2 g/bhp-hr for NO_x beginning with the 2007 model year diesel engines has forced manufacturers to come up with new ways to meet the new regulations. Two of the most likely options to meet these lower limits are selective catalytic reduction (SCR) for NO_x and diesel particle filters (DPF) for the soot. SCR utilizes an injection of a urea solution to reduce engine out NO_x to N₂. Two problems that exist are HDDVs need to accommodate extra weight for enough urea onboard to support a HDDV refueling cycle and there is a risk of ammonia slip out of the tailpipe. DPFs trap soot particles from engine out exhaust with different filter surfaces. In order to regenerate the surface of the filter, there is often an oxidation catalyst placed upstream of the filter which intentionally oxidizes engine out NO to NO₂ which can burn the trapped soot from the filter surface. This particular step presents a potential problem with interfering with the NO₂/NO ratio as more trucks will be emitting more NO₂. Since NO locally removes tropospheric ozone, higher level ozone results if NO is lowered. If NO₂ is emitted directly then ozone levels would be expected to increase even more.



Instead of using SCR, some trucks have taken advantage of the CAAP 50% funding to use alternative fueled trucks. When these engines are operated under stoichiometric conditions, they emit very little NO_x. However, in order to emit very little NO_x, engine out exhaust is passed through a TWC that reduces NO_x to ammonia. While ammonia is currently not a regulated mobile source emission this process remains a legal

one. These alternatively fueled trucks can cost to as much as 2-3 times that of a new diesel HDDV and yet there seems to be few emissions benefits measured by RSD worth the expense.

On a fleet-wide basis as of May 2010, very few trucks had been outfitted with SCR technology to lower NO_x to meet the new standards. The CAAP has legislated an accelerated schedule that has sped up the fleet penetration of lower emitting trucks. Part of this accelerated strategy has been to phase in the forced retirement or replacement of older model years. Currently, engines with model year pre-1994 are no longer allowed entry into the ports. Model years 1994-2003 are only allowed in if they have been retrofitted with a DPF that meets a level 3 verified diesel emission control strategy (VDECS) as of January 1, 2010 or are Class 7 trucks. However, as usual, a loophole was taken advantage of with the intermediate model year engines. As the rule was written, only Class 8 trucks which are all heavier than 33,001 lbs gross vehicle weight (GVW) are subject to the more stringent emissions limit. Instead of complying with the lower emissions limit, most truck operators with engines model year 1994-2003 opted to use Class 7 trucks which are 26,000-33,000 lbs GVW and are exempt from this regulation. This means that those operating Class 7 trucks get a free two year extension to comply with the CAAP strategy. The final phase is to ban all trucks that do not meet the 2007 emission standard regardless of Class or model year starting January 1, 2012.

The on-road PM and NO_x emissions of trucks measured at the Port of LA, Peralta and the Port of Houston are decreasing with model year 1995 and newer. However, each

site has yet to reach the PM and NO_x standard levels of 0.035 and 1.3 g/kg, respectively. Only certain trucks at the Port of LA that combust natural gas under stoichiometric conditions with TWC show measureable NO_x emissions below the standard. The NO_x from these trucks is instead reduced and emitted as ammonia, which is currently not a regulated pollutant for on-road vehicles.

The emissions comparison at three different locations revealed that the average model year of trucks at the Port of Houston in 2009 was similar to the average model year of trucks at the Port of LA in 2008. Both the fleet average and emissions by model year, starting with MY 1995, for NO and NO_x at the Port of Houston were more similar to the similarly aged fleet at Peralta. The similar NO and NO_x emissions from these two sites are most likely due to the similarly observed speeds and accelerations. Both the fleet average and emissions by model year, starting with MY 1995, for NO₂ at the Port of Houston were however more similar to the similarly aged fleet at the Port of LA. A closer evaluation of the driving modes, specifically VSP, at the Port of Houston and the Port of LA shows that both sites have lower average VSP (less than 2 kw/tonne) relative to the average VSP at Peralta (about 6 kw/tonne). NO₂ was shown to have higher average values for lower average VSP bins for all three measurement years at Peralta. It was determined that the relatively lower NO₂ at Peralta compared to the Ports of Houston and LA for model year 1995-2003 is related to the higher VSP observed at Peralta. While the Port of Houston and the Port of LA have similar fleet average NO₂ emissions for similarly aged fleets, the NO₂ originates from two different places. The fleet fraction

at the Port of Houston shows that 78% of the fleet is model year 1995-2003 which are pre-control trucks. The fleet fraction at the Port of LA shows that only 34% the fleet was model year 1995-2003 and 50% of the fleet was model year 2009 and newer. The contribution of NO₂ emissions from the mid-range model years at Houston is similar to the contributions of NO₂ emissions from both the mid-range model years and the newest model years at the Port of LA.

HDDV Exhaust On-Road Sampling Prototype

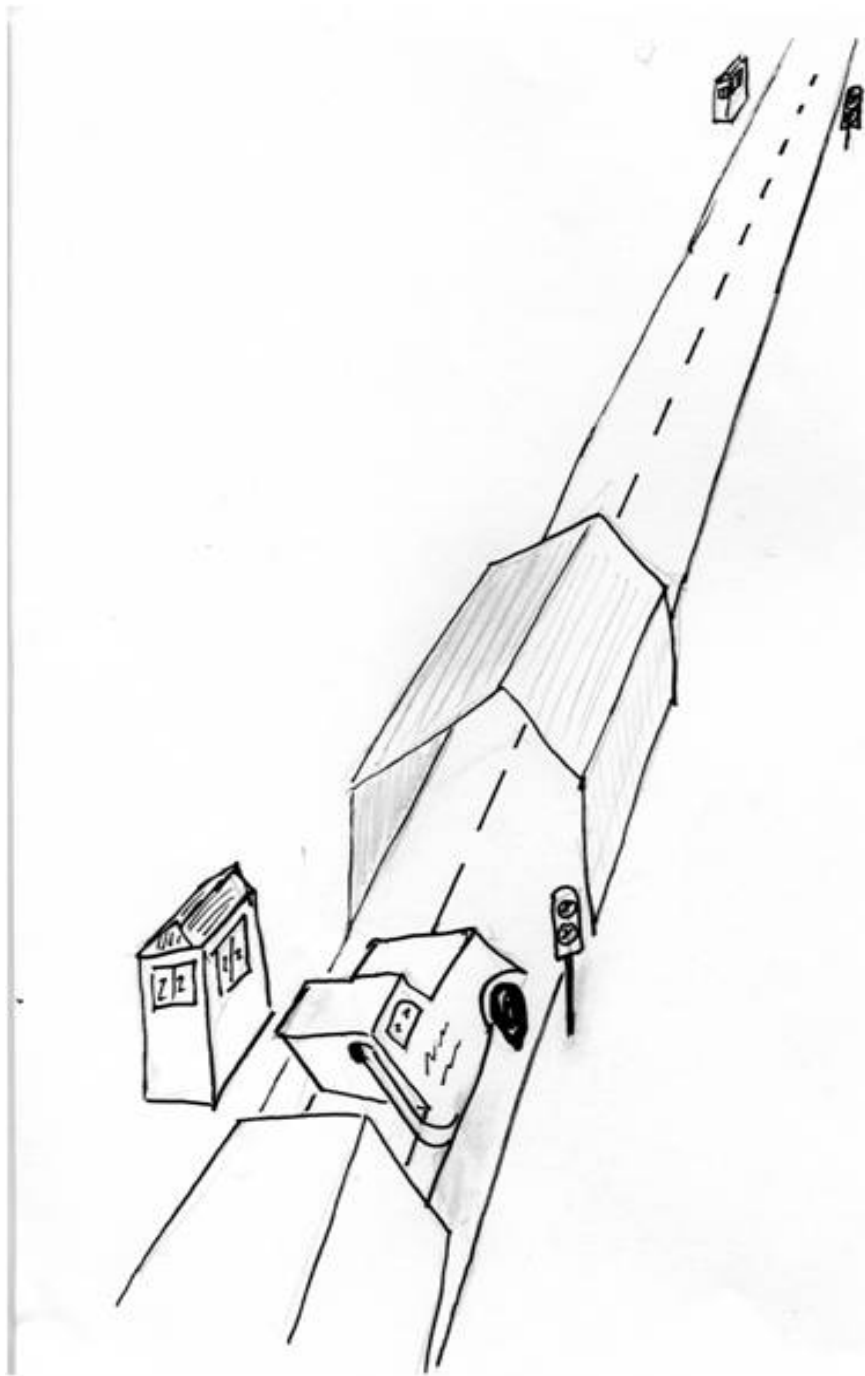
Remote sensing of light duty vehicles (LDV) has been accumulating measurements since the late 1980's. The lighter weight of these vehicles makes it possible to also measure the exhaust on a chassis dynamometer as is done at emissions testing facilities. Chassis dynamometer exhaust measurements can be in real time or can be integrated by allowing the diluted exhaust into large gas sampling bags and subsequently measuring the bag contents. Measuring integral vehicular exhaust allows the performance and emission quality of the car to be evaluated over multiple and different cycles that attempt to mimic normal driving as would be observed on the road. These same integral tests for HDDVs are more complex and more expensive. The chassis dynamometer required for HDDVs needs multiple personnel to attach the axles to absorption brakes to measure power and torque. The exhaust is also insulated and

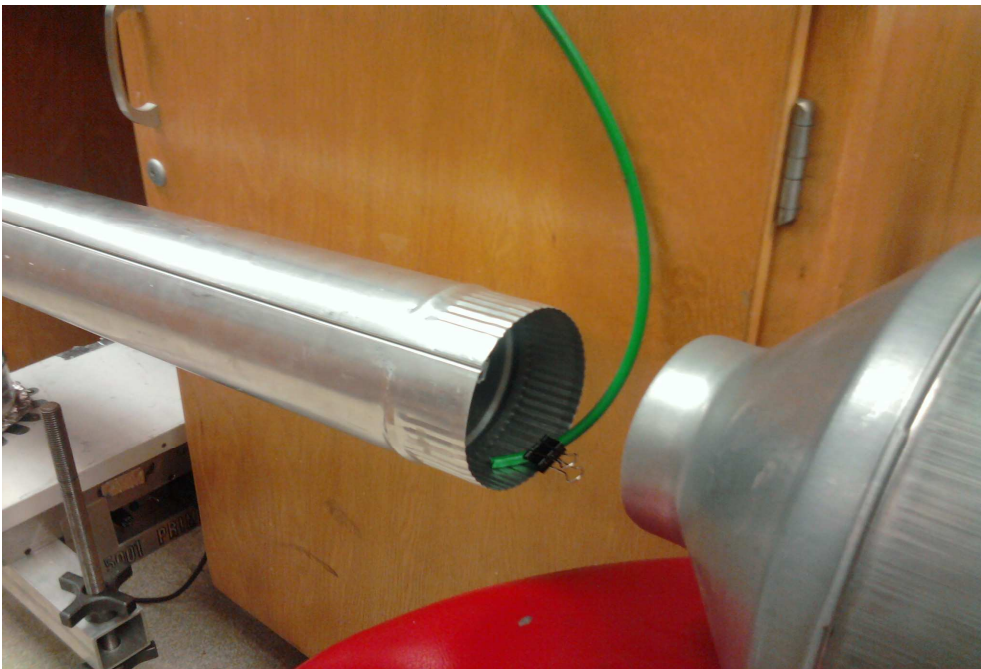
transported to a dilution tunnel. For LDVs one trained technician can perform about 10-12 IM240 emission tests in one hour which cost 25 dollars each. For comparison, there were 15 HDDVs tested a total of 104 tests for the ETaPS project at the University of West Virginia over a period of six weeks. That is about 2.5 HDDV tests a day.

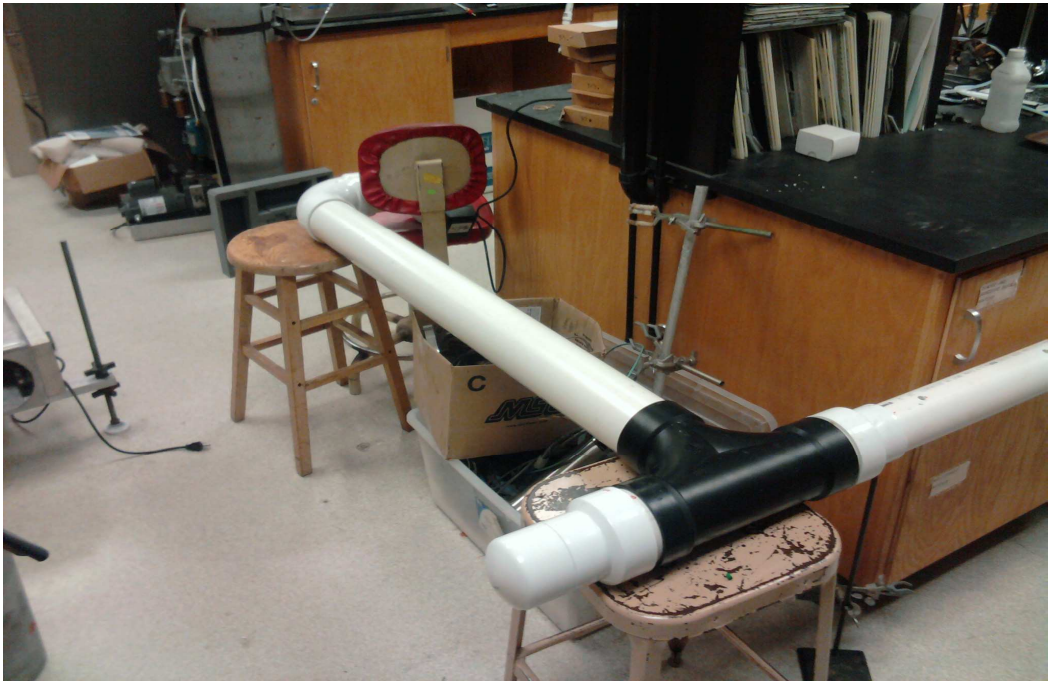
It is therefore a useful idea to sample integral HDDV exhaust on the road in a simple and inexpensive way. The following proposal is one possible solution using current analyzers being used at LDV dynamometer testing facilities. Imagine a large tent that is fifty feet long, fifteen feet wide and about twenty feet high at its apex. This structure would overlay a section of road highly populated with HDDV traffic like the on-ramp to an interstate from a weigh station. The idea is that the length of the tent allows exhaust from an accelerating HDDV to be contained and will consist of multiple accelerator positions as a HDDV up-shifts gears to match interstate speed. Down the right hand side of the tent there is a fifty foot long pipe about fourteen feet above the roadway with fifty holes drilled one foot apart. An inline air fan draws air from inside the tent through the holes and down the pipe to a set of emission analyzers. As a truck drives through the tent the first hole collects exhaust and ideally the fan's sampling speed roughly matches that of the passing truck so that the exhaust being delivered down the sampling pipe passes the next hole at the same time new exhaust is added. This creates an integral lump of exhaust that is measured by the analyzers as an average of a fifty foot cycle over seven to ten seconds of acceleration. A cartoon drawing of this setup is shown in Figure 35.

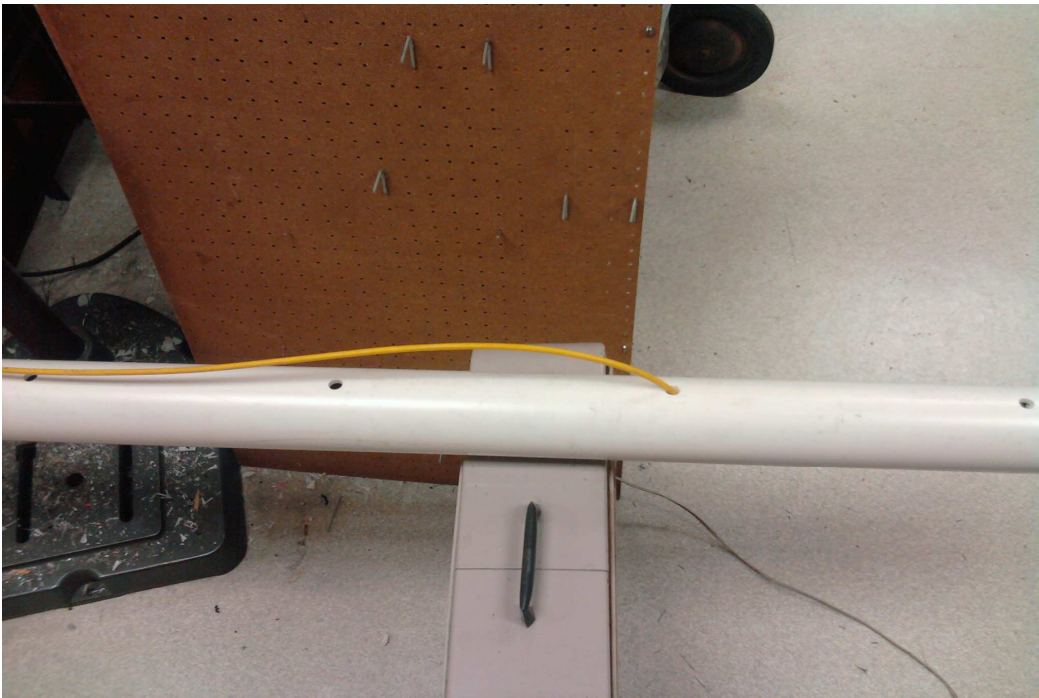
Fifty feet of 3-inch diameter PVC pipe was purchased from Home Depot. Only 25 feet of pipe was assembled because there was not enough lab space. The fluid dynamic equations used to calculate air flow for the hypothesized sampling system were obtained from an online calculator found at www.pipeflowcalculations.com. The calculations for the sampling system assumed that air would be drawn from the center down to the instrument analyzers. For this case, each 25 foot section of pipe would need holes drilled one foot apart increasing in diameter away from the center of the length of pipe in order to keep equal air flow across each orifice. Incremental increases in the diameters of holes drilled changed every 6th hole. Therefore the diameter increments starting from the end away from the center are; 17/32", 1/2", 15/32", 7/16", and 27/64." The drill bits available did not have the resolution to make these small increments. Instead, the 1/2" drill bit was used for each section. The first two sections were treated as 1/2" holes and the last three sections of holes had extra shavings removed to increase their diameters. Proof of concept experiments were performed with a cylinder of CO₂ injecting two plumes of gas into the sampling system. The FEAT 5001 unit was adapted to this sampling system as a detector. One CO₂ plume was injected at the intake of the FEAT unit and the second CO₂ plume was injected at the far end of the sampling tube. The CO₂ injections were controlled by a solenoid valve and the difference between the recorded peaks is effectively the response time for the sampling system. The calculated Δt was one second for 25 feet of 3-inch diameter pipe and 5 feet of 4-inch diameter pipe with hole sizes described previously. The observed Δt was 4 ± 0.2 seconds which

indicates that less air flow than expected is being provided from the current fan. However, a four second response time is sufficient for this design and the expected speeds of passing trucks. Figure 36- Figure 40 show pictures of the described experiment. Figure 41 shows a sample recording of the CO₂ injections repeated five times. The x-axis is a time scale measured in 10Hz samples.

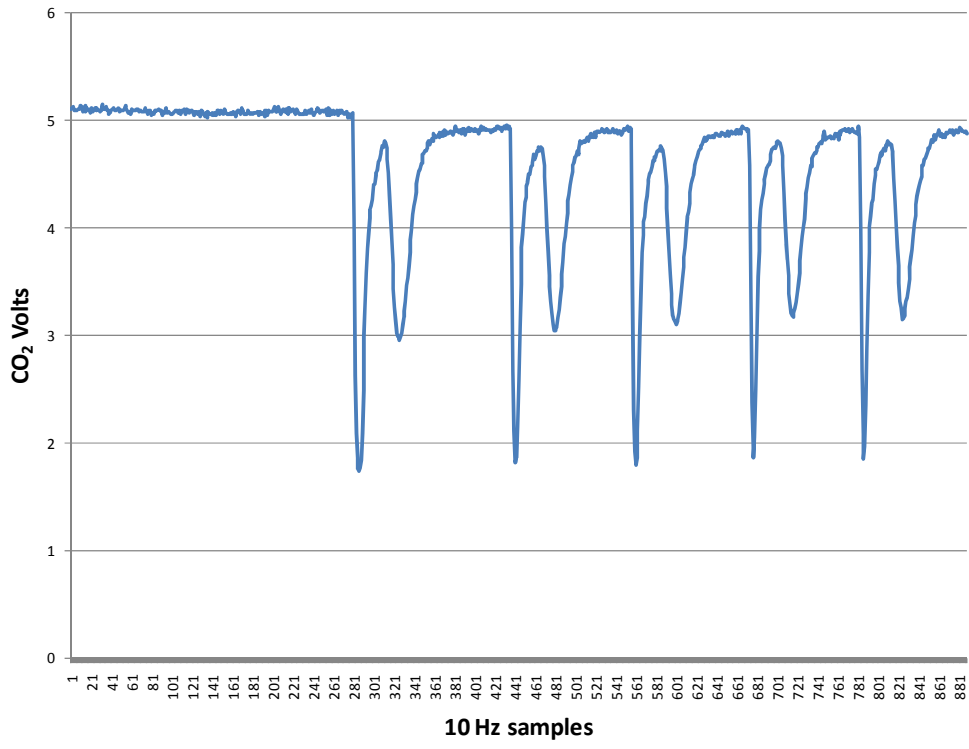




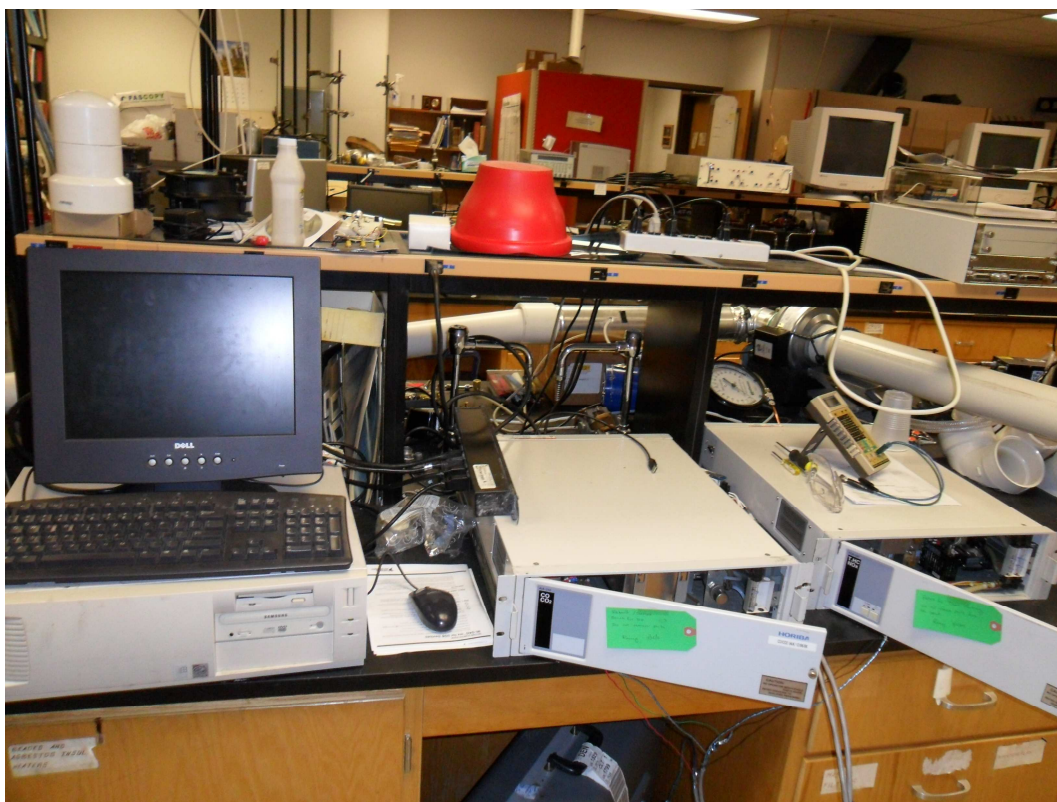




CO₂ injection test



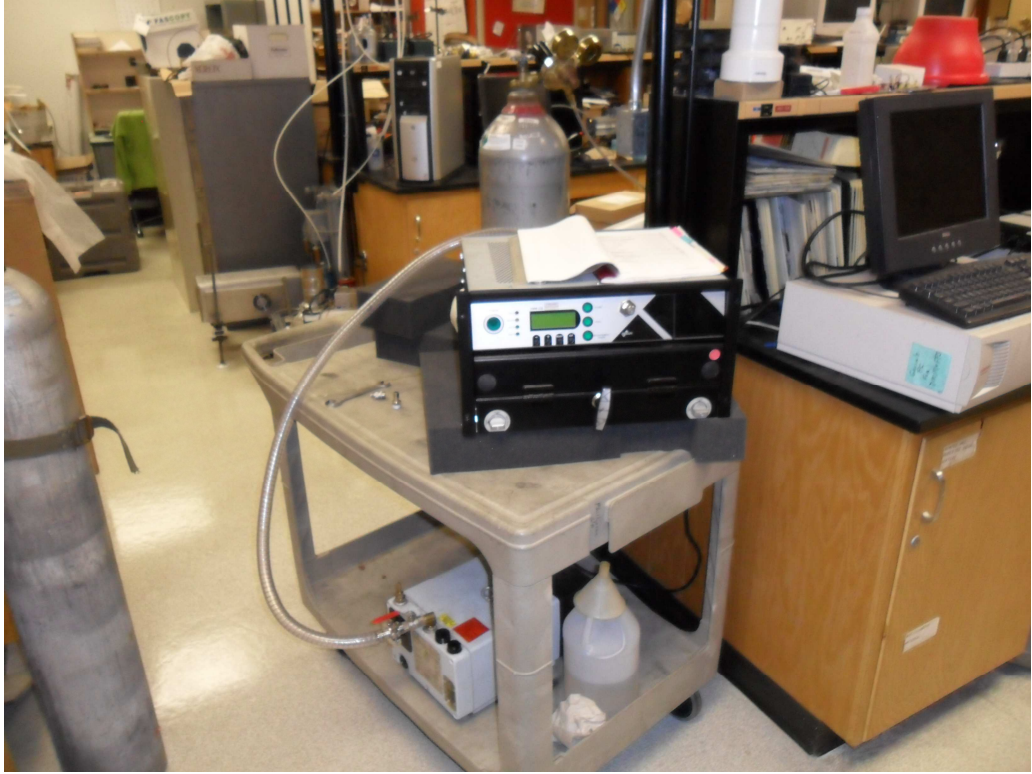
A smaller five-foot prototype was built for lab testing. Five, half inch holes were drilled one foot apart in a three inch diameter PVC pipe available from Home Depot. Air flowed through the holes down the pipe and transferred to a four inch diameter pipe through a t-connector with one side blocked (Figure 38). A Fantech FG 4XL fan was placed at the end of the four inch diameter pipe and blew air into a four inch diameter aluminum duct situated perpendicular to the fan. The sampling tubes for each instrument were drilled into the aluminum air duct. An external air pump was required to supply the analyzers with the correct sample flow rate. A table of the correct pressures for each inlet can be found in Appendix B. Two Horiba Analyzers were each setup to measure two species of exhaust. The Horiba AIA measured CO and CO₂ with a flow cell and infrared spectroscopy. The Horiba FLA measured THC by flame ionization and NO by chemiluminescence. This setup as described does not measure NO₂ and ideally a second Horiba CLA would be needed and properly calibrated to the NO₂ setting so the NO/NO₂ ratio can be measured. A Dekati Mass Monitor was supplied to measure fine particle emissions. Figure 42-Figure 46 show the setup as described above.





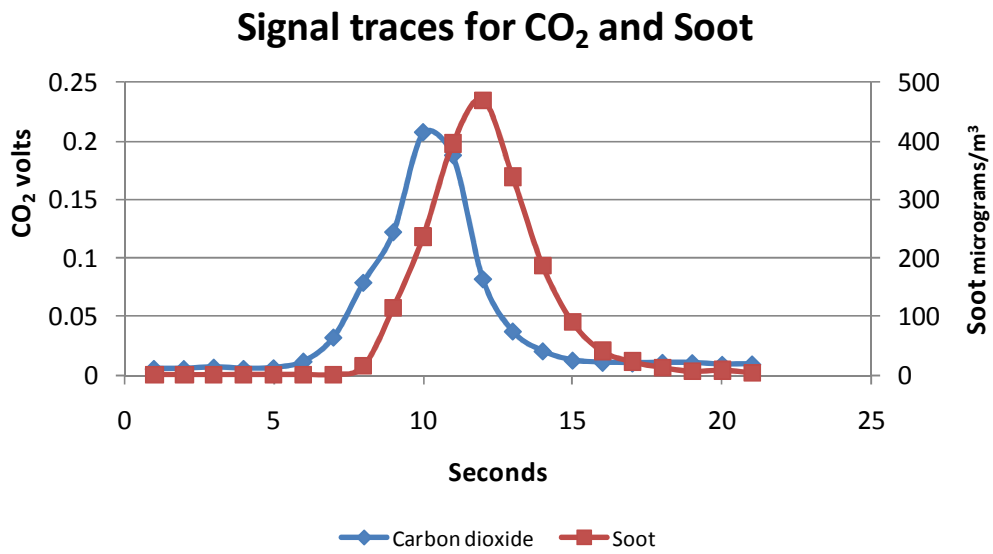
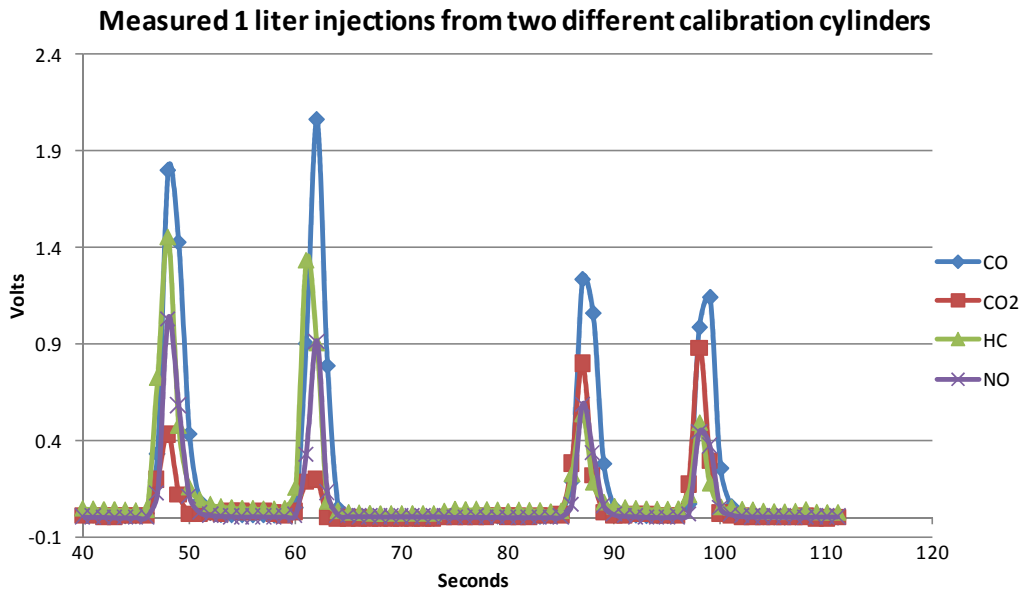






Two certified calibration gas mixture cylinders were used to test this sampling system. These gas cylinders are the same ones used to calibrate RSDs. The first is the University of Denver's FEAT cylinder which has 6% CO, 6% CO₂, 0.6% HC, and 0.3% NO. The second cylinder is used to calibrate an ESP 4600 RSD which has 3% CO, 12% CO₂, 0.15% HC, and 0.15% NO. There is about a 10:1 dilution ratio with this length of sampling pipe. The detection limit for this apparatus was not explored but is expected to be low enough to accommodate any levels of regular diesel exhaust. Typical peaks from a 10:1 dilution are shown in the top picture in Figure 47 and an example of a corresponding smoke signal for half a liter of synthesized particles diluted with half a liter of calibration gas is shown in the bottom picture of Figure 47. There is a two second lag in response time for the maximum observed signals between the IM Analyzers and the DMM. Even with a 10:1 dilution the integral signal to noise ratio can range from 20-100 depending on cylinder and gas species. There was not a proper standard for smoke as there was for the other gaseous species. Therefore in order to test the response time difference for the Dekati Mass Monitor (DMM), a small vial of ethyl benzene was burned inside a large inverted beaker. Once the flame was extinguished the one liter gas syringe sampled half a liter of the smoke that was created in the beaker. The remaining half a liter was then filled with cylinder gas. This synthetic exhaust sample with mixed smoke particles and gases was injected into one of the holes in the sampling pipe. The resulting ratio of soot to CO₂ calculated from the bottom graph in Figure 47 is comparable to a well maintained 1995 HDDV. The expected emissions signals, with on-

road speeds from actual trucks, should have very little error based on the signal to noise and level of detection for the one liter injections in this setup.



Just like remote sensing calculations, the data from the IM analyzers are ratioed to CO₂ and compared to the ratios in the cylinders. Figure 47 shows four measured samples of one liter injections. The integral under each peak was summed and converted to a concentration using the calibration curves supplied by ESP. The calibration curves and the equations used for this analysis can be found in Appendix C. Those concentrations are then ratioed to the CO₂ value. Table 8 compares the relative concentrations and ratios between the two cylinders used in the experiments. When the correct equations are applied to each gas and the two peaks are averaged, the ratios measured are within the uncertainty of the calculated values from the cylinders. The measured HC ratios are expected to be three times the calculated ratios because the calculated ratios are in propane units and the measured values are from a flame ionization detector which is calibrated as a carbon counting method. One propane unit would be counted as three carbon units in flame ionization. These results show that if there is sufficient exhaust captured by the sampling pipe, a drive through on-road HDDV IM program could be successful. They also show that as little as a half liter of typical exhaust is plenty to achieve a good signal to noise ratio. We believe that as truck emissions become more regulated, non-intrusive truck exhaust emissions measurements such as those from this truck shed can provide useful data at weigh stations and border crossings.

	Cylinders		Calculated		Measured	
	FEAT(%)	ESP(%)	FEAT ratio	ESP ratio	Average FEAT ratio	Average ESP ratio
CO	6	3	1	0.25	1.06 ±5.2%	0.26 ±5.2%
CO ₂	6	12	-	-	-	-
HC	0.6	0.15	0.3*	0.0375*	0.28 ±2.4%	0.04 ±2.4%
NO	0.3	0.15	0.05	0.0125	0.05 ±3.8%	0.01 ±3.8%

Table 8 Actual cylinder concentrations (left two columns). Calculated emission ratios to CO₂ (middle two columns). Average measured ratios of two injections from each cylinder (right two columns). *Average measured HC are in ppm Carbon and are expected to be about three times the calculated HC as the HC used for calibration was propane therefore the calculated ratios for HC are multiplied by three. Measured uncertainties are calculated from a separate experiment of repeatability of the measurements using the ESP cylinder. Uncertainties are the square root of the sum of the squares for the cylinder certification and the standard error of the mean for each pollutant.

3. Light-Duty Gasoline Vehicles

Comparison of Colorado's Inspection Maintenance Program with OBD and RSD

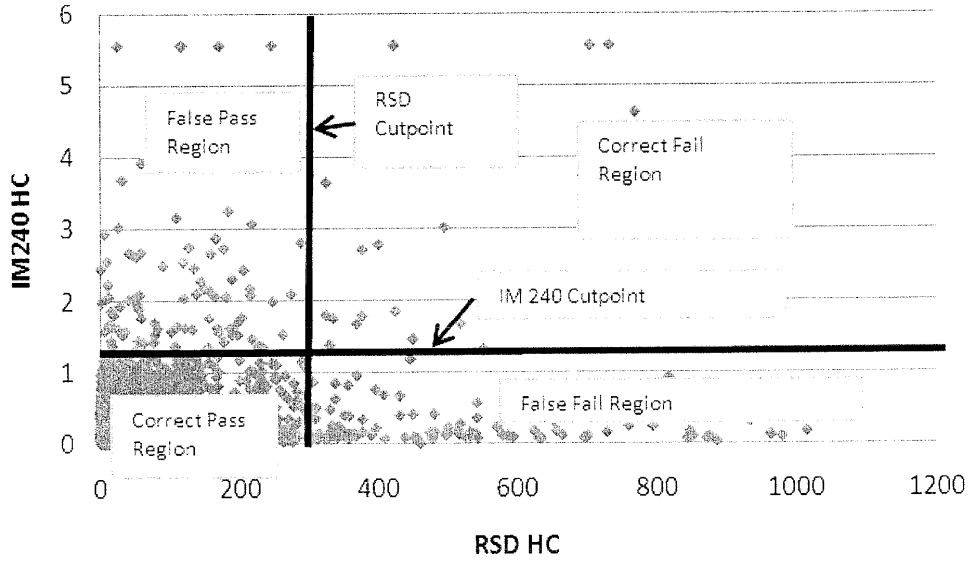
Currently, Colorado is one of the few states that does not require motorists to pass an On-Board Diagnostic computer (OBD) test as part of its Inspection and Maintenance (I/M) program (60). Instead, motorists are subject to a visual inspection, a gas-cap pressure test, and a dynamometer test of tailpipe emissions every two years in order to qualify for their vehicular registration certificate. Remote sensing is used as part of this program to “Clean Screen” or to award motorists an effective passing grade on their required emissions test if they are measured as suitably low emitters by various vans throughout the Denver area. This option gives motorists a chance to mail in the required payment for the test and not have to wait at a testing facility. Environmental Systems Products (ESP) conducts these measurements with remote sensing vans and currently clean screens at least 200,000 vehicles a year. If you assume the average distance a motorist is to a testing facility is five miles (61) and the fleet average fuel economy is 20 miles per gallon then the Clean Screen program has saved 100,000 gallons of gasoline from being burned. The average price of gasoline at the pumps in Colorado reached as high as \$3.70 during the spring of 2011 (62). So the clean screen process would have cumulatively saved \$370,000 just from motorists not commuting to the testing facility.

Implementation plans involving a larger contribution of remote sensing as part of a state's emission program have been proposed by Hoshizaki *et al.* as early as 1973 (63). They present multiple drive-through options for a preliminary RSD test to a state's mandatory emission test. A simple demonstration of using remote sensing in an emission program is placing the instrument right before the testing facility to potentially Clean Screen a larger portion of the fleet. This improves the convenience to motorists by decreasing the wait times that are usually associated with the IM240 test. A recent evaluation of the Colorado Automotive Inspection and Readjustment program (AIR) was submitted for the Office of the State Auditor by *dKC de la Torre Klausmeier Consulting, Inc.* Klausmeier *et al.* (61) concludes that remote sensing is ineffective for identifying gross polluting vehicles, which are generally the top 1% of the fleet which can be responsible for more than 30% of the on road emissions, and also that remote sensing is ineffective as a sole method for controlling emissions. The former conclusion comes from Klausmeier's Figure D-9, where it shows single remote sensing measurements against the corresponding IM240 measurements from only 1998 model year passenger vehicles (Figure 48, D-9) totaling 5,268 measurements. According to Klausmeier, the 1998 model year was chosen because it had the most data and it was a year with substantial modeled emissions reductions from the AIR program. Klausmeier concludes that because there was such a small number of data points that were successfully identified above the IM240 limit *and* the remote sensing limit that remote sensing would

be an ineffective approach for a “Dirty Screen” that would identify the high emitters of the on road fleet.

The emissions of a broken vehicle will vary regardless of test or method, especially so for high emitters (64). The same is true, if not more so, with remote sensing data since they are instantaneous snap shots which for some vehicles are throttle position dependent. The problem is the variability of the emissions from the individual vehicles especially when they are compared from different days. This is exactly what is being demonstrated in Klausmeier’s Figure 48 (D-9) because the RSD measurements are only the most recent measurement before that vehicle’s IM240 test. The numbers are correct for each test on the day of collection and the intrinsic vehicular variability is what drives the “false fails” and “false passes” in Figure 48 (D-9). It is interesting to note that in Klausmeier’s report the very next figure shows how well fleet averages of IM240 measurements correlate with remote sensing measurements.

Figure D-9
Colorado Automobile Inspection and Readjustment (AIR) Program
Correlation Between IM240 Test Results and Rapid Screen Results
for 1998 Model-Year Passenger Vehicles



Source: Colorado Department of Public Health and Environment Rapid Screen and IM240 data.

Correct Pass: Below the established cutpoint for both the Rapid Screen and IM240 tests.

False Pass: Below the established cutpoint for Rapid Screen but above IM240 cutpoint.

False Fail: Below the established cutpoint for the IM240 test but above the Rapid Screen cutpoint.

Correct Fail: Above the established cutpoint for both the Rapid Screen and IM240 tests.

The Colorado RSD data sets contain measurements of on-road emissions. On-road emissions are what the I/M programs are supposed to reduce. Thus Colorado's RSD data can be used to compare how well or badly the OBD computer results compare to an actual test of exhaust emissions (The Colorado IM240 test) and both of those to the on-road emissions that the programs are supposed to reduce. A benefit of these data is that remote sensing data can also be used to help to improve the I/M program. This analysis was performed on the most recent years of data available (2008-2009) from the Colorado data sets. Microsoft Access was used as the analysis program. In the database containing the IM240 and OBD data, records were chosen with fields for vehicle information (make, model, year, fuel, vehicle type) and test results. Test lane records have an overall test result column but this includes the emission test result as well as a visual inspection result. For the purpose of intercomparisons between test lane (IM240), RSD, and OBD, only the emissions result field was used for the IM240 test. This resulting 2009 I/M database contains 657,436 vehicles. Also, results and emissions of vehicles were chosen and matched from the RSD database to the IM240 database based on the initial IM240 test, no second chance test was awarded, only non-idle tests were conducted, and only stations operated by ESP were considered. For the sake of simplicity the OBD results were only interrogated if the light was ON at the time of the IM240 test and no further interrogation was performed as to why the light was ON. The RSD database was restricted to only Colorado license plates. Additional restrictions selected only RSD records that included Y's for the emission flag and only when the ambient temperature

was above 45 F to avoid steam plumes. There are over 8 million identified license plates in the 2009 RSD database, of which there were 1,160,698 unique plates. 246,523 of these unique plates were successfully matched to the 2009 IM240 database. This matched database is referred to as the 2009 IM/RSD database. By default, there is some age bias in the RSD database compared to the registered fleet because the majority of the on-road fleet is newer cars in part because they drive more often, at least on the freeways where RSD measurements are made.

Conversely, the IM240 database is age biased for an older fleet because the four newest model year cars are exempt from IM240 tests unless change in ownership occurs. Emission reductions and benefits were calculated for RSD by interrogating the 2009 IM/RSD database for vehicles with the criteria that the vehicle was measured ≥ 1 time at least 30 days prior to its initial IM240 test and that it was measured ≥ 1 time at least 30 days after its initial IM240 test. These criteria effectively reduce the size of the available fleet in 2009 for selection to assess the on-road emissions reductions to 463,105 RSD measurements from 57,524 vehicles. However, even with these selection criteria there are still tens of thousands vehicles left to determine emissions benefits. The emissions benefits for the IM240 program were taken from Klausmeier *et al.* report to the Colorado State Auditor (61) as well as the identifiable HC emissions from the 2009 IM/RSD database. To account for the Clean-screen contribution of the on-road fleet, a total of 20,000 vehicles were added to the 2009 IM/RSD database in proportion to Klausmeier's report for the total on-road fleet. There were 5,649 vehicles (7%) from the 2009 IM/RSD

database that initially failed their IM240 test. The identified on-road HC emissions of these failures averaged 192 ppm. The average on-road HC emissions for the 2009 IM/RSD fleet were 50 ppm. The Clean Screen program in Colorado allows on-road vehicles to not submit to their biennial IM240 test if they are measured multiple times with readings below a certain cut point. Since, there are about 200,000 vehicles a year that pass a clean screen test these vehicles are not represented in the IM240 data and need to be accounted for in the total on-road fleet calculation. If the average on-road HC emissions for the Clean-screen fleet were 20 ppm then the percent of total on-road HC emission identified by RSD can be estimated. The total contribution of on-road HC emissions is sum of weighted averages of the 2009 IM/RSD and Clean-screen fleets, or;

2009 IM/RSD average of 50ppm*75%(fleet)/100 = 37.5

Clean-screen average of 20ppm*25%(fleet)/100 = 5

37.5 + 5 = 42.5

The identified on-road HC failures make up 7% of the 2009 IM/RSD fleet, including the Clean-screen fleet. The contribution of the HC failures is

$192\text{ppm} * 7\%(\text{fleet}) = 13.4$. Therefore, RSD identified 32% ($13.4/42.5$) of the on-road HC emissions from only 7% of the on-road fleet. From these identified failures, the eligible OBD equipped vehicles (MY 1996 and newer) were interrogated for their OBD result. OBD failed 50% of the initial IM240 failures ($50\% * 3.5\% \text{ fleet}$) averaging 180ppm HC and failed 20% of the initial IM240 passes ($20\% * 55\% \text{ fleet}$) averaging 26ppm HC. When summed together, these contribute to 12.8% failure rate of the OBD eligible fleet. The

fraction of identified on-road HC emissions from an OBD only program is,
 $180\text{ppm} * 1.7\%(\text{fleet}) + 26\text{ppm} * 10.4\%(\text{fleet}) = 5.7$. $5.7/42.5 = 13\%$. According to this analysis, an OBD only program would identify 13% of the on-road emissions from 12.8% of the on-road fleet.

Figure 49 (D-10) shows an r^2 value of 0.994 which is outstanding. This figure clearly shows that these two tests are measuring the same thing, at least with fleet averages. Figure 50 repeats the analysis in Figure 49 from the 2008 Colorado databases for IM240 and RSD and reports an r-squared value of 0.988. The method of matching records for this 2008 database is described below for the 2009 datasets except that the 2008 database did not have before and after I/M test criteria for emissions reduction analysis.

Figure 51 shows IM240 data plotted against remote sensing data collected at the entrance to an emissions testing facility. All model years are represented in this graph and the data are separated into the categories correct passes, correct failures, false passes or false failures.

Table 9 shows the values for characterizing single remote sensing measurements using a pass/fail cut point of 300ppm HC, which is the same cut point used by Klausmeier in Figure 48. The accuracy of remote sensing's ability to successfully clean screen HC emissions within one hour of IM240 tests is 97%. The arithmetic used to calculate this percentage from Table 9 is;

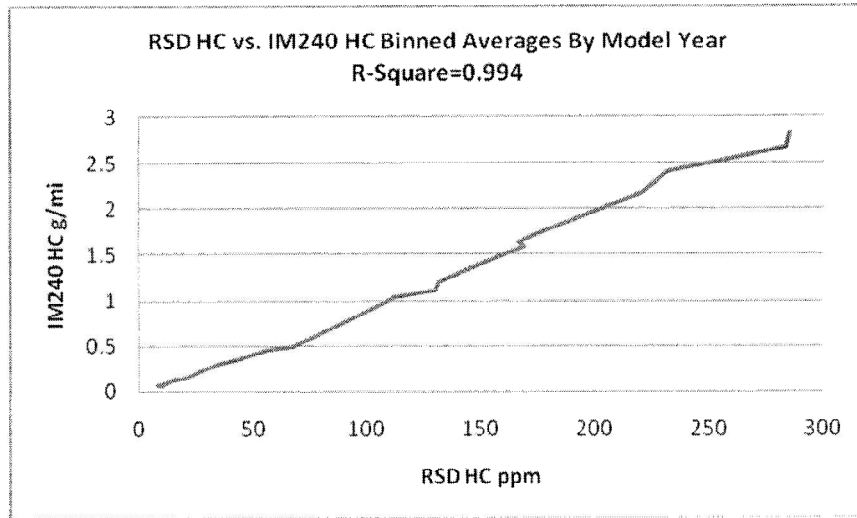
Correct passes / (Correct passes + False passes) or;

$$3001 / (3001 + 92) = 97\%$$

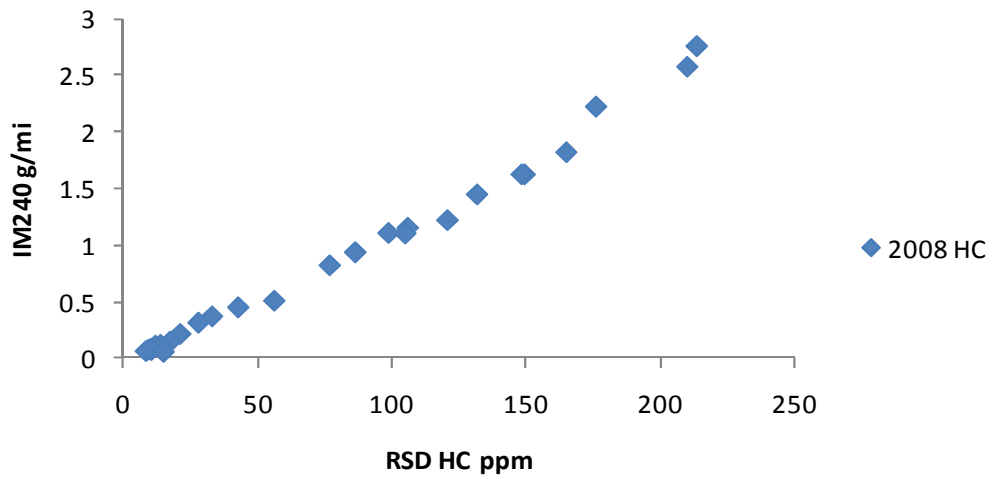
This 300ppm cut point would have identified 71.3% of the supposedly repairable IM240 HC emissions. However, this cut point would lose 28.7% of the supposedly repairable IM240 HC emissions.

Table 10 shows the results of a theoretical 20ppm HC cut point which would send home about half of the incoming fleet. This program would have identified 140 vehicles that failed the IM240 test, and would have identified 95.3% of the supposedly repairable IM240 HC emissions. This 20ppm cut point identifies 24% more repairable IM240 HC emissions while only losing 4.7% of the repairable IM240 HC emissions from the falsely passed vehicles all for sending 50% less vehicles to the IM240 than the 300ppm cut point.

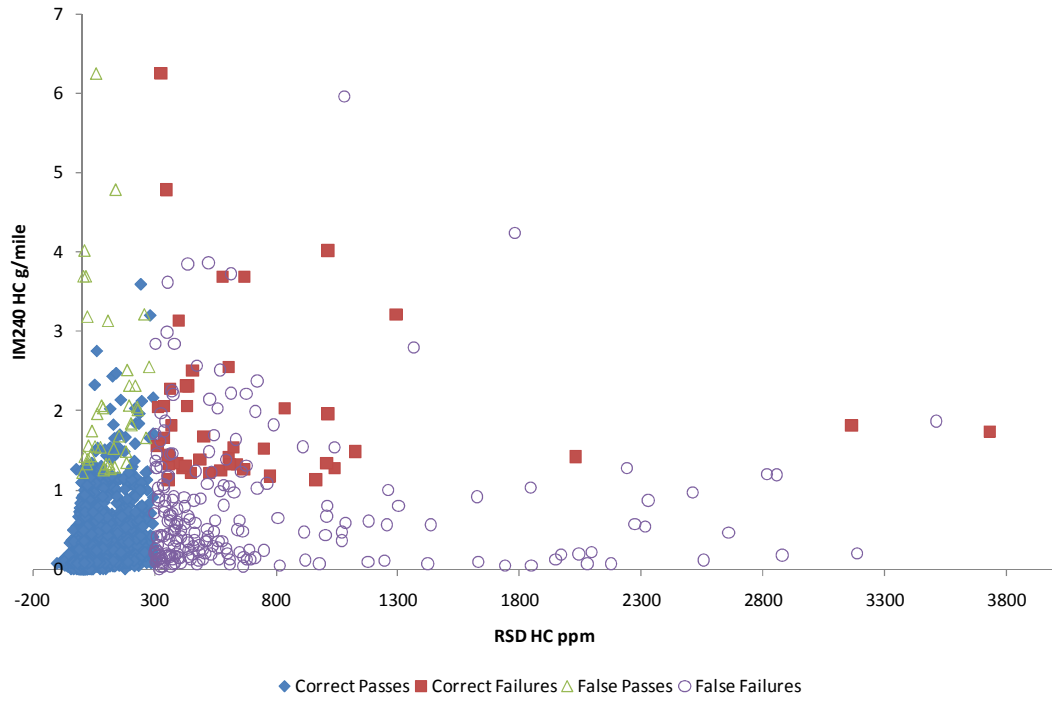
Figure D-10



2008 HC



IM240 vs RSD single measurements for all model years at the entrance to an I/M facility



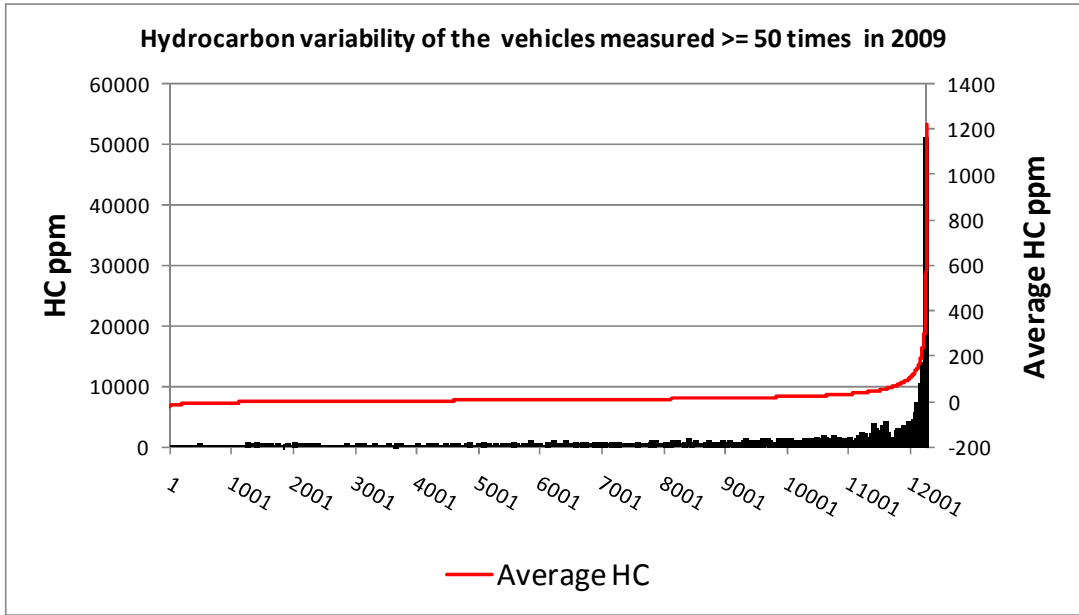
Category	Number
Correct Passes	3001
Correct Failures	64
False Passes	92
False Failures	221

Table 9 Values shown are from vehicles identified using a remote sensing HC cut point of 300ppm. IM240 results were used to confirm the remote sensing results by looking at the vehicles that passed the overall emission test and the vehicles that failed the emission test. This 300 ppm cut point could be used to send home 91% of the fleet but at a loss of 12% of the IM240 failing emissions.

Category	Number
Correct Passes	1645
Correct Failures	140
False Passes	16
False Failures	1577

Table 10 Values shown are from vehicles identified using a remote sensing HC cut point of 20ppm. IM240 results were used to confirm the remote sensing results by looking at the vehicles that passed the overall emission test and the vehicles that failed the emission test. This 20 ppm cut point could be used to send home 49% of the fleet but at a loss of 4.7% of the IM240 failing emissions.

The problem of vehicle emission variability can be shown in Figure 52 with remotely sensed vehicles measured at least fifty times in 2009, which there are over 12,000 unique vehicles. The vehicles in the highest 1%, which represent 19% of the average emissions, are shown in Figure 53 and are ordered by average ppm HC. This fleet is newer since the criteria only include on-road vehicles and is the reason why the top 1% of the fleet produces 19% not 30% of the emissions. Only the minimum, maximum and average values are reported for each vehicle. The maximum HC reading for each vehicle is represented by the top of each bar and the minimum HC reading is represented by the bottom of each bar. The average HC reading is shown as a line. Note the difference between the left and right y-axis scales. There are very few vehicles which are consistently emitting high HC with low variability. The fourth bar from the right in Figure 53 averages 870 ppm HC. This vehicle has relatively lower variability but never achieves zero or negative HC readings. There is also a vehicle with a maximum HC reading of 50,000 ppm. That's 5% HC in the exhaust emitted on the road! However, this vehicle has a larger range of emissions and averages 680 ppm HC. Both of these vehicles are polluting but the vehicle with 5% HC could either show up in Klausmeier's "false fail" region or the "false pass" region depending on the day. Regardless, it is a gross polluting vehicle at least occasionally and was identified by remote sensing. Using this fleet of high emitters measured at least 50 times in 2009 only a few needed to be repaired for large reductions in HC. Such a query can be achieved using RSD criteria of one or multiple measurements on a single vehicle.



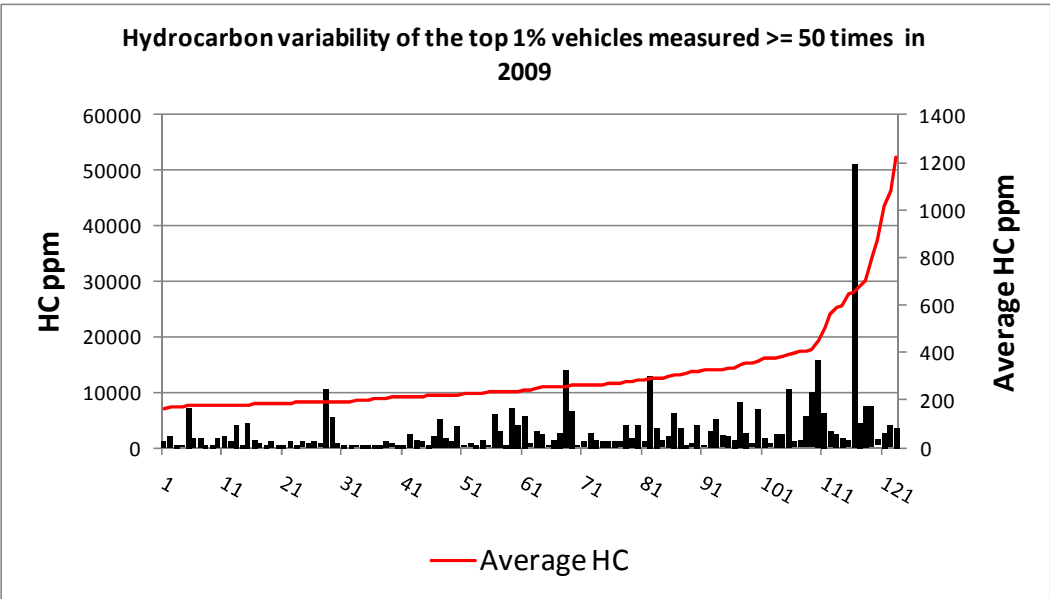
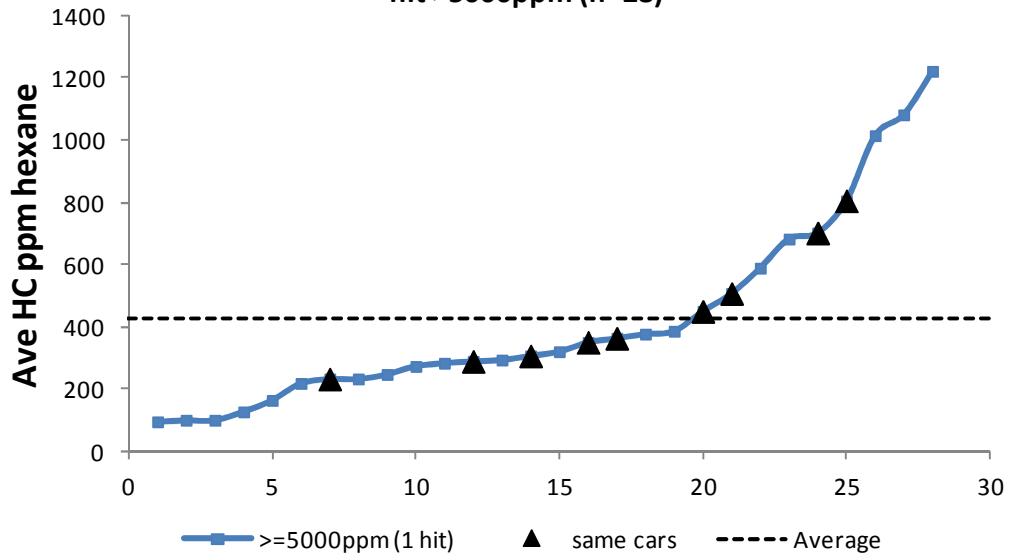
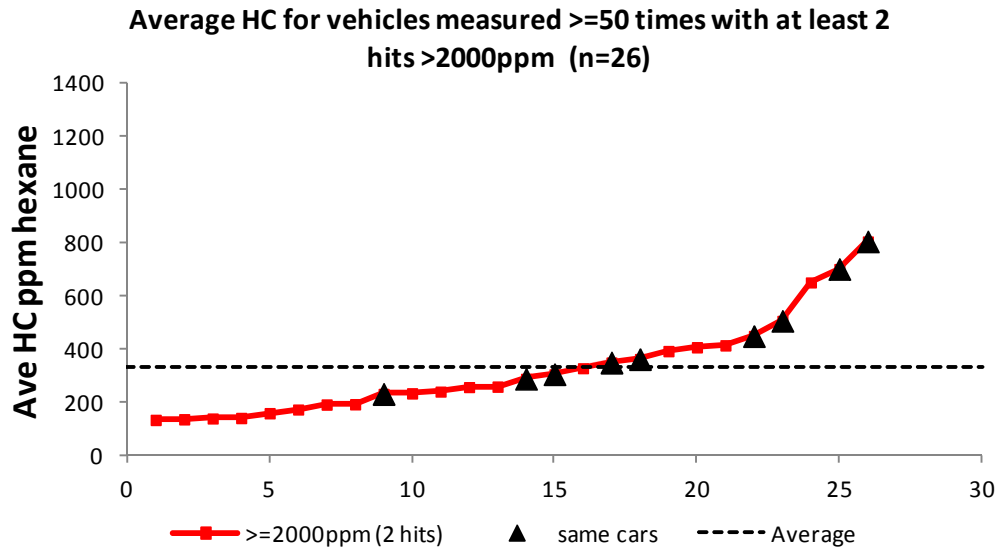


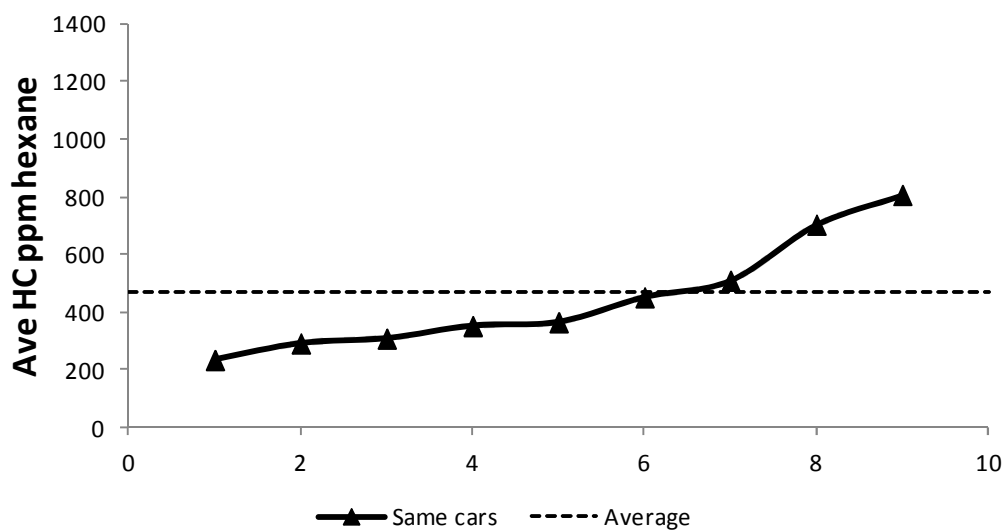
Figure 54 plots the average HC emissions for the vehicles produced from a criterion of at least one hit ≥ 5000 ppm HC. Figure 55 plots the average HC emissions for the vehicles produced from a criterion of at least 2 hits ≥ 2000 ppm HC. For each figure the horizontal dashed line represents the average HC for the plotted vehicles. Only 28 and 26 vehicles are shown in each figure, respectively. Each figure represents about the same fraction of the sampled fleet in Figure 52 (0.2%) with somewhat similar average HC emissions. If these cut points selected all vehicles that could be repaired, the 5000ppm cut point could reduce HC emissions by 6% and the 2000ppm cut point could reduce HC emissions by 4%. For both queries, the lowest average HC value for a single car is still above 100ppm HC. The 9 triangles shown in Figure 54 and Figure 55 represent vehicles (0.07% of the fleet shown in Figure 52) that are produced from both queries and are shown by themselves in Figure 56. The variability between IM240 tests and remote sensing tests can be reduced by using remote sensing at the entrance to a testing facility. If the vehicle passes its remote sensing test at a testing facility then the motorist may leave and mail in the payment, or proceed directly to the payment center without passing the chassis dynamometer test. If the vehicle fails its remote sensing test then it enters the facility to get a confirmatory IM240 test.

Average HC for vehicles measured ≥ 50 times with at least 1 hit >5000 ppm (n=28)





Average HC for vehicles measured ≥ 50 times with at least 2 hits >2000 ppm and at least 1 hit >5000 ppm (n=9)



Realistically, an I/M program using RSD selection criteria would want to repair more than 28 vehicles. This can be achieved using more stringent RSD cut points and data are available to compare what RSD cut points would work best. For about three months there were remote sensing measurements made on 3,378 vehicles entering the emission facility in Ken Caryl, Colorado. When the remote measurements were matched for vehicles measured on the same day and right before their initial IM240 test, there were 156 vehicles that failed the emission test. Of these, 35 failed only on NO_x and RSD will not be accountable for identifying them directly because high emitting cars with higher CO and HC tend to have lower NO_x.

Using a stringent cut point, remote sensing at an emissions testing facility can easily send home 50% of the customers with a pass and send the other 50% for an IM240 test and still capture 90% of the cars that would have failed if every car was subjected to an IM240 test. This can be achieved by setting a one-point fail limit of 20ppm hydrocarbons. At Ken Caryl, this 20 ppm HC cut point would have sent 1,717 out of 3,378 cars (51%) to an IM240 test. These tested cars would have identified 114 of the 156 failures for either the CO or HC portion of the emissions test, or both. Subsequently, 26 vehicles, which represent 0.8% of the fleet, were also selected from this HC cut point that only failed the NO_x portion of the IM240 emission test. These NO_x only failures were measured by RSD with an average of 1330 ppm NO and represent 23% of the on-road NO_x failures and 25% of the IM240 NO_x failures. This drive through RSD program improves efficiency of the current I/M program in addition to the convenience factor for

the motorists. Sending home 50% of the incoming motorists would save many hours of waiting and perhaps idle emissions. The 10% loss in vehicular failure rate is acceptable because they only contribute to 4.8% of the IM240 HC.

Cost Analysis of Colorado's Inspection Maintenance Program with OBDII and RSD

The state of Colorado is unique in two ways when it comes to air care programs. 1) Colorado is the only state, out of the current 34 states with an I/M program (60), that uses only a tailpipe emissions test in order to register a vehicle and 2) Colorado has acquired over 15 years of remote sensing, IM240 and OBDII data from motorists. This is one of the largest if not the largest set of data for comparative emissions from three different tests anywhere in the world. With the introduction of the On-Board Diagnostic (OBD) computer in 1996 proponents hoped that this program would solve all the problems of broken vehicles and higher emitting vehicles driving on the road. This relies on the motorist to notice the light that is illuminated when the computer recognizes a malfunction in the emissions system and then take the car into a shop to have a technician interrogate the computer to fix any problem, if there was one to begin with. The OBD computer does not measure any emissions but is rather intended as a predictor of future emissions. There are many possibilities for this program not to work as well as expected and there are studies of many different manufacturers that have documented issues with OBD (65,66). Motorists tend to ignore the light if the car is driving fine and the

computer recognizes a loose electrical connection or loose gas cap as a future emission problem. Every other state with an emission testing program uses the OBD computer at least in part to pass the certification test for registration. Some places like Chicago have moved into an OBD only program in which no emissions are measured.

Adding a criterion to these vehicles that they had to have at least one RSD measurement at least 30 days before their initial IM240 test and at least one RSD measurement at least 30 days after their IM240 test leaves 57,524 vehicles for which we can assess the on-road emissions change which occurred at least within the two months surrounding the IM test. These are the RSD-I/M vehicles. Rob Klausmeier reported to the State Auditor that the 2008 repair costs for 57,000 IM240 vehicles (6% of the total fleet) were \$12,400,000. That is \$215 per car. The repair costs are assumed to be the same in 2009.

There were 5,649 vehicles from the RSD-I/M fleet that initially failed the IM240 test. Before and after remote sensing identified that these vehicles averaged 83ppm reduction for hydrocarbons (HC). The average on-road HC for the total measured fleet was 50ppm HC. A proportional number to represent the clean screened vehicles of 20,000 vehicles is added to the RSD-I/M fleet to calculate the total fleet. These clean screened vehicles are assumed to have an average of 20ppm HC. The initial failures represent 7.3% of the sampled fleet. They identified 33% of the on-road HC emissions and showed a 14.3% HC reduction after their initial IM240 test. This reduction

percentage becomes 15.5 tons HC per day using the 2009 HC inventory data estimated from Klausmeier's report. The cost per ton HC per day for IM240 is then;

$$\$215 \text{ per car} * 5,649 \text{ cars} / 15.5 \text{ tons HC per day} = \$78,400 \text{ per ton HC per day}$$

OR *\$12,100,000 total cost extrapolated to the total fleet*

If the repair costs are used from the 2005 EPA study (40), namely \$316 per car for IM240 failures then the above numbers are;

$$\$316 \text{ per car} * 5,649 \text{ cars} / 15.5 \text{ tons HC per day} = \$115,000 \text{ per ton HC per day}$$

OR *\$17,900,000 total cost extrapolated to the total fleet*

This EPA study also reported that repairs cost \$453 per car using an OBDII only program. Using a statistically similar fleet to the RSD-I/M vehicles then, conservatively, 12% would have failed an OBDII only program and received only a 6% HC benefit or 6.5 tons HC per day. The tons HC per day cost for this program is;

$$\$453 \text{ per car} * 9,240 \text{ cars} / 6.5 \text{ tons HC per day} = \$640,000 \text{ per ton HC per day}$$

OR *\$25,000,000 total cost extrapolated to the total fleet*

An OBDII only program in Colorado in 2009 would have achieved only about 40% of the on-road emission reductions of the current program. The cost per ton per day of these reductions would have been 5-8 times larger than the current program costs. The overall cost for an OBDII only program in 2009 would have been about 2 times the total cost of the current program. What is very interesting is that the average value of 20 ppm HC used for the clean screen fleet was chosen before the analysis of the drive through

RSD at an I/M facility for which the 20ppm HC was the cut point for selecting 50% of the vehicles for an IM240 test and still captured 90% of the failures.

References

1. Stedman, D. H. (1989) *Environ Sci Technol* **23**, 147-149
2. Bishop, G. A., and Stedman, D. H. (1990) *Environ Sci Technol* **24**, 843-847
3. Lawson, D. R., Groblicki, P. J., Stedman, D. H., Bishop, G. A., and Guenther, P. L. (1990) *J Air Waste Manage* **40**, 1096-1105
4. Stedman, D. H., Bishop, G. A., Peterson, J. E., and Guenther, P. L. (1991) On-Road Remote Sensing of CO Emissions in the Los Angeles Basin. in *Final report to the California Air Resources Board under Contract No. A932-189*
5. Stedman, D. H., Bishop, G. A., Peterson, J. E., Guenther, P. L., McVey, I. F., and Beaton, S. P. (1991) On-Road Carbon Monoxide and Hydrocarbon Remote Sensing in The Chicago Area. in *Final Report to the Illinois Dept. of Energy and Natural Resources, ILENR/RE-AQ-91/14*
6. Ashbaugh, L. L., Lawson, D. R., Bishop, G. A., Guenther, P. L., Stedman, D. H., Stephens, R. D., Groblicki, P. J., Parikh, J. S., Johnson, B. J., and Huang, S. C. (1992) On-Road Remote Sensing of Carbon Monoxide and Hydrocarbon Emissions During Several Vehicle Operating Conditions. in *Presented at AWMA/EPA Conference on PM10 Standards and Nontraditional Particulate Source Controls, Phoenix, AZ*
7. Bishop, G. A., Stedman, D. H., Peterson, J. E., Hosick, T. J., and Guenther, P. L. (1993) *J Air Waste Manage* **43**, 978-988
8. Lawson, D. R. (1993) *J Air Waste Manage* **43**, 1567-1575
9. Stedman, D. H., Bishop, G. A., Peterson, J. E., and Hosick, T. (1993) Provo Pollution Prevention Program: A Pilot Study of the Cost-Effectiveness of an On-Road Vehicle Emissions Reduction Program. in <http://www.feat.biochem.du.edu/assets/databases/Utah/Provo.pdf>
10. Bishop, G. A., Zhang, Y., McLaren, S. E., Guenther, P. L., Beaton, S. P., Peterson, J. E., Stedman, D. H., Pierson, W. R., Knapp, K. T., Zweidinger, R. B., Duncan, J. W., Mcarver, A. Q., Groblicki, P. J., and Day, J. F. (1994) *J Air Waste Manage* **44**, 169-175
11. Butler, J. W., Gierczak, C. A., Jesion, G., Stedman, D. H., and Lesko, J. M. (1994) On-Road NOx Emissions Intercomparison of On-Board Measurements and Remote Sensing. in *Final Report (Ford Motor Co.), CRC Report No. VE-11-6*
12. Guenther, P. L., Bishop, G. A., Peterson, J. E., and Stedman, D. H. (1994) *Sci Total Environ* **147**, 297-302
13. Stedman, D. H., Bishop, G. A., Beaton, S. P., Peterson, J. E., Guenther, P. L., McVey, I. F., and Zhang, Y. (1994) On-Road Remote Sensing of CO and HC Emissions in California. in *Final Report, Contract No. A032-093, California Air Resources Board*
14. Stedman, D. H., Bishop, G. A., Zhang, Y., and Guenther, P. L. (1994) *Traffic Technology International* **94**, 194-198

15. Stedman, D. H., Zhang, Y., Bishop, G. A., Beaton, S. P., and Guenther, P. L. (1994) On-Road Carbon Monoxide and Hydrocarbon Remote Sensing in the Chicago Area in 1992. in *Final report to American Petroleum Institute*
16. Zhang, Y., Bishop, G. A., and Stedman, D. H. (1994) *Environ Sci Technol* **28**, 1370-1374
17. Stedman, D. H., and Bishop, G. A. (1995) *John Wiley & Sons, Inc*, 359-369
18. Zhang, Y., Stedman, D. H., Bishop, G. A., Guenther, P. L., and Beaton, S. P. (1995) *Environ Sci Technol* **29**, 2286-2294
19. Bishop, G. A., and Stedman, D. H. (1996) *Accounts Chem Res* **29**, 489-495
20. Stedman, D. H., Bishop, G. A., Aldrete, P., and Slott, R. S. (1997) *Environ Sci Technol* **31**, 927-931
21. Stedman, D. H., Bishop, G. A., and Slott, R. S. (1998) *Environ Sci Technol* **32**, 1544-1545
22. Wenzel, T. (2001) *Environ Sci Policy* **4**, 359-376
23. Wenzel, T. (2003) *Environ Sci Policy* **6**, 153-166
24. Burgard, D. A., Bishop, G. A., Stadtmuller, R. S., Dalton, T. R., and Stedman, D. H. (2006) *Appl Spectrosc* **60**, 135a-148a
25. Stedman, D. H., Bishop, G. A., and Stadtmuller, R. (2007) On-Road Remote Sensing of Automobile Emissions in the Chicago Area: Year 7, September 2006. in *Coordinating Research Council Contract No. E-23-9*
26. Bishop, G. A., Peddle, A. M., Stedman, D. H., and Zhan, T. (2010) *Environ Sci Technol* **44**, 3616-3620
27. Bishop, G. A., Burgard, D. A., and Stedman, D. H. (2004) On-Road Remote Sensing of Automobile Emissions in the La Brea Area: Year 3, October 2003. in *Coordinating Research Council Contract No. E-23-4*
28. Bishop, G. A., and Stedman, D. H. (2008) *Environ Sci Technol* **42**, 1651-1656
29. Bishop, G. A., Morris, J. A., and Stedman, D. H. (2001) *Environ Sci Technol* **35**, 1574-1578
30. Heywood, J. B. (1988) *Internal Combustion Engine Fundamentals*, McGraw-Hill Publishing Company, St. Louis
31. Bowman, C. T. (1975) *Prog Energ Combust* **1**, 33-45
32. Hillard, J. C., and Wheeler, R. W. (1979) *SAE Transportation* **88**; **790691**
33. Vioculescu, I. A., and Borman, G. L. (1978) *SAE Transportation* **87**; **780228**
34. (2010) 2010 update San Pedro Bay Ports clean air action plan. The Port of Los Angeles; Port of Long Beach: Los Angeles
35. Schuchmann, B. G., Bishop, G. A., and Stedman, D. H. (2009) Remote Measurements of On-Road Emissions from Heavy Duty Diesel Vehicles in California ; Year 2.
36. (<http://www.cumminswestport.com/products/islg.php>) Specifications for the stoichiometric NG ISL-G Cummins engine.
37. (1998) Summary of Test Results from Wisconsin EPA OBD Project. in *Report No. SR98-10-02*, Sierra Research: Sacramento, CA

38. Trimble, T. (2000) Analysis of the OBDII Data Collected From the Wisconsin I/M Lanes. in *EPA-420-R-00-014; US Environmental Protection Agency, Office of Transportation and Air Quality: Ann Arbor, MI*
39. Durbin, T. D., and Norbeck, J. M. (2002) *J Air Waste Manage* **52**, 1054-1063
40. Gardetto, E., Bagian, T., and Lindner, J. (2005) *J Air Waste Manage* **55**, 1480-1486
41. Pope, D. J. (2009) Particle Matter Measurements for Inspection Maintenance Programs. in *Department of Natural Sciences and Mathematics, University of Denver, Denver*
42. Maricq, M. M. Evaluation of a prototype tailpipe PM sensor. Ford
43. Singer, B. C., Harley, R. A., Littlejohn, D., Ho, J., and Vo, T. (1998) *Environ Sci Technol* **32**, 3241-3248
44. EPA. (2002) Highway Diesel Progress Review.
45. (2008) California Code of Regulations. in *Title 13, Section 2027*; <http://www.arb.ca.gov/regact/2007/drayage07/finreg1209.pdf>
46. (2008) California Code of Regulations. in *Title 13, Section 2025*
47. (2007) 2006 Estimated Annual Average Emissions: Statewide. in *California Air Resources Board* <http://www.arb.ca.gov/ei/emissiondata.htm>
48. Harley, R. A., Marr, L. C., Lehner, J. K., and Giddings, S. N. (2005) *Environ Sci Technol* **39**, 5356-5362
49. Stedman, D. H. (2004) *Environ Chem* **1**, 65-66
50. Fujita, E. M., Stockwell, W. R., Campbell, D. E., Keislar, R. E., and Lawson, D. R. (2003) *J Air Waste Manage* **53**, 802-815
51. Lemaire, J. (2007) *Österreichische Ingenieur und Architekten-Zeitschrift* **152**, 1-12
52. (2003) California Code of Regulations. in *Title 13, Section 2702(f) and 2706(a)*
53. Jimenez, J. L., McClintock, P., McRae, G. J., Nelson, D. D., and Zahniser, M. S. (1999). in *Proceedings of the 9th CRC On-Road Vehicle Emissions Workshop, CA*
54. Lenner, M. (1987) *Atmos Environ* **21**, 37-43
55. http://www.cumminswestport.com/pdf/CWI-ISL_G_Brochure_MED.pdf **2009**, Brochure for Cummins Westport ISL-G
56. USEPA 2007 Highway Rule. in <http://www.epa.gov/otaq/highway-diesel/index.htm>. http://www.us.sgs.com/ulsd_testing.htm?serviceId=10010630&lobId=19649
57. Bishop, G. A., Holubowitch, N. E., and Stedman, D. H. (2008) Remote Measurements of On-Road Emissions from Heavy Duty Diesel Vehicles in California ; Year 1.
58. Li, S. C., and Williams, F. A. (2002) *J Eng Gas Turb Power* **124**, 471-480
59. Biniwale, R. B., Pande, J. V., Dhakad, M., Labhsetwar, N. K., and Ichikawa, M. (2008) *Catal Lett* **123**, 164-171
60. EPA. (2003) Major Elements of Operating I/M Programs. in *Office of Transportation and Air Quality*

61. Klausmeier, R., Darlington, T., Kahlbaum, D., and Wolff, G. (2009) Evaluation of the Colorado Automobile Inspection and Readjustment (AIR) Program. in *Prepared for the Colorado Office of the State Auditor*
62. (2011) Gas Buddy: http://www.coloradogasprices.com/Retail_Price_Chart.aspx.
63. Hoshizaki, H., Wood, A. D. Kemp, D. D. (1973) Vehicle Inspection Instrumentation. in *Prepared for the California Air Resources Board*
64. Bishop, G. A., Stedman, D. H., and Ashbaugh, L. (1996) *J Air Waste Manage* **46**, 667-675
65. EPA. (2011) OBD Readiness Testability Issues <http://www.epa.gov/oms/regs/im/obd/regtech/420b11022.pdf>. in *Transportation and Regional Programs Division; Office of Transportation and Air Quality*
66. EPA. (2011) IM OBD Vehicles Readiness Exception List. in *Office of Transportation and Air Quality* <http://www.epa.gov/otaq/regs/im/obd/regtech/420f08009.pdf>

Appendix A

External flow rates and pressure settings for HDDV sampling system

- Air pump for the three sample inlets (CO/CO₂, NO, and HC) -10 psi (69 kPa)
- FID fuel pressure-22 psi (150 kPa)
- Zero air pressure for FID and NO- 20 psi (138 kPa)
- DMM- all internally regulated based upon vacuum pump

Appendix B

Data collected at Fullerton Municipal Airport

Peralta 2010 Temperature and Humidity Data										
Time	4/26	4/26	4/27	4/27	4/28	4/28	4/29	4/29	4/30	4/30
	°F	%H	°F	%H	°F	%H	°F	%H	°F	%H
5:53	54	93	56	83	58	87	55	40	49	63
6:53	56	87	56	83	59	84	57	32	54	57
7:53	58	81	57	80	62	65	59	29	59	44
8:53	64	65	57	80	64	52	60	27	62	38
9:53	68	57	59	75	65	49	63	23	65	29
10:53	71	53	61	72	65	49	65	22	68	32
11:53	69	57	64	63	66	47	66	19	69	29
12:53	71	53	66	59	67	42	65	28	72	24
13:53	71	53	65	61	66	43	66	29	72	20
14:53	74	48	64	63	66	43	66	32	70	25
15:53	73	48	63	68	66	40	65	37	70	21
16:53	70	53	64	65	63	45	66	31	67	26

Data collected at Daugherty Field in Long Beach

Port of LA 2010 Temperature and Humidity Data										
Time	5/3	5/3	5/4	5/4	5/5	5/5	5/6	5/6	5/7	5/7
	°F	%H	°F	%H	°F	%H	°F	%H	°F	%H
5:53	55	86	56	90	58	84	59	75	58	90
6:53	59	81	59	84	59	81	61	72	62	78
7:53	65	61	63	73	61	78	64	65	66	63
8:53	68	57	65	68	64	70	64	63	70	51
9:53	73	46	67	63	65	68	67	59	70	61
10:53	75	45	65	65	66	65	68	59	72	53
11:53	77	42	67	61	68	61	69	57	75	45
12:53	81	35	69	57	68	61	67	61	79	36
13:53	80	37	68	59	67	66	69	55	79	34
14:53	77	43	68	61	67	63	70	53	79	31
15:53	76	45	67	63	66	65	72	46	77	28
16:53	74	45	68	61	64	70	70	44	73	29

Appendix C

The following equations were solved for the purpose of the observed results. Better equations will be needed for future development of the truck shed.

For HC and NO, all points under the peak of interest were summed and corrected for any baseline offset. The summed values (x) were then used to solve the following equations;

$$\text{HC\%} = 360*(x)/10,000$$

$$\text{NO\%} = 100*(x)/10,000$$

The curves for CO and CO₂ were each treated in two sections. For CO, all individual points greater than 1 volt were summed (x) and fitted with the exponential equation;

$$\text{CO\%} = [486.75*\exp(0.621*(x))]/10,000$$

All individual points less than 1 volt were summed (x) and fitted with the linear equation;

$$\text{CO\%} = [777.62*(x) - 24.355]/10,000$$

For CO₂, all individual points greater than 2 volts were summed (x) and fitted with the following equation;

$$\text{CO}_2\% = 0.6551*(x) - 0.0278$$

Please note that for the experiments performed in this document no individual point ever exceeded 2 volts.

All individual points less than 2 volts were summed (x) and fitted with the following equation;

$$\text{CO}_2\% = 0.8878*(x) - 0.5471$$

The total CO₂ % for an individual peak is the sum of these two calculated CO₂ percentages.

